The Dynamic Platelet Function Assay (DPFA): Assessment of platelet translocation behaviour on von Willebrand Factor (VWF) in pregnancy, neonates and adults

AUTHOR(S)

Jonathan James Cowman

CITATION

Cowman, Jonathan James (2015): The Dynamic Platelet Function Assay (DPFA): Assessment of platelet translocation behaviour on von Willebrand Factor (VWF) in pregnancy, neonates and adults. Royal College of Surgeons in Ireland. Thesis. https://doi.org/10.25419/rcsi.10807433.v1

DOI

10.25419/rcsi.10807433.v1

RCSI

The Dynamic Platelet Function Assay (DPFA): Assessment of platelet translocation behaviour on von Willebrand Factor (VWF) in pregnancy, neonates and adults

Jonathan Cowman

PhD **2015**

Declaration

I declare that this thesis, which I submit to RCSI for examination in consideration of the award of a higher degree PhD is my own personal effort. Where any of the content presented is the result of input or data from a related collaborative research programme this is duly acknowledged in the text such that it is possible to ascertain how much of the work is my own. I have not already obtained a degree in RCSI or elsewhere on the basis of this work. Furthermore, I took reasonable care to ensure that the work is original, and, to the best of my knowledge, does not breach copyright law, and has not been taken from other sources except where such work has been cited and acknowledged within the text.

Signed_____

10116231

Student Number _____

29/05/2015

Date _____

Table of Contents

Publications

Published papers

FITZGIBBON, S., **COWMAN**, J., RICCO, A. J., KENNY, D. & SHAQFEH, E. S. 2014. Examining platelet adhesion via Stokes flow simulations and microfluidic experiments. Soft Matter, 11, 355-67.

WALSH, T. G., BERNDT, M. C., CARRIM, N., **COWMAN**, J., KENNY, D. & METHAROM, P. 2014. The role of Nox1 and Nox2 in GPVI-dependent platelet activation and thrombus formation. Redox biology, 2, 178-86.

LUCITT, M. B., O'BRIEN, S., **COWMAN**, J., MEADE, G., BASABE-DESMONTS, L., SOMERS, M., KENT, N., RICCO, A. J. & KENNY, D. 2013. Assaying the efficacy of dual-antiplatelet therapy: use of a controlled-shear-rate microfluidic device with a well-defined collagen surface to track dynamic platelet adhesion. Analytical and bioanalytical chemistry, 405, 4823-34.

Published abstracts

MULLERS, S., **COWMAN**, J., BURKE, N., Murray, A., FLOOD, K., TULLY, E., O' CONNER, H., Dempsey, M., DICKER, P., GEARY, M., KENNY, D. AND MALONE F. 2015. Significant differences in dynamic platelet behavior in gestational hypertension and preeclampsia compared with intrauterine growth restriction suggesting alternate pathways in utero-placental disease. American journal of obstetrics and gynecology, 210: S48.

MULLERS, S., BURKE, N., **COWMAN**, J., KEARNEY, M., FLOOD, K., O' CONNER, H., DICKER, P., TULLY, E., GEARY, M., KENNY, D. AND MALONE F. 2015. Platelet function in intra-uterine growth restriction: altered platelet behaviour as a cause or a consequence of utero-placental disease. American journal of obstetrics and gynecology, 212, S125-S126.

QUINN N., **COWMAN** J., GEOGHEGAN S., FERGUSON B., SHARPE T., KENNY D. & MOLLOY E.J. 2014. Preterm Infants Exhibit Increased Platelet Adhesion To VWF Under Conditions Of Arterial Shear. Archives of Diseases in Childhood, 99: A211-A212.

Submitted papers

COWMAN, J., DUNNE, E., OGLESBY, I., BYRNE, B., RALPH, A., VOISIN, B., MULLERS, S., RICCO, A.J. and KENNY, D. 2015. Age-related changes in platelet function are more profound in women than in men; platelet function changes with age (Submitted for publication in Scientific Reports).

RALPH, A., SOMERS, S., **COWMAN**, J., VOISIN, B., HOGAN, E., DUNNE, H., DUNNE, E., BYRNE, B., RICCO, A.J., KENNY, D. and WONG, S. 2015. Enhancements to a platelet tracking method of shear-mediated platelet interactions with von Willebrand factor (Submitted for publication in Transactions on Image Processing).

Manuscripts in preparation

COWMAN, J., QUINN N., GEOGHEGAN S., DUNNE, E., BYRNE, B., RALPH, A., VOISIN, B., MULLERS, S., RICCO, A.J., MOLLOY, E.J. and KENNY, D 2015. Platelet translocation behaviour on von Willebrand Factor (VWF) is significantly different in preterm versus full-term infants.

COWMAN, J., MULLERS, S., BYRNE, B., RALPH, A., VOISIN, B., RICCO, A.J., Malone, F. and KENNY, D. 2015. Platelet translocation behaviour is altered during pregnancy and pregnancy with utero-placental disease.

MEADE, G., O'BRIEN, S., SOMERS, M., **COWMAN**, J, BYRNE, B., McATAMNEY C., MURPHY R., FOLEY, D., O'REILLY, B., KENT, N., RICCO, A.J. and KENNY, D. 2015. Platelet behavior on von Willebrand factor under arterial fluid shear differs between healthy individuals and patients with cardiovascular disease on dual antiplatelet therapy.

COLLINS, A. DUNNE, E., RALPH, A., VOISIN, B., **COWMAN**, J., OGLESBY, I., McFADDEN, S., WONG, S., BYRNE, B., RICCO, A.J. and KENNY, D. 2015. Aspirin inhibits stable adhesion in vitro and in vivo.

Posters and oral presentations

COWMAN, J., DUNNE, E., QUINN, N., GEOGHEGAN S., MOLLOY E.J., RICCO A.J. and KENNY, D. 2014. Platelets from premature neonates have increased platelet affinity for von Willebrand factor (VWF) under arterial shear compared to platelets from term neonates. Scientific and Standardization Committee (SSC), Milwaukee, USA 2014. **Top rated abstract, Oral presentation**.

COWMAN, J., COLLINS, A., DUNNE, E. and KENNY, D. 2014. Platelet function changes with age. Human Disease Mapping (HDM), RCSI Dublin. Oral Presentation.

COWMAN, J., COLLINS, A., DUNNE, E., EGAN, K., SOMERS, M., RALPH, A., VOISIN, B., WONG, S., HOGAN, E., GEOGHEGAN, S., QUINN, N., RICCO, A.J., MOLLOY, E.J. and KENNY D. 2013. Age influences platelet behavior on von Willebrand factor. UK Platelet Conference, Birmingham. Poster Presentation.

COWMAN, J., SOMERS, M and KENNY, D. 2011. Thrombus formation on collagen is inhibited by $P2Y_{12}$ inhibition. Haematology Association of Ireland, Wicklow (Ireland). Oral Presentation.

Awards

Young investigator award and travel fund. Top rated abstract at the Scientific and Standardization Committee (SSC), Milwaukee, USA 2014.

List of abbreviations

ADAMTS-13	A disintegrin and metalloproteinase with thrombospondin motif-13
AA	Arachidonic Acid
ADP	Adenosine di-phosphate
BFP	Bio-membrane force probe
BOT	Botrocetin
BBS	Bernard Soulier Syndrome
BSA	Bovine Serum Albumin
$C_6H_{12}O_6$	Dextrose
CFL	Cell Free Layer
CT	Closure Time
CVD	Cardiovascular Disease
CEPI	Collagen and Epinephrine
CADP	Collagen and ADP
COX	Cyclooxygenase
dH_2O	Deionised Water
$DiOC_6$	Dihexyloxacarbocyanine iodide
DPFA	Dynamic Platelet Function Assay
ECM	Extracellular matrix
EtOH	Ethanol

F-L	Fahraeus–Lindquist layer
FITC	Fluorescein Isothiocyanate
GT	Glanzmann's Thrombasthenia
GP	Glycoprotein
HCT	Haematocrit
IUGR	Intrauterine growth restriction
KH_2PO_4	Potassium dihydrogen phosphate
LTA	Light Transmission Aggregometry
LRR	Leucine-rich repeat
MFI	Mean fluorescent intensities
$MgCl_2.6H_20$	Magnesium Chloride Hexahydrate
MSD	Mechano-sensitive domain
NaCL	Sodium chloride
$NaHCO_3$	Sodium bicarbonate
OT	Optical Tweezers
P2Y	Purinergic Receptor Y
PBS	Phosphate Buffered Saline
PCI	Percutaneous Coronary Intervention
PET	Preeclampsia
PIH	Pregnancy induced hypertension
PMMA	Polymethylmethacrylate

PFA-100	Platelet Function Analyser-100
PRP	Platelet Rich Plasma
PPP	Platelet Poor Plasma
PSA	Pressure Sensitive Adhesive
PS	Polystyrene
RBCs	Red Blood Cells
SD	Standard Deviation
SEM	Standard Error of the Mean
TRAP	Thrombin Receptor Agonist Peptide
TxA_2	Thromboxane A2
WBCs	White Blood Cells
VWD	von Willebrand Disease
VWF	von Willebrand Factor
VWFpp	von Willebrand Factor pro-peptide

List of figures

List of tables

Summary

Platelets are a key constituent in haemostasis and thrombosis. Platelet function testing has clinical benefit, through identifying those who are potentially at risk to bleeding or thrombosis. Empirically, the challenge is to produce tests that can effectively replicate the flow and shear environment that platelets experience *in vivo*.

Our research group, previously developed a Dynamic Platelet Function Assay (DPFA), that uses novel parallel plate flow chambers coated with purified human VWF and custom-designed platelet tracking software (Kent et al., 2010, Lincoln et al., 2010). This custom-designed platelet tracking software was capable of deriving novel parameters of platelet function that related to the biological activity of platelets *in vivo*. However, the reliability and the clinical relevance of the measured parameters of the DPFA were unclear, and there were errors in its platelet tracking process. A primary objective of this PhD thesis was to investigate the above issues through validation and clinical evaluation of the DPFA. Validation of the assay was achieved computationally using an ideal data set, which determined the percentage systematic error for each measured parameter of platelet behaviour, and biologically using a $P2Y_1$ receptor inhibitor MRS2179. Clinical evaluation was performed in adults, neonates, healthy pregnancy and pregnancy with utero-placental disease, through observation and recording of subtle changes in the behavior of platelets translocating on VWF.

The results conveyed in this thesis, validated, clinically evaluated and enhanced the DPFA, through the refinement and adaptation of its platelet tracking software and parameter outputs. It is concluded that the DPFA is capable of detecting subtle changes in platelet function. These changes in platelet function are cognizant to the behaviours of platelets *in vivo*. It is recommended that future work should seek to enhance and further understand the assays outputs.

Acknowledgements

Thanks **Science Foundation Ireland** for funding this project.

Particular thanks and appreciation to my supervisor **Prof. Dermot Kenny** for affording me the opportunity to do my PhD in his lab. I would like to thank him for his patience, guidance and supervision throughout. I arrived in **Dermot's** lab as a boy but left as a man.

I would like to acknowledge **Prof. Antonio (Tony) Ricco** for his assistance during my PhD. It was inspiring to have conversations and pints down the Swan with a NASA scientist.

I would like to express appreciation to the Biomedical Diagnostics Institute (BDI) and CVD1 research group in RCSI and DCU. **Eimear Dunne,** who was always there any time I had questions or needed clarification. Our project manager, **Dr. Barry Byrne,** who I plagued during my PhD. Thank you for proof reading my PhD chapters and the football debates. **Dr. Irene Oglesby,** thanks for the direction with my writing style. **Siobhan McFadden,** thanks for the chats and providing me with blood collections for my experiments. **Martin Somers,** thanks for helping me somewhat understand the very basic concepts of software design. **Peter McCluskey,** I am honestly shocked at your knowledge of practically anything that exists. **Dr. Niamh Gilmartin,** thanks for your help and advice. I would also like to thank **Dr. Nigel Kent** of the Dublin Institute of Technology (DIT) and **Dr. Conor Burke** associate director (commercialisation) in BDI. **Dr. Gerardene Meade,** thank you for help and advice during the early days of my PhD.

I would like to acknowledge the contributions of my collaborators during my PhD. **Prof. Eric Shaqfeh** and **Dr. Sean Fitzgibbon** of Stanford University in California. Thanks **Dr. Nuala Quinn**, **Dr Sarah Geoghegan** and **Prof. Eleanor Molloy** of Holles street maternity hospital in Dublin. My first visit to the Neonatal Intensive Care Unit (NICU) was amazing. Thanks **Prof. Brian Meenan** and **David Bishop** of the University

of Ulster's Nanotechnology and Integrated Bioengineering Centre (NIBEC). For their support and clinical facilitation, a warm thanks to **Prof. Fergal Malone, Dr. Liz Tully** and **Dr. Sieglinde (Siggy) Müllers** of the Rotunda hospital in Dublin. Thank you **Siggy** for helping me during the past two years, I learned a lot from you about pregnancy and utero-placental disease. I would like to acknowledge **Prof. Robert Montgomery,** Blood Research Institute, Milwaukee, WI, USA for providing von Willebrand Factor (VWF) for my studies. Thanks to the guys in the Irish Centre for High-End Computing (ICHEC), **Dr. Adam Ralph**, **Dr. Simon Wong** and **Dr. Bruno Voisin**.

I would like to thank everyone in Molecular and Cellular Therapeutics (MCT). In particular, **Olwen Foley**, **Kay McKeon**, **Mary Ledwith** and **Anne Grady**. Phlebotomists **Una**, **Helen** and **Pauline**. Thanks **Dr. Maria Morgan** for the evening chats we had when I was working late and providing the office with chocolate.

Thank you to **Dr. Heiko Dussmann** and **Brenton Cavanagh** in RCSI for all the help with the microscope. Whenever I had a problem you guys would always sort it out.

To the porters **Frank D**, **Frank B**, **Brian**, **Eddie, Dave** and **Phil**, some of you I worked with over the summer many years ago before starting my PhD. It was a real experience and one I will not forget.

I have made many friends in RCSI who have moved on to greener pastures. I'd like to acknowledge **Niamh Cooke**, **Aideen Collins** and **Ana Lopez-Alonso**. Thanks to **Karl Egan**, you are one of the most genuine blokes I have ever met. **Seamus** (Shambosis) **Allen**, we had some craic over the years, enjoyed your joke of the day. The lovely **Naadiya Carrim** (Benzema), thanks for being a great friend and listening to me moan. **Emily Reddy** (Reddy), what can I say; we had some serious craic in the office, the laughs about Father Ted, the Simpsons and South Park. The office was so quiet without you that I actually got some work done. My favourite Indian **Kalyan Golla** (Prof. Golla), number one in my eyes. Missed you dearly when you left for the states, hopefully you'll be back in your "real" home (Ireland) soon. The Italian stallion **Annachiara Mitrugno** (Ms. Italia), teaching you English and I pretending to learn

Italian was mighty. **Tadhg** (lord wellington) **Mcgivern,** some man for one man, never have I heard someone use the word “well” as much as you. **Thea Tilly,** we had the craic, will never forget that house party at yours, sore heads all round the next day. **Tony** (T-Bad) **Walsh**, I have multiple names for you, missed all our football chats. **Graham Kelly** some man for the pints. To my gym buddies and friends **John O’Brien** and **Damir Vareslija** thank for you “setting the tone” in the gym and the pints down the Swan.

Finally, I would like to thank my family and friends from home, you know who you are, for always being there for me whenever I was down or needed someone to talk to. In particular, I would like to thank my parents **Seamus** and **Nenette** who I dedicate this thesis too. Thank you for everything you have provided me with in life. There were times where I struggled but you always encouraged me and I got there eventually.

“Physical fitness is not only one of the most important keys to healthy body, it is the basis of dynamic and creative intellectual activity”

John F. Kennedy 1960

Chapter 1

Introduction

1.1 The platelet

In the blood stream there are 3 types of circulating cells, platelets, white blood cells (WBCs) and red blood cells (RBCs). Platelets are small discoid-shaped cells ranging from 2–5 μm in diameter with a thickness of 0.5 μm and are produced by megakaryocytes in the bone marrow. The normal platelet count is approximately 150-450 x 10^3 platelets per microlitre (μL) of blood in humans. Platelets have a lifespan of 7-10 days after which time they are cleared by macrophages in the liver and spleen.

1.1.1 Haemostasis

Platelets have a fundamental role in haemostasis (Figure 1.1). In the arterial circulation, damage to the vascular wall, results in the exposure of vascular/subendothelial matrix proteins. The proteins that are exposed are primarily collagens. Von Willebrand Factor (VWF) present in blood plasma, binds to this exposed collagen, resulting in a conformational change in the structure of VWF. This structural change in VWF allows it to capture platelets from flowing blood. VWF captures platelets via its interaction with the platelet glycoprotein (GP) Ib-IX-V complex. Platelet movement is slowed, allowing the platelet to interact with collagen via the platelet immunoglobulin-like receptor GPVI. The platelet GPVI receptor generates powerful platelet activation signals and this results in inside-out activation of platelet integrins α2β1 and αIIbβ3 and cytoskeletal remodelling, which leads to platelet spreading, granule secretion and release of thromboxane A_2 (a potent mediator of platelet activation). The activation of fibrinogen receptor αIIbβ3 modulates stable platelet adhesion and aggregation at the site of vascular damage (Watson, 2009).

The importance of platelets in haemostasis is highlighted by rare platelet bleeding disorders such as Bernard-Soulier syndrome (BSS) and Glanzmann's thrombasthenia (GT). BSS is caused by defects in the platelet glycoprotein (GP) Ib-IX- V complex which results in macrothrombocytopenia. Macrothrombocytopenia is thrombocytopenia with an increase in platelet size (Li et al., 1995, Andrews and Berndt, 2013). Thrombocytopenia refers to low platelet counts and is generally

defined as platelet counts (< 150 x 10^3 per µL of blood in healthy adults). GT is caused by defective or low levels of the fibrinogen receptor integrin αIIbβ3 which results in reduced platelet aggregation (Nurden, 2006).

1.1.2 Thrombosis

Platelets play a key role in thrombosis (Figure 1.1), namely the formation of a thrombus in a vessel that results in obstruction of blood flow. Venous and arterial thrombosis occurs where thrombi form in a vein or artery respectively. Venous thrombosis is mainly mediated by the coagulation cascade whereas arterial thrombosis is mainly mediated by the activity of platelets. Venous thrombosis is initiated by a tissue factor, which activates the coagulation response (Esmon, 2009). Deep vein thrombosis is the most common form of venous thrombosis and is characterised by the formation of a blood clot in the deep veins of the leg. The blood clot can dislodge and become a moving clot (embolus) and travel to the lungs resulting in the formation of pulmonary embolism (Hwang and Schulman, 2013). Arterial thrombosis occurs at sites of vascular damage, where platelets adhere and aggregate uncontrollably. Arterial thrombosis can also occur as fats and cholesterol are deposited along the artery wall, forming atherosclerotic plaques. These plaques can rupture causing platelet adherence and aggregation in the vessel which result in occlusion of the vessel (Previtali et al., 2011).

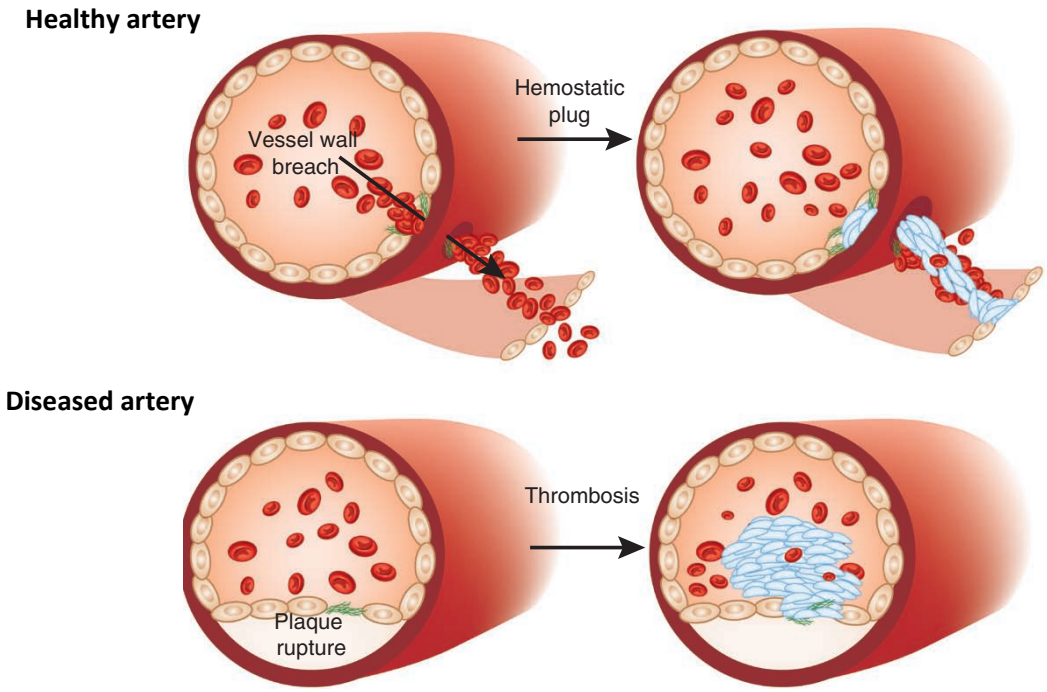

Figure 1.1 Haemostasis versus thrombosis formation. Damage occurs via trauma at the endothelial wall of the healthy artery. Platelets sense this damage; they adhere and rapidly interact with one another forming a thrombus. The thrombus seals the wound and supresses bleeding. In the diseased artery, plaque rupture causes platelet activation within the vessel. This restricts blood flow leading to thrombosis. (Adapted from Jackson, 2011).

1.2 The effects of shear on platelet adhesion to exposed collagen

Platelets are small and thus are affected by the distribution of RBCs in the blood vessel. This phenomenon is known as Fahraeus–Lindquist effect where the RBCs migrate to the centre of the vessel forcing the platelets to the vascular wall (Fahraeus, 1931). Platelets are therefore in an optimal location to respond to vascular damage. Upon damage of the vessel wall, collagen fibres present in the sub-endothelial layers are exposed to the flowing blood. The dynamic forces of the blood influence how platelets respond to the exposed vascular collagen and create shear within the vessel. Shear refers to the frictional force that RBCs apply to the platelets when contacting the damaged vascular wall. This force results in shear-induced deformation of the platelet at the wall and dictates what receptors the platelet utilises for adhesion to the damaged surface. Hence at different shear rates, platelets use different platelet receptors to modulate the adhesion on the exposed vascular surfaces (Kroll et al., 1996). Under venous shear conditions (< 1000 s^{-1}), platelet adhesion to collagen is predominately mediated by platelet-collagen immunoglobulin-like receptor, GPVI. GPVI engagement with collagen causes intracellular signalling and activation of integrins α2β1, αIIbβ3 (Yip et al., 2005).

Under conditions of arterial shear (> 1000 s^{-1}), platelet adhesion to the exposed collagen is initiated by the platelet-VWF receptor interaction. VWF binds to the exposed collagen and undergoes a conformational change that allows VWF to engage with the platelet. Next, the VWF tethers the platelet and slows the platelet's movement, allowing platelet receptor GPVI to interact with the collagen, resulting in activation of integrin α2β1, αIIbβ3 and subsequent adhesion of the platelet to the damaged surface. Under pathological shear conditions (> 10,000 s^{-1}), platelet activation is not required and is exclusively mediated through VWF-platelet interactions in the absence of αIIbβ3 adhesive function (Jackson et al., 2009).

1.3 Platelet adhesion receptors

Platelets contain several key receptors on their surface, which modulate primary platelet adhesion to exposed vascular surfaces. Platelet adhesion receptors GPIb-IX-V complex (initiation of platelet adhesion), GPVI (platelet activation) and integrin

αIIbβ3 (stable platelet adhesion and aggregation) have central roles in the haemostasis process. These receptors are adapted to function under high-shear stress conditions (Yip et al., 2005). This thesis, will focus on platelet adhesion to immobilised VWF under arterial shear conditions in the absence of collagen. Platelet adhesion to immobilised VWF is a two-step dynamic process by which the GPIb-IX-V complex mediates initial platelet attachment and integrin αIIbβ3 supports irreversible attachment of the platelet (Savage et al., 1996).

1.3.1 Glycoprotein (GP) Ib-IX-V complex

The GPIb-IX-V complex, mediates initial platelet adhesion to collagen at the site of vascular damage, via its interaction with VWF under high-shear stress conditions. There are approximately 25,000 copies of GPIb-IX-V per platelet. The GPIbα of the GPIb-IX-V complex interacts with VWF resulting in transmembrane signaling events, activation of αIIbβ3 and platelet aggregation (Canobbio et al., 2004).

The GPIb IX-V complex consists of four subunits, GPIbα, GPIbβ, GPIX and GPV. All of the subunits belong to a leucine-rich repeat (LRR) superfamily. Disulphide bonds link GPIbα to two GPIbβ subunits and these are non-covalently bonded with GPIX and GPV in a ratio of 2:4:2:1 (Andrews and Berndt, 2013). Notably, the cytoplasmic tail of the GPIbβ subunit contains the membrane proximal sequence RRLRARARARA and blocking of this sequence has been shown to inhibit platelet activation (Martin et al., 2003). Genetic mutations in either of the subunits GPIbα, GPIbβ or GPIX of the GPIb-IX-V complex can cause BSS (Li et al., 1995, Andrews and Berndt, 2013). GPIb-IX-V complex also has other roles *in vivo* other than binding VWF including binding to αMβ2 (MAC-1) which promotes leukocyte migration and adhesion on mural vascular thrombi (Michelson, 2007), or binding of P-selectin on endothelial cells or activated platelets (Andrews et al., 2003).

1.3.1.1 Glycoprotein Ibα structure

GPIbα (Figure 1.2A) is the major ligand-binding subunit of the GPIb-IX-V complex. It comprises of an N-terminal flanking sequence which has seven leucine-rich repeats each containing 24 amino acids, a leucine-rich C-terminal flanking sequence, an

anionic sequence which has three sulphated tyrosine, a mucin-like macroglycopeptide region which contains two cysteines that bind GPIbα and GPIbβ together via disulphide bonds and finally a 96 amino acid long cytoplasmic tail (Dong et al., 2001, Luo et al., 2007). The association of GPIbα with A1-VWF (Figure 1.2B) results in the characteristic tethering of platelets from circulation at the site of vascular damage under high-shear stress conditions. GPIbα also contains the binding sites MAC-1, thrombin, P-selectin, Factor XII and high molecular weight kininogen (Berndt et al., 2001).

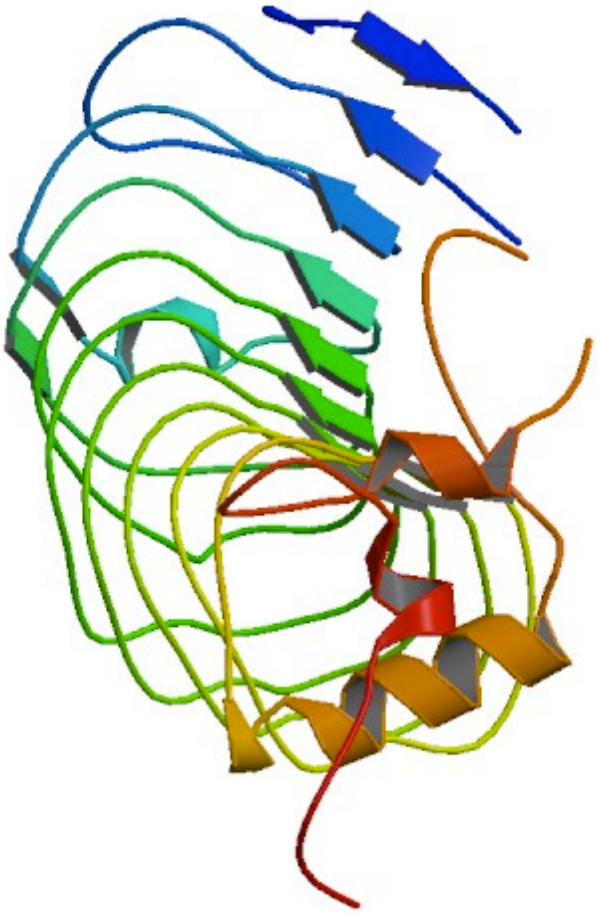

Figure 1.2 Crystal structure of the von Willebrand Factor binding domain of glycoprotein Ib alpha. Protein chains are colored from the N-terminal to the C-terminal using a rainbow colour gradient (Huizinga et al., 2002, RCSB Protein Data Bank 10.2210/pdb1m0z/pdb).

1.3.2 Platelet integrin αIIbβ3

Platelet integrin αIIbβ3 is the most abundant platelet receptor consisting of approximately 50,000 - 80,000 copies per platelet (Wagner et al., 1996). The structure of αIIbβ3 consists of αIIb and β3 subunits that are non-covalently associated, with one membrane-spanning region bound to a short cytoplasmic tail consisting of 20 and 40 amino acid residues, respectively. The αIIbβ3 heterodimer consists of an N-terminal globular head containing the ligand binding region and 2 C-terminal rod-like tails containing the cytoplasmic domain (Hato et al., 2002). Integrin αIIbβ3 plays an essential role in regulating platelet adhesion to VWF and is critical for platelet aggregation and thrombus formation (Nesbitt et al., 2002). In its inactive state, αIIbβ3 has a poor binding affinity for VWF and fibrinogen. Integrin αIIbβ3 can be activated via agonist-induced stimulation such as adenosine diphosphate (ADP), thrombin or engagement of the GPIb-IX-V complex with VWF or GPVI with collagen, which results in inside-out signaling, ultimately resulting in conformational changes in the structure of αIIbβ3 (Ma et al., 2007).

A critical pathway for inside-out activation of αIIbβ3 occurs as cleaved thrombin binds to the protease-activated receptor 1 (PAR1) which is found on the plasma membrane of platelets. Phospholipid hydrolysis occurs at the site of thrombin binding, resulting in inositol trisphosphate (IP3) and diacylglycerol (DAG) generation, increasing cytosolic free Ca^{2+}. Calcium-dependent guanine nucleotide exchange factor CALDAG-GEFl and protein kinase C (PKC) are activated with the increased concentration of Ca^{2+} and DAG, leading to the conversion of Ras-related protein 1 (RAP1) from a GDP to a GTP-bound form. The activation of RAP1 recruits Rap1-GTP-interacting adaptor molecule (RIAM) and talin 1 (binding partner of RIAM) to the plasma membrane. Talin 1 interacts with the αIIbβ3 integrin β3 tail resulting in activation of the integrin (Shattil et al., 2010, Mehrbod et al., 2013). Conformational changes occur such as dissociation of the α and β tail of the integrin rendering the αIIbβ3 competent to bind its ligands such as fibrinogen. A study utilising monoclonal antibodies (monovalent Fab' fragment) directed against αIIbβ3 demonstrated that during activation of platelets with thrombin that there was an increased surface

expression of αIIbβ3 epitopes. These epitopes were functional and could bind fibrinogen mediating platelet aggregation (Niiya et al., 1987). Increased surface expression of αIIbβ3 has been positively associated with increased platelet aggregation in healthy volunteers and those with acute coronary syndrome (Yakushkin et al., 2011). Integrin αIIbβ3 not only has a role in platelet aggregation but also provides stable adhesion upon interaction with VWF.

1.4 Von Willebrand Factor (VWF)

Von Willebrand Factor (VWF) is a multimeric blood plasma glycoprotein which acts as a bridging molecule between the sub-endothelial matrix and platelets. VWF's major role is to regulate the initial platelet interactions with vascular proteins such as collagen and to facilitate platelet aggregation and spreading on exposed vascular surfaces. VWF is produced in the endothelial cells and stored in Weibel-Palade bodies, platelet alpha-granules and is found in the extracellular matrix (ECM) (Ruggeri and Ware, 1992, Siedlecki et al., 1996). The VWF that is released from the Weibel-Palade bodies consists of ultra-large structures that are highly-thrombogenic (Ruggeri, 2007, Wagner, 1993, Fernandez et al., 1982). These highly thrombogenic ultra-large VWF structures are regulated by a disintegrin and metalloproteinase with thrombospondin motif (ADAMTS-13). ADAMTS-13 cleaves the VWF at Tyr1605/Met1606 within the A2 domain of VWF breaking the VWF down into smaller, less-thrombogenic structures (Michelson, 2007, Dong et al., 2002). ADAMTS-13 cleavage is of key importance and has to be highly controlled. Deficiency of ADAMTS-13, results in the production of abnormally-large VWF multimers which cause excessive platelet aggregation *in vivo* (Furlan et al., 1997). The VWF found in the platelet alpha-granules is only released upon platelet activation and enhances platelet aggregation at the site of vascular injury (Michelson, 2007, Kulkarni et al., 2000).

In vivo, VWF forms multimers via disulfide-linked bonds and can reach sizes up to 20,000 kDa. VWF has binding sites for platelet receptor glycoprotein (GP) Ib, αIIbβ3, fibrin and factor VIII (Yuan et al., 2012, Sadler, 1998). VWF circulates in the plasma typically at a concentration of 10 µg/mL and only binds to platelets in its elongated,

active conformation. VWF's transition from a globular, inactive state to an active conformation occurs upon exposure to vascular collagen and or shear stress (Ruggeri and Mendolicchio, 2007, Lenting et al., 2010). A study utilising microfluidic flow chambers to monitor VWF response to varying hemodynamic shear rates showed that the VWF at low shear rates (10-1000 s^{-1}) remained in its closed globular configuration. However, at higher shear rates (5000 s^{-1}) VWF adopts an open elongated configuration. This process is reversible in the absence of any vascular surface such that the closed globular structure reformed once the shear rate decreased below the critical threshold (Schneider et al., 2007). VWF can also be converted to its active conformation *in vitro* using non-physiological modulators like botrocetin, a C-type snake venom lectin (Fukuda et al., 2005) or ristocetin an antibiotic from the bacterial host *Amycolatopsis lurida* (Dong et al., 2001).

1.4.1 The structure of VWF

VWF is encoded on the short arm of chromosome 12 and is approximately 178 kilo-bases in length with 52 exons (Mancuso et al., 1989). Expression of the VWF gene is confined to megakaryocytes and endothelial cells (Ruggeri and Ware, 1993). VWF in its mature form consists of approximately 2050 amino acids (275 kDa) spanning the molecular domains D'-D3-A1-A2-A3-D4-B1-B2-B3-C1-C2 (Michelson, 2007) (Figure 1.3A). However, more recently Zhou et al., (2012) challenged this theory and re-annotated the molecular domains within VWF (Figure 1.3B). Each monomer of VWF contains 10 O-linked and 12 N-linked oligosaccharide chains (Titani et al., 1986). VWF also contains a high content of cysteine residues, which play an important role in linking the VWF subunits together, forming higher-order structures of VWF. Disulfide bonds exist within mature VWF, which comprises of an amino terminal (residues 283-695) with 30 cysteine residues and a carboxyl-terminal (residues 1908-2050) with 18 cysteine residues. Dimers are formed via association of VWF monomers within the carboxyl terminal regions, linked by disulfide bridges (Marti et al., 1987, Ruggeri and Ware, 1993). These dimers then form multimers as disulfide bridges are formed at the amino terminal of the D3 domain (Mendolicchio and Ruggeri, 2005).

VWF is produced in the endothelial cells and dimerizes in the endoplasmic reticulum through disulfide bonds between C-terminal CK domains. This leads to the formation of “tail-to-tail” proVWF which multimerize in the Golgi apparatus. This occurs via furin, which cleaves the propeptide between the D1D2 domains resulting in “head-to-head” disulfide bonds between D3 domains. The end product is a VWF multimer that is stored in highly compact tubules forming the Weibel–Palade bodies (Huang et al., 2008). The VWF multimers present in the storage granules are ready for release via the action of von Willebrand Factor polypeptide (VWFpp). The role of VWFpp is vital for multimerisation and intracellular storage of the mature von Willebrand factor and in its absence VWF multimers are not stored (Haberichter et al., 2002). The different functional domains on VWF have specific roles. These include FVIII, bound by the D’ region of VWF. The three A-domains (A1, A2 and A3) within VWF are responsible for platelet-VWF mediated adhesion to the exposed ECM. The A1 domain contains the binding region for GPIbα on the surface of the platelet, facilitating initial platelet interactions with exposed ECM protein. The A1 domain also has binding sites for heparin and collagen. The A2 domain is a target for cleavage by ADAMTS13 and the A3 binds to collagen enabling platelet integrin to interact with the Arg-Gly-Asp (RGD) of the C1 domain of VWF (Mendolicchio and Ruggeri, 2005).

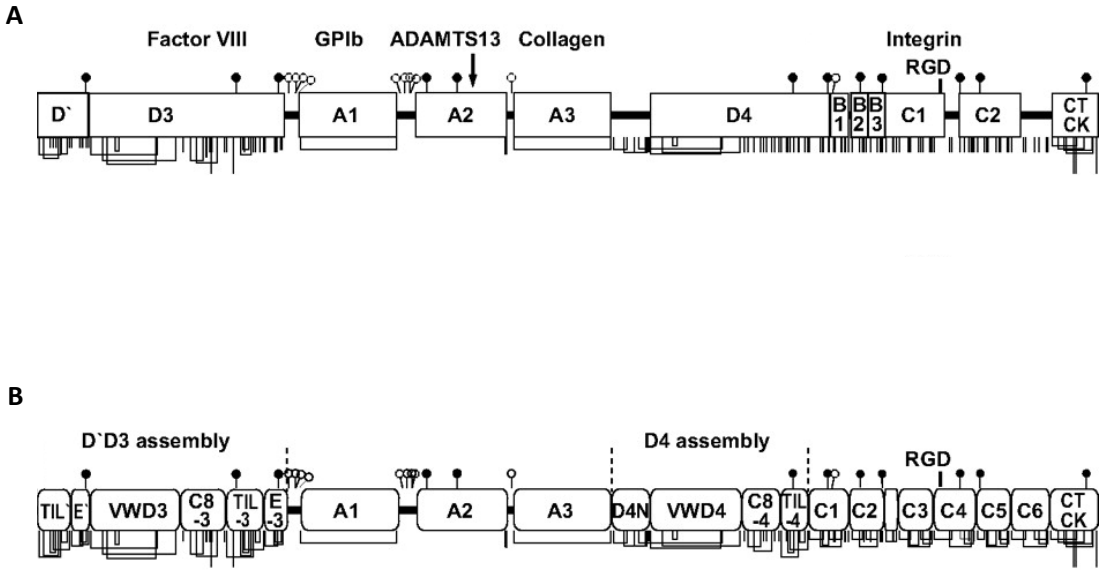

Figure 1.3 The mature structure of VWF. (A) Image showing commonly used domain assignment in the literature, the mature VWF (2050 amino acids) subunit that contains recognition sites for FVIII, collagen, GPIbα, ADAMTS13 and integrin αIIbβ3. (B) Re-annotated domain assignment by Zhou et al, 2012. (Adapted from Zhou et al, 2012).

1.5 Platelet adhesion to immobilised VWF under arterial shear conditions

VWF circulates in plasma and upon vascular damage collagen fibres are exposed to the flowing blood. VWF binds to this exposed collagen mainly via VWF's A3 domain but also via the A1 domain (Cruz et al., 1995, Lankhof et al., 1996, Morales et al., 2006). The immobilisation of VWF to collagen, in addition to shear stress at the wall of the vessel causes a conformational change in the structure of VWF. The VWF adopts its open elongated form, exposing the protected A1 domain to flowing blood (Watson, 2009, Ruggeri and Mendolicchio, 2007, Ulrichts et al., 2006). The A1 domain of VWF is subsequently recognised by the platelet receptor complex glycoprotein (GP) Ib-IX-V (GPIbα). This interaction between the platelet and VWF has a fast 'on-rate' association, which is ideal for platelet capture under arterial shear conditions (Doggett et al., 2002). Circulating platelets in plasma are tethered to the VWF following platelet interactions with the exposed A1 domain of VWF. This initial GPIbα-A1-VWF interaction can result in the formation of membrane platelet tethers (smooth cylinders of lipid bilayer) that are influenced by the haemodynamic drag of RBCs (Jackson, 2007). An increase in shear rate results in a significant elongation of the platelet tethers. Platelet tether formations are unlikely to play a significant role under venous shear conditions, as the number of platelet tethers formed at lower shear conditions is minor compared to those at arterial shear conditions (Dopheide et al., 2002). However, under arterial shear it appears that platelet tethers play a pivitol role in supporting platelet matrix interactions and platelet-platelet adhesion that is primarily mediated through GPIbα-A1-VWF interactions (Reininger et al., 2006, Jackson, 2007). Platelets translocate (stop start motion of the platelet) as GPIbα-A1-VWF bonds are formed and broken on the damaged endothelial surface. Platelet engagement with VWF induces downstream signaling events, which result in remodeling of the platelet cytoskeleton and shape changes from disc-shaped cells to irregular-shaped spheres (Yuan et al., 1999). This shape change is optimal for platelet rolling and is associated with increased platelet rolling velocities (Maxwell et al., 2006). Platelet translocation eventually slows the platelet, allowing engagement of platelet receptors with a slow 'on-rate' association (such as GPVI) to interact with collagen. The result is signalling events which activate the platelet integrins α2β1 and αIIbβ3.

Another mechanism of platelet integrin αIIbβ3 activation was recently described by Zhang et al., (2014). Zhang and colleagues demonstrated that the VWF-A1 association with platelet GPIbα under shear stress results in the unfolding of a hitherto-unidentified structural domain between the macroglycopeptide region and the transmembrane helix (juxtamembrane stalk region) of the GPIbα subunit. This region is the mechano-sensitive domain (MSD), which unfolds under shear stress, resulting in a change in conformation of the neighbouring GPIbβ and GPIX. This change in conformation causes transmission of a signal across the cell that can eventually result in activation of platelet integrin αIIbβ3. The activation of αIIbβ3 promotes stable platelet adhesion and aggregation at the site of vascular damage (Watson, 2009). A schematic representation illustrating selective adhesion of platelets to immobilised VWF is shown in Figure 1.4.

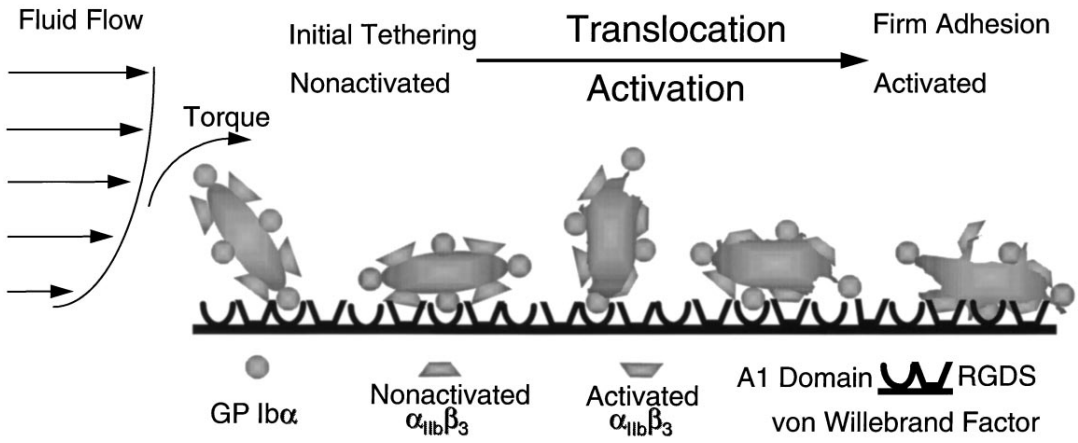

Figure 1.4 Platelet interactions with immobilised VWF. Circulating platelets tether to immobilised VWF via GPIbα-A1-VWF interaction. The haemodynamic forces of blood flow (torque) break the initial GPIbα-A1-VWF bond causing the platelet to move into a rolling state. New bonds are formed and broken between the GPIbα-A1-VWF resulting in the stop start motion of the platelet, referred to as platelet translocation. Platelet translocation continues until αIIbβ3 is activated and binds to the RGDS sequence in the C1 carboxyl terminal domain of VWF. The result is firm adhesion of the platelet to VWF. (Adapted from Ruggeri, 1997).

1.6 Regulation of the VWF-GPIbα interaction

The structural and biophysical basis of the interaction between VWF-GPIbα *in vivo* and how it is regulated is currently unclear. It has been shown that the D'D3 amino terminal of VWF can play a protective role in shielding the A1 domain of VWF from GPIbα when VWF is found in its inactive state (Madabhushi et al., 2012, Ulrichts et al., 2006). Ulrichts et al., (2006) reported that the D'D3 amino terminal limits the A1 domain's accessibility to GPIbα, due to its close proximity to the A1 domain of VWF. Following VWF immobilisation to collagen, the A1 domain of VWF is free to bind to GPIbα. Experimental evidence has shown the cleavage of the D'D3 amino terminal sequence of VWF results in a VWF-GPIbα interaction. Subsequent addition of an isolated D'D3 fragment to the cleaved VWF was demonstrated to inhibit this VWF-GPIbα interaction. The A2 domain of VWF can also shield the VWF-A1 from GPIbα. Although direct binding of A2 to A1 domain within full length VWF has not been demonstrated to date, the use of a recombinant polypeptide against the A2 domain was shown to effectively block the interaction of VWF with GPIbα under high flow conditions (Martin et al., 2007).

The A1A2A3 tri-domain of VWF has a protective role in preventing spontaneous binding of GPIbα to VWF. The A1A2A3 tri-domain contains the functional regions for platelet adhesion; A1 interacts with GPIbα, A2 is the site of ADAMTS-13 cleavage and A3 recognises vascular collagen. The tri-domain (amino acids 1238-1874) fragments of VWF can be synthesised *in vitro*. These fragments have similar characteristics to full-length VWF *in vivo*, making them suitable for studying the regulatory mechanisms of VWF activation. Analysis of A1A2A3 tri-domain recombinant proteins demonstrate that the stability of the VWF-A1 is linked to the interactions between the A domains. Termination of A1A2A3 association, results in a conformational change to the A1 domain, promoting platelet activation and thrombus formation (Auton et al., 2010). Arterial shear flow studies with fibrinogen confirm that intact tri-domain A1A2A3 inhibits the ability of platelets to bind to fibrinogen. Truncating this sequence reverses the above process. Finally, the association of the A1A2A3 tri-domain complex has an auto-inhibitory role in protecting the A1 domain of VWF, thus preventing spontaneous binding of VWF to circulating platelets in flow under

normal conditions in the absence of vascular damage or plaque rupture (Auton et al., 2012).

The N-terminal flanking region of the A1 domain, the amino acid sequence 1238-1260, located outside the disulphide loop, can regulate GPIbα binding. Studies using 1238 and 1261-A1A2A3 VWF fragments, show that deletion of amino acid residues 1238-1260 can alter the stability of the A1 of the tri-domain complex. Using thermal unfolding (e.g. applying heat to denature proteins), it has been shown that deletion of this amino acid sequence (1238-1260) resulted in enhanced binding to GPIbα (Auton et al., 2012). Nowak et al., (2012) highlighted the importance of the N-terminal flanking region by examining the effect of *O*-linked glycosylation of VWF, where oligosaccharide chains are linked via the hydroxyl groups of Serine or Threonine residues. The absence of *O*-linked glycosylation on VWF, under static conditions (mediated by enzymatic cleavage), allowed VWF to adopt a more tightly-folded conformation protecting the A1 domain from GPIbα. However, under shear stress it was found that removal of *O*-linked glycosylation (which occurs around the 1238-1260 amino sequence between the D3 and A1 domains) resulted in VWF unfolding, enhancing its ability to bind collagen. Therefore, glycosylation affects the accessibility of the A1 domain within the VWF, particularly between the D3 and A1 regions (1238-1260). These actions protect the A1 from the platelet GPIbα rather than having a direct effect on the VWF-A1 GPIbα bond. *O*-linked glycosylation enhances and protects the stability of the 1238-1260 amino acid residue sequence by providing rigidity to the amino backbone and preventing unwanted platelet-VWF interactions under normal circulatory conditions (Nowak et al., 2012).

The VWF-A1 N-terminal flanking region (1238-1260) regulates the VWF-GPIbα interaction by impeding the interaction at low force, but providing stabilisation as force increases (Ju et al., 2013). The initial interaction of VWF-GPIbα behaves as a biphasic mechanism such that bond lifetimes are initially prolonged then shortened as force increases (Yago et al., 2008). Increased bond lifetimes result in the force deceleration (catch bonds) of the platelet and decreased bond lifetimes result in force acceleration (slip bonds) of the platelet, as the GPIbα dissociates from VWF (Ju

et al., 2013). Catch and slip bonds can be defined as bond lifetimes that initially increase (catch bond) then decrease (slip bond) with applied force. These catch and slip mechanisms are not just unique to platelets, and have been shown to play a role in selectin-ligand bonds that mediate rolling and tethering of leukocytes on vascular surfaces (Marshall et al., 2003, Lou et al., 2006).

Kim et al., (2010) examined GPIbα dissociation from VWF at low forces (10pN) using optical tweezers (OT). The study highlighted that when using A1-VWF constructs (1261-A1) at low forces, GPIbα could flex between two slip bond states known as a flex bond. One state in low force was followed by a second state with higher force with a 20-fold greater lifetime. OT utilises infrared laser light to manipulate individual molecules within cells and therefore, make them suitable for investigating GPIbα-VWF interactions (Block, 1992). Ju et al., (2013) examined how GPIbα dissociates from VWF in a construct containing the N-terminal flanking region (1238-A1) in order to elucidate its mechanism. Firstly, using a bio-membrane force probe (BFP), Ju and colleagues showed that sequence lengths of VWF could influence the GPIbα dissociation behaviour from VWF. A BFP was used as it is very sensitive technique for measuring single molecular bonds (Gourier, 2008). BFPs are very versatile and can be used with a wide range of forces (0.1 pN to 1 nN). This is because the stiffness of the force sensor allows the end-user to set the force measurements at will (Merkel et al., 1999). Ju et al., (2013) used the BFP to show that full-length VWF formed catch-slip bonds, 1238-A1 constructs formed slip-catch-slip and 1261-A1 constructs formed slip bonds only. Ju and colleagues observed when using low forces (< 15 pN), the same flex bond in the 1261-A1 constructs which were originally described by Kim et al., (2010). Another study ustilising Atomic Force Microscopy (AFM), Yago et al., (2008) did not reach similar conclusions.

Ju et al., (2013) using flow chambers coated with VWF, identified that bond lifetimes regulate platelet-rolling velocities. Slower rolling velocities were associated with longer bond lifetimes and *vice versa*. Catch bonds have stronger bond lifetimes than slip bonds and this suggests that catch bonds regulate flow-enhanced rolling on VWF. Platelet rolling velocities on full-length and VWF-A1 constructs were shown to

be governed by their respective catch/slip bond dissociation behaviours of GPIbα from VWF (Yago et al., 2008, Yago et al., 2004, Ju et al., 2013). Ju and colleagues demonstrated that the N-terminal flanking terminal region present in the 1238-A1 constructs formed slip/catch/slip bonds but not in the 1261-A1, where slip only bonds were observed. Thus, the N-terminal flanking region controls platelet rolling and stability of VWF-GPIbα dissociation to increasing force. The addition of soluble Q1238-E1260 (contains N-terminal flanking region) could successfully rescue the catch bond in 1261-A1 constructs but resulted in a reduction in GPIbα binding lifetimes with VWF and 1238-A1 constructs.

1.7 Platelet function assays

There are a number of platelet function tests available for clinical use. While these tests are useful there are several major drawbacks with most of these tests, these include the volume of blood used, technical difficulties, the fact that a single agonist is used at a maximal concentration and significantly that most of these assays do not assess platelet function in a manner that occurs in the arterial system.

Current platelet function tests measure blood clotting time (PFA-100 analyser), platelet aggregation (Light Transmission Aggregometry, Whole Blood Aggregometry, VerifyNow®, Plateletworks™) and platelet adhesion (Impact Cone and Plate(let) Analyzer).

1.7.1 Platelet Function Analyser (PFA-100)

The Platelet Function Analyser measures time-to clot-occlusion. It is microprocessor-controlled and has disposable test cartridges coated with either collagen and epinephrine (CEPI) or collagen and ADP (CAPD). The PFA-100 uses citrated whole blood that is aspirated through the device under high shear conditions (5000 to 6000 s^{-1}) (Harrison and Lordkipanidze, 2013). Platelets interact with the CEPI or CAPD-coated surface which results in adhesion, activation and aggregation of platelets. The time taken for platelets to occlude the aperture is measured and reported as the closure time (CT) (Kundu et al., 1995). This device is advantageous as it is simple, rapid and does not require specialised training (Harrison and Lordkipanidze, 2013).

However, the diagnostic potential of the PFA-100 assay is limited due to its insensitivity in detecting mild platelet bleeding tendencies (Hajdenberg, 2004).

1.7.2 Light transmission aggregometry (LTA)

LTA measures platelet aggregation in platelet-rich plasma (PRP) induced by agonists such as ADP, arachidonic acid, epinephrine and collagen. Platelet poor plasma (PPP) is used to calibrate the system. The PPP represents 100 percent aggregation. The PRP prior to aggregation causes light scattering. Upon addition of agonists to the stirred PRP, platelets become activated and aggregate, reducing light scattering and increasing the light transmitted. The amount of aggregation is therefore directly proportional to the amount of transmitted light (Born, 1962). The system offers advantages in terms of being able to test multiple agonists. However, LTA has disadvantages including (i) it is labour intensive, (ii) it requires expertise, (iii) large volumes of blood and (iv) is non-physiological. The diagnostic potential of LTA is limited and is relatively insensitive to pre-existing aggregates or early-phase aggregation (Harrison and Lordkipanidze, 2013, Thompson et al., 1986).

1.7.3 Whole blood aggregometry (WBA)

Improvements to classical LTA to make it more physiological include the use of whole blood aggregometry (WBA), which was first described in the early 1980s (Cardinal and Flower, 1980). WBA uses whole blood rather than PRP to assess platelet aggregation. The assay measures the change of electrical impedance as opposed to light transmission, as measured by LTA. Addition of the agonist to blood causes platelet sticking between two platinum electrodes. Over time, impedance increases as aggregation occurs between the electrodes, hence correlating with the degree of platelet aggregation. Comparative studies of WBA versus LTA gave similar results (Nicholson et al., 1998). WBA eliminates the centrifugation steps needed for LTA, but still requires expertise and is insensitive to small platelet aggregates (< 100 platelets) while being relatively expensive (Harrison and Lordkipanidze, 2013). In recent times, an impedance-based multichannel platelet analyser has become available (Roche Multiplate device). This device has been shown to be comparable with LTA, have similar intra-individual variability but can be performed more rapidly

(Seyfert et al., 2007). The Multiplate device is useful in predicting the risk of early drug-eluting stent thrombosis in those patients with poor responses to clopidogrel (Sibbing et al., 2009).

1.7.4 VerifyNow®

The VerifyNow® is a point of care test that measures whole blood aggregation. Blood drawn in sodium citrate is aspirated into the device; a steel ball mixes lyophilised fibrinogen-coated beads and a single agonist. Platelet aggregation is measured via a detector that measures transmitted light. The device uses a total of 3 separate cartridges to measure $P2Y_{12}$, aspirin and αIIbβ3 inhibition individually. The $P2Y_{12}$ cartridge has two chambers containing the agonists ADP and TRAP. The aspirin cartridge contains arachidonic acid and the αIIbβ3 cartridge contains TRAP. The major advantage of this device is that it uses whole blood and is user-friendly. However, it suffers from a number of drawbacks including that the cartridges are expensive, can only measure a single anti-platelet drug response and has limited sensitivity (Harrison, 2009, Bal Dit Sollier et al., 2010).

1.7.5 Plateletworks™

Plateletworks™ is another point of care test that that uses platelet count to measure platelet aggregation. Whole blood in EDTA is passed through an aperture, which interrupts a constant electrical response, providing an electrical impulse. This electrical impulse is used to provide a baseline platelet count. The platelets are activated within device via agonists such as collagen, arachidonic acid or ADP and platelet count is measured. The difference between the baseline platelet count and platelet count after addition of the agonist is used to determine the degree of platelet aggregation (Hussein et al., 2013). The advantages of this device include that it is user friendly and it has a low sample volume (2 mL of blood per assay). However, the assay is highly time dependent and fails to predict adverse cardiovascular events (Seidel et al., 2011).

1.7.6 The IMPACT [Cone and Plate(let) Analyzer (CPA) technology]

Cone and platelet technology examines platelet adhesion to extracellular matrix (ECM) under defined shear conditions (venous, arterial or pathological shear). The

device gives two result outputs including platelet surface coverage and mean aggregate size (Varon et al., 1997). This technology is now commercially available as the IMPACT platform. It is possible to perform an experiment in 130 μL of blood. The blood is placed in polystyrene wells coated with ECM. An arterial shear rate of 1800 s^{-1} is applied for 2 minutes. Platelet adhesion is assessed, once washing and staining of the plate has occurred. The analysis is performed using image analysis software provided with the system. The system has been shown to be sensitive to aggregation defects in patients with storage pool disease, severe von Willebrand disease and epinephrine response deficiency (Shenkman et al., 2008). However, experience with the system is limited and the test does not reliably predict cardiovascular events (Breet et al., 2010).

1.7.7 Summary of platelet function testing

Platelet function testing has the potential to provide clinical benefit. This is supported in the literature by studies which have demonstrated that high platelet reactivity as measured by platelet function assays is associated with an increased risk of thrombotic events (Brar et al., 2011, Parodi et al., 2011, Bliden et al., 2007). The technical challenge here is to produce tests that can effectively replicate the flow and shear environment that platelets experience *in vivo*. Currently, the only clinically-validated assay of platelet function under high shear conditions is the PFA-100. However, this assay has failed to reliably detect platelet hyperreactivity and thus identify prothrombotic states (Gorog and Fuster, 2013). This thesis will discuss the optimisation and clinical validation of a physiological assay of platelet function under arterial shear conditions.

1.8 The Dynamic Platelet Function Assay (DPFA)

Parallel plate flow chambers have been used over the past three decades and have become indispensible research tools for studying platelet interactions with vascular matrix proteins under defined rheological conditions (Roest et al., 2011). Previously, our research group developed a flow-based assay of platelet function using novel parallel plate flow chambers coated with purified human VWF and custom-designed platelet tracking software (Kent et al., 2010). This assay is termed the “Dynamic

Platelet Function Assay (DPFA)" (described in detail in the methods section of Chapter 2). In brief, blood is pumped through custom-made parallel plate flow chambers with channel dimensions of 50 μm height 2 mm width, coated with VWF under arterial shear (1,500 s^{-1}). Platelet interactions with VWF are recorded using an Andor camera at a frame rate of 30 frames/second. A platelet tracking algorithm is then used to accurately identify individual platelets in each frame of an image sequence of 500 frames (corresponding to the first 16.7 seconds of image acquisition). The platelet algorithm accurately identifies individual platelets in each frame of an image sequence of 500 frames (corresponding to the first 16.7 seconds of image acquisition). The software using an Image Processing Toolkit in MatLab (MATLAB, 2011) detects the size and (x,y) centroid position of each of the platelets in the imaged area against a continuously changing background. Platelet tracks are constructed as each individual platelet's movement is tracked from one frame to the next. A weighted distance matrix is generated between the platelet track's current position and other platelets on the frame that gives preference to platelet movement in the direction of flow over cross-stream movement. Each track is extended by assigning the original platelet to a platelet positioned in the next frame, using a set of rules to the weighted distance matrix. Each platelet in the image sequence is linked using a list of tracks with (x,y) positions and area (A) that relate to each individual platelet's movement. The result is a list of platelet tracks corresponding to the associated positions over time for each platelet in an image sequence. Using this information, we can derive multiple parameters of platelet translocation behaviour (Chapter 2, Table 2.4).

There are some advantages but some limitations to the DPFA. Advantages of the DPFA include:

- Use of whole blood, thereby limiting manipulation of the platelets.
- Low volume blood requirement (< 100 μL)
- Use of a shear environment (1500 s^{-1}), mimicking conditions that platelets experience *in vivo* in the arterial system.

- Ability to measure multiple behaviours of platelets translocating on VWF in real-time.
- Evidence in our laboratory also demonstrates that the assay is sensitive to platelet inhibitors such as aspirin (manuscript in preparation), clopidogrel (manuscript in preparation) and ReoPro (Lincoln et al., 2010).

Limitations of the DPFA include:

- Requires expertise.
- Knowledge of platelet function.
- Labour intensive process.
- Surface only contains immobilised VWF, thereby neglects effects of platelet receptors such as GPVI.

1.9 Thesis aims

The aim of the thesis is to validate, clinically evaluate and enhance the DPFA

In order to achieve this aim, this thesis sets out to:

- Validate and improve the accuracy of the custom-designed platelet tracking software (Chapter 3).
- Determine the biological factors that can influence dynamic platelet adhesion to VWF (Chapter 3)
- Establish a normal reference range for the healthy donor population (Chapter 3)
- Characterise platelet function in adults, neonates, healthy pregnancy and pregnancy with utero-placental disease (Chapter 4,5 & 6).
- Finally, to explore a synthetic surface that has the ability to capture donor VWF from plasma (Chapter 7).

Chapter 2

Materials and methods

2.1 Reagents and buffers

Table 2.1 List of experimental reagents

Reagent	Abbreviation	Source
Bovine Serum Albumin	BSA	Sigma Ireland
von Willebrand Factor	VWF	Prof. Robert Montgomery Milwaukee USA
2'-Deoxy-N6-methyladenosine 3,5-diphosphate diammonium salt	MRS2179	Sigma Ireland
Phosphate Buffered Saline	PBS	Sigma Ireland
Trizma® base	Tris Base	Sigma Ireland
3.2% Trisodium citrate	CIT	Sigma Ireland
Pressure Sensitive Adhesive	PSA	Adhesives Research, Limerick, Ireland
Polymethylmethacrylate	PMMA	Ensinger Plastics, UK
3,3'-Dihexyloxacarbocyanine Iodide	$DIOC_6$	Invitrogen, Carlsbad, CA, USA
Microscope slides (24x50mm)	N/A	VWR Germany
Ethanol	EtOH	Sigma Ireland
19-gauge butterfly needle	N/A	Beckman Dickinson, Oxford UK
Polypropylene syringe	N/A	Beckman Dickinson, Oxford UK
Parallel plate flow devices	N/A	BDI, DCU, Ireland
Bio-compatible platinum-cured silicone tubing	N/A	Thermo Fisher Scientific, Denmark
Platelet Gp Screen kit	N/A	BIOCYTEX, Marseille, France
Dextrose	$C_6H_{12}O_6$	Sigma Ireland
Sodium chloride	NaCl	Sigma Ireland
Sodium bicarbonate	$NaHCO_3$	Sigma Ireland
Potassium chloride	KCl	Sigma Ireland
Potassium dihydrogen phosphate	KH_2PO_4	Sigma Ireland
Magnesium Chloride Hexahydrate	$MgCl_2.6H_20$	Sigma Ireland
Mouse anti-human CD42b	AK2	AbD Serotec USA

Table 2.2 Stock solutions of JNL

	Component	FW	Amount	Dilution	FC
JNL A	60mM Dextrose	180.2	5.4g/500ml	10X	6mM
JNL B	1.3M NaCl	58.44	37.99g/500ml	10X	130mM
	90mM Na Bicarb	84.01	3.78g/500ml	10X	9mM
	100mM Na Citrate (Tribasic,dehydrate)	294.1	14.7g/500ml	10X	10mM
	100mM Tris base	121.14	6.06g/500ml	10X	10mM
	30mM KCl	74.56	1.12g/500ml	10X	3mM
JNL D	8.1mM KH_2PO_4 (monobasic anhydrate)	136.1	0.55g/500ml	10X	0.81mM
JNL E	90mM $MgCl_26H_2O$	203.3	1.83g/100mls	100X	0.9mM

1. JNL A, JNL B, JNL D and JNL E were stored in the fridge at 4^oC.
2. Before use, aliquots of JNL A, JNL B, JNL D and JNL E were taken from the fridge and allowed to come to room temperature (RT).
3. 10 mL of each JNL A/B/D and 1 mL of JNL E were mixed together.
4. 40 mL of deionized water was added to the solution and ACD (38mM citric acid anhydrous, 75mM sodium citrate tribasic dihydrate, 124mM dextrose) was used to pH the solution to 7.4.
6. The JNL solution was made up to 100 mL with deionised water.

2.2 Experimental equipment

Table 2.3 List of experimental equipment

Experimental equipment	**Source**
NEMESYS precision microfluidic syringe pump	Cetoni GmbH, Korbussen, Germany
Sysmex-KX21N haematology analyser	Sysmex Corp., Kobe, Japan
Digital EM-CCD camera (iXON EM+)	Andor Technology, Belfast, Ireland
Zeiss Axiovert-200 epi-fluorescence	Carl Zeiss Microscopy, LLC, United States
BD FACSCanto II	BD Biosciences, San Jose, CA 95121-1807, USA

2.3 Research ethics

Ethical approval for all studies was obtained from the Medical Research Ethics Committees of the Royal College of Surgeons in Ireland, Beaumont Hospital, Rotunda Hospital and National Maternity Hospital, Holles St., Dublin, Ireland (Appendix A). All blood samples were collected in accordance with the declaration of Helsinki. Written informed consent was obtained from all donors prior to phlebotomy. For donors under the age of 18, written, informed consent was provided by parents or guardians.

2.4 Blood collection

Venous blood was drawn from the antecubital vein using a 19-gauge butterfly needle connected to a sterile polypropylene syringe. Blood was drawn into 3.2 % (w/v) trisodium citrate anticoagulant (1:9 volume of citrate to blood, final citrate concentration of 0.32 %). Blood samples were kept at room temperature with gentle rocking and used within 1 hour of phlebotomy. Whole blood cell counts were recorded for each donor, using a Sysmex-KX21N haematology analyser (Sysmex Corp., Kobe, Japan).

2.5 The Dynamic Platelet Function Assay (DPFA)

2.5.1 Assembly of parallel plate flow chambers

The parallel plate flow chambers were made up of 3 parts and assembled (Figure 2.1). Part (A) consisted of a 25 x 55 mm polymethylmethacrylate (PMMA) top plate with inbuilt 1/16-inch polypropylene inlet and outlet attached via epoxy glue. Part (B) comprised of a pressure sensitive adhesive (PSA) layer containing the microfluidic channel of interest that is 50 μM in depth, 2 mm in width and 35 mm in length. Finally part (C) a microscope glass coverslip (24 x 50 mm).

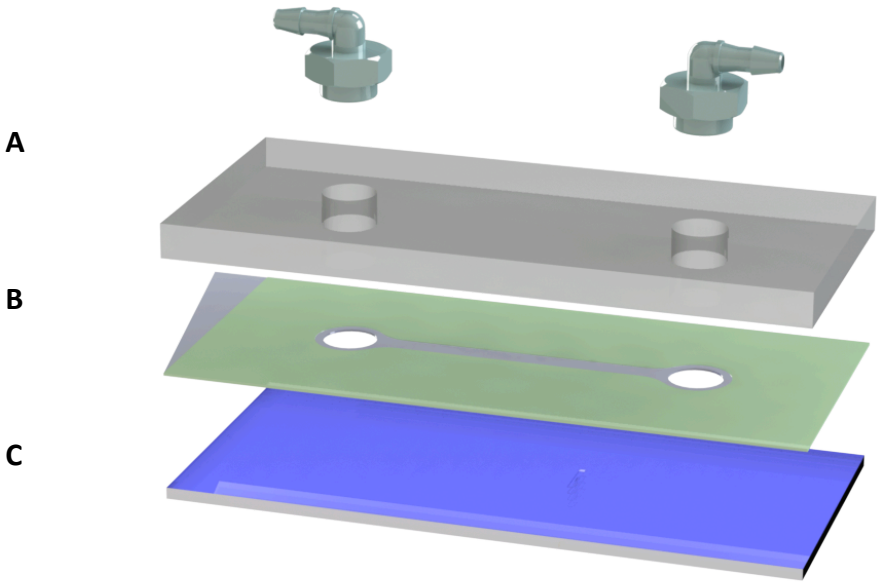

Figure 2.1 Parallel plate flow chamber layers (A) PMMA top layer. (B) Pressure sensitive adhesive containing the microfluidic channel. (C) The coverslip. The assembled flow chamber has channel dimensions of large aspect ratios (50 µm in height 2 mm width).

2.5.2 Preparation of parallel plate flow chamber

The channel of the assembled parallel plate flow chamber was coated with 100 µg/mL of the vascular protein von Willebrand Factor (VWF), that is diluted in phosphate buffered saline (PBS) buffer overnight at 4 °C (Figure 2.2). The channel was then washed 3 times with PBS, blocked with 1 % BSA in PBS for 1 hour at room temperature, followed by a final 3 washes with PBS buffer prior to blood perfusion.

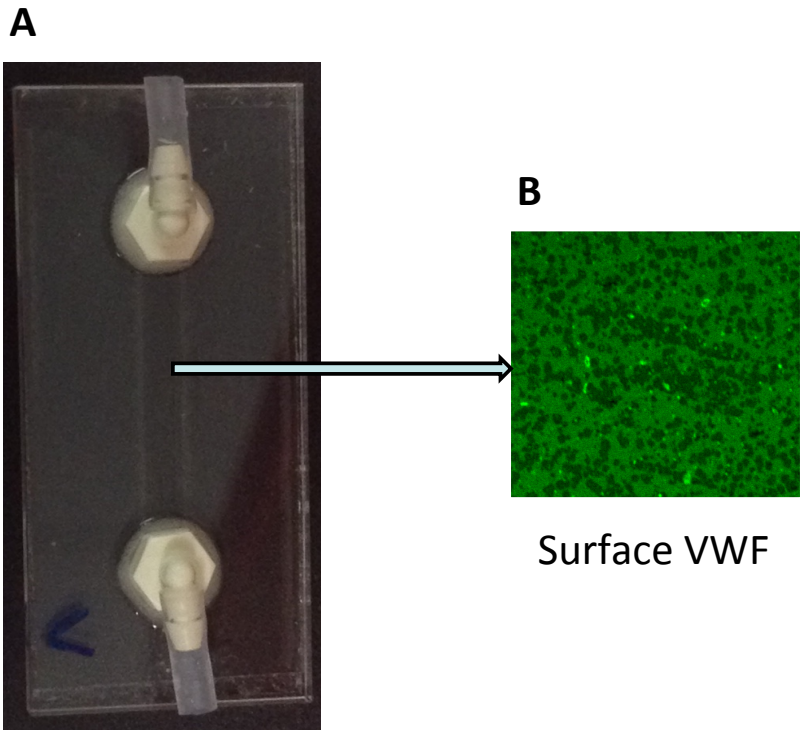

Figure 2.2 Coated channel of parallel plate flow chamber with VWF. (A) Assembled flow chamber (B) Microscope image of the channel coated with VWF, stained with sheep-anti-human fluorescein isothiocyanate (FITC)-labelled anti-VWF antibody.

2.5.3 Labeling of platelets with fluorescent dye

Blood was drawn in 3.2 % trisodium citrate (10 % v/v). 200 µL of blood was aliquoted to an eppendorf. 1 µM 3,3'-dihexyloxacarbocyanine iodide ($DiOC_6$) fluorescent dye was added to the blood. This dye is not specific to platelets but localises to the endoplasmic reticulum and mitochondria of platelets. This dye has been used previously to visualise platelets translocating on VWF (Lincoln et al., 2010, Kent et al., 2010). The dye allowed the platelets to be visualised in real-time. Blood was incubated with the dye for 10 minutes at 37 °C prior to perfusion.

2.5.4 Perfusion of blood and image acquisition in parallel plate flow chamber

The parallel plate flow chambers were mounted on an inverted microscope (Zeiss Axiovert-200 epi-flouresence). A NEMESYS syringe pump was used to draw the blood across the surface of the flow chamber containing the immobilised VWF. The DPFA requires < 100 µL of blood per flow run. A flow rate (Q) of 75 µL/min was used. This flow rate gives an arterial shear rate (γ) of 1,500 s^{-1}, corresponding to a shear stress (τ) of 6 Pa (6 N/m^2) at the wall of the surface where the platelets interact. Images were captured using a vacuum-cooled (-80 °C) digital EM-CCD camera (iXON EM+, Andor Technology, Belfast, Ireland) connected to MetaMorph (version 7.7, Molecular Devices Ltd., UK) illuminated with an Osram 103-W mercury light source and a fluorescein isothiocyanate (FITC) filter set providing excitation and emission at 490 nm and 528 nm, respectively (Chroma Technology Corp, Vermont, USA). A total of 1000 Images were acquired at 30 frames per second using a 63x objective (512 x 512 pixel, 128.768 x 128.768 µm) field of view for visualisation of platelet interactions with the VWF in real time (Figure 2.3).

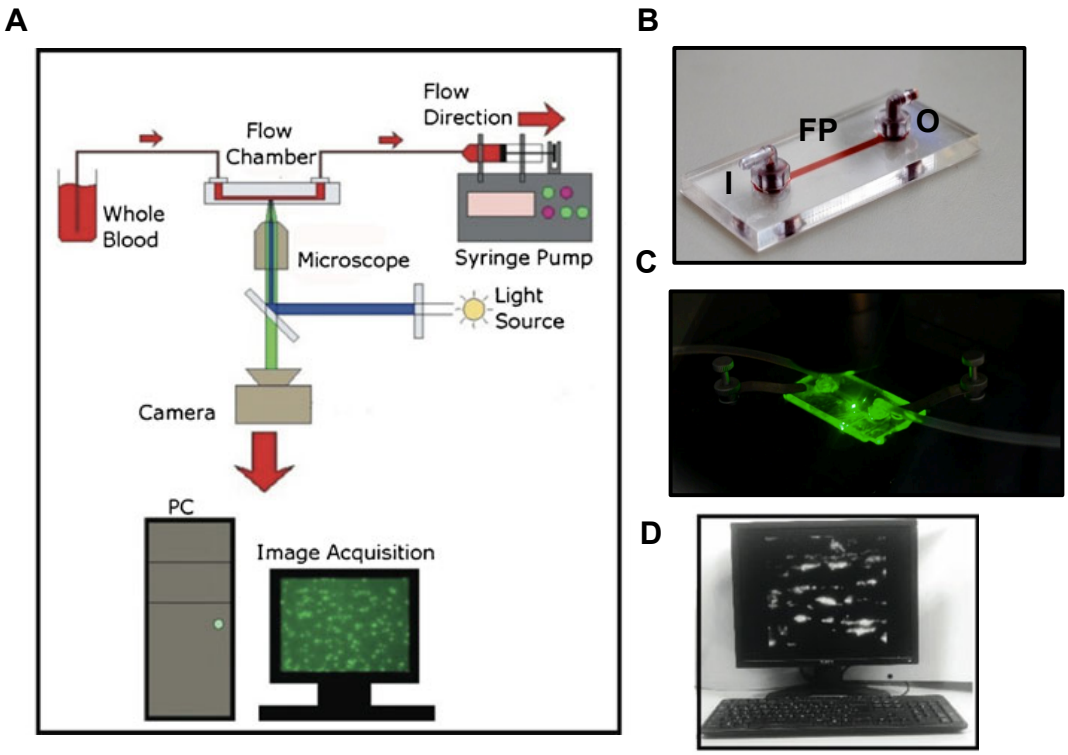

Figure 2.3 The Dynamic Platelet Function Assay (DPFA). (A) Schematic representation of assay system with mounted microfluidic parallel-plate flow chamber illustrating blood perfusion with a syringe pump, Zeiss Axiovert-200 epi-flouresence inverted microscope enclosed in a 37 °C chamber fitted with an Andor camera connected to PC with MetaMorph software for image capture. (B) Parallel plate flow chamber containing an inlet (I), an outlet (O) and 50 µm in height 2 mm width channel which defines the flow path (C) Microfluidic parallel-plate flow chamber mounted in the stage area of the inverted microscope. (D) PC with metamorph software. (Adapted from Lucitt et al., 2013).

2.5.5 Platelet tracking algorithm software

Platelet tracking software was used to track platelet movement on VWF. This software has previously been described Lincoln et al., (2010) and Kent et al., (2010). The original platelet tracking software used a probability function and cut-off based on the typical movement of a platelet on a clutter-free, smooth surface. That is to say, there was a strong preference for platelet movement in a narrow angle in the direction of the flow. However, this approach had errors in its tracking process due to merging and separating of platelet groups and/or movement around obstructions. The main source of mistracking related to platelet fragmentation. Platelet fragmentation occurs where a single platelet track is recorded as a set of smaller tracks. Over the past four years, significant enhancements to this software programme have been undertaken with the help of software engineers, Martin Somers Dublin City University (DCU), and the Irish Centre for High End Computing (ICHEC, Grand Canal Dock, Dublin). These enhancements include a less directional distance weighting method of tracking that allows us to identify those platelets, which are part of a platelet group and to track them as they merge and split from the group. This allows for construction of the full platelet track. The process of the enhanced method of platelet tracking is described in the sections below.

2.5.5.1 Masking of platelet images

Platelets interacting with VWF are imaged using an Andor camera at a frame rate of 30 frames per second. A total of 1000 images are acquired. The first 500 images are assessed using the platelet tracking software. The platelet software accurately identifies the centroid positions of individual platelets in each frame for the image sequence of 500 frames (corresponding to the first 16.7 seconds of image acquisition). The software masks each platelet (Figure 2.4) using an Image Processing Toolkit in MatLab which detects the size and (x,y) centroid position of each of the platelets in the imaged area against a continuously changing background (MATLAB, 2011, Lincoln et al., 2010).

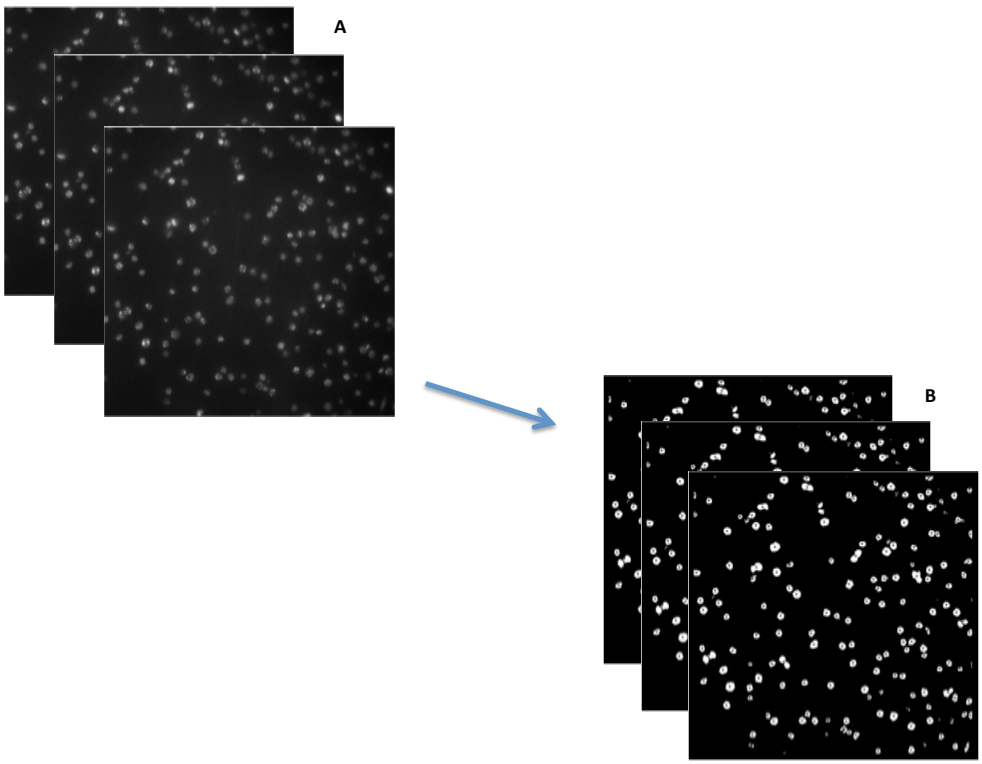

Figure 2.4 Masking of platelet images. (A) Acquired platelet images (B) Masking of platelets captured in (A)

2.5.5.2 Generation of platelet tracks

Once all the platelets on each of the 500 frames are masked, platelet tracks are constructed. The platelet tracks are constructed as each individual platelet's movement is tracked from one frame to the next. A weighted distance matrix is then applied between the platelet track's current position and other platelets on the frame which gives preference to platelet movement in the direction of flow over cross-stream movement. Each track is extended by assigning the original platelet to a platelet positioned in the next frame, using a set of rules to the weighted distance matrix (Appendix B). Each platelet in the image sequence is linked using a list of tracks with (x,y) positions and area (A) that relate to each individual platelet's movement. The result is a list of platelet tracks corresponding to the associated positions over time for each platelet in an image sequence (Figure 2.5). Once all the track sequences have been constructed some are rejected based on two rejection criteria: tracks less than 10 frames or platelet areas less than 3 μm^2. The first action is to remove fragmented tracks and the second action is to remove tracked objects that are too small to be considered platelets.

2.5.5.3 Measured platelet behaviors

The tracked platelet movement is then used to generate a total of six platelet translocation behaviours that relates to the biological activity of platelets on VWF (Table 2.4).

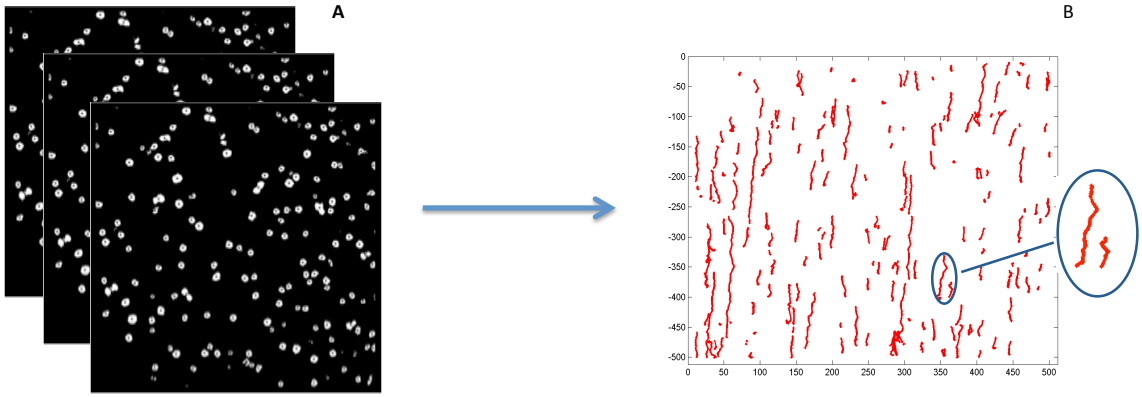

Figure 2.5 Generation of platelet tracks. (A) Masked platelets (B) Worm plot of tracked platelet movement on VWF (red).

Table 2.4 List of measured platelet behaviors

Number	Parameter	Definition
1	Platelet tracks	The number of platelets that interact with VWF
2	Platelet translocation	The number of platelets that travel >1.5 the average radius of the platelet
3	Weighted median speed	The speed a translocating platelet moves in the direction of flow (μm/second)
4	Static platelets	The number of platelets that travel <1.5 the average radius of the platelet
5	Unstable platelet interactions	Platelets that interact with VWF for a period that is greater than 10 frames but less than 490 frames
6	Percentage of platelet surface coverage	Percentage of platelet surface coverage on the final frame (500)

2.5.6 Statistical analysis

In order to address the variability of the assay related to blood condition and experimental error, each donor's blood was run in triplicate (unless otherwise stated) through the DPFA. All runs from each cohort were then analysed, and runs outside the mean ± 2SD were removed before each donor's parameters were averaged over 3 or less eligible runs. This process allows us to detect and remove any extreme outliers in order to determine a normal reference range. A ± 2SD cutoff was chosen as this is a frequently used in determining cutoff values for diagnostic tests (Singh, 2006). The numerical analysis was done with the Prism 5.0a software (GraphPad Software, Inc.). *P* values < 0.05 were considered significant. All graphs in this thesis are presented as mean ± standard error of the mean (mean ± SEM) unless otherwise stated.

2.6 The ideal data set

The ideal data set was developed by software engineers at DCU and ICHEC, in conjunction with the RCSI research group. The data resulting from this validation study is under review in Transactions on Image Processing (Ralph *et al.*, 2015, Appendix B). The ideal data sets contained images with known values of platelet translocation behaviour, in addition to a range of different platelet translocation behaviours that were experienced experimentally. Objects (Figure 2.6) similar to the size of a platelet were placed on each image in the data set. Each object had 'no noise' i.e. an intensity of one and a background of zero. On each start frame (frame 1) 25 objects were placed randomly on the image in the absence of overlapping objects. Each image set contained a known number of ideal tracks (objects) that equaled the final number of objects on the last frame (frame 500). Objects were added at regular intervals on subsequent frames, care was taken to ensure by frame 500 that the expected number of tracks had been achieved. For sets where there was no overlapping of objects a perfect tracking system would identify all object tracks and any deviations in this number would be down to mistracking. A fraction of objects were assigned as translocating (movement greater than 1.5 times the radius of the object). Each of the translocating objects had identical tracks that moved at 100 pixels at 1 pixel/frame before stopping. Static objects had no movement hence

had a translocating distance of zero. The translocating objects moved in the direction of the flow and there was no restriction on merging and separating events of objects after frame 1.

For each of the measured platelet translocation behaviours (minus unstable platelet interactions parameter) (Table 2.4), the values were fixed: final object count (50, 100, 150, 200, 250, 300, 350, 400), the fraction of static platelets (10 %, 20 %, 30 %) and the translocating speed (0.5, 1.0, 1.5 pixels/frame). There were a total of 3 runs per experiment.

In summary, a novel platelet tracking software was designed and verified as accurate. The design was based on a weighted distance matrix using custom-developed idealized data sets, which determined the percentage systematic error for key individual parameters of platelet translocation of biological relevance (discussed in detail in Chapter 3).

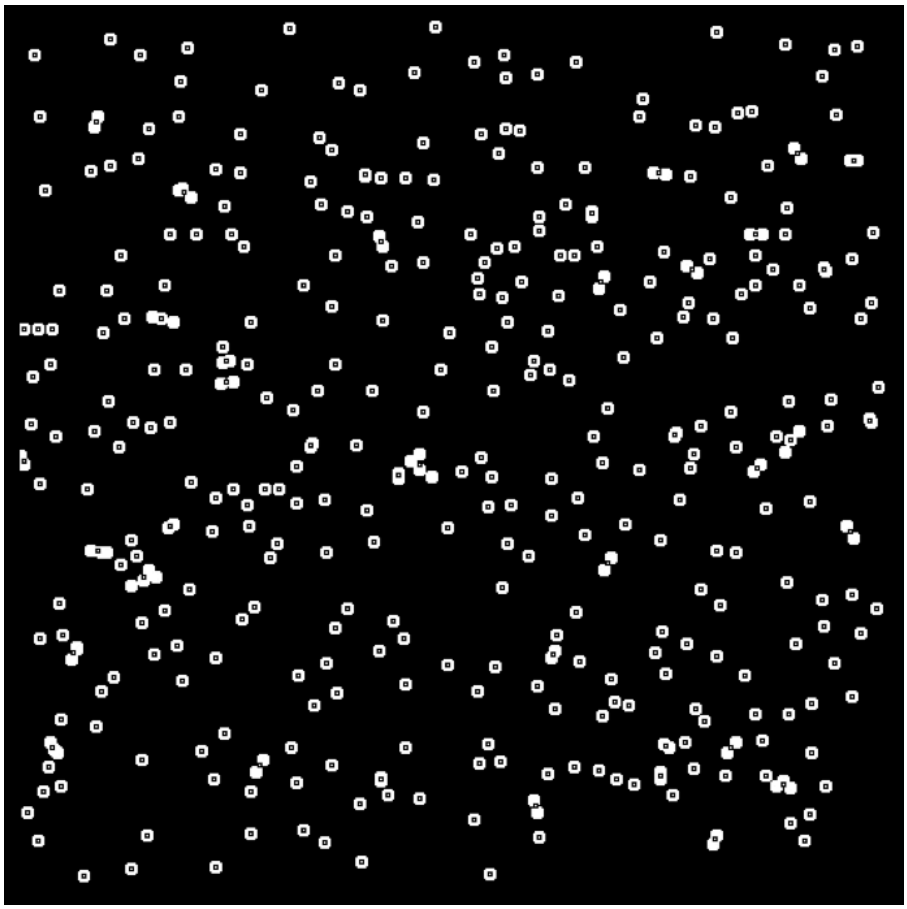

Figure 2.6 The ideal data set with objects mimicking platelet size. An image of a frame generated for the ideal data set with the centroid position of each platelet masked by the platelet tracking software to enable analysis of platelet translocation behaviour.

2.7 Platelet glycoprotein quantitation

The levels of platelet glycoproteins (GpIIIa, GpIb and GpIa) were assessed using a Platelet GP Screen kit (BIOCYTEX, Marseille, France) via flow cytometry, using a BD FACSCanto II (San Jose, CA 95121-1807, USA) with FACSDiva software. A total reaction volume of 60 µL consisted of monoclonal antibody (CD61, CD42b or CD49b), diluted whole blood (1:4) or calibrated bead suspension and florescent stain (anti mouse IgG FITC).

2.7.1 Assay calibration

Firstly the assay was calibrated using a log FSC versus log SSC cytogram to minimise the background noise by drawing a gate around the main single bead population (Figure 2.7A). A histogram (log FL1 versus count) was generated. The fluorescent peaks corresponded to different platelet glycoproteins that were gated and the mean fluorescence intensity (MFI) was recorded (approximate MFI: 1662 CD61, 10858 CD42b and 43039 CD49b) (Figure 2.7B). Approximately 10,000 beads were gated in the window.

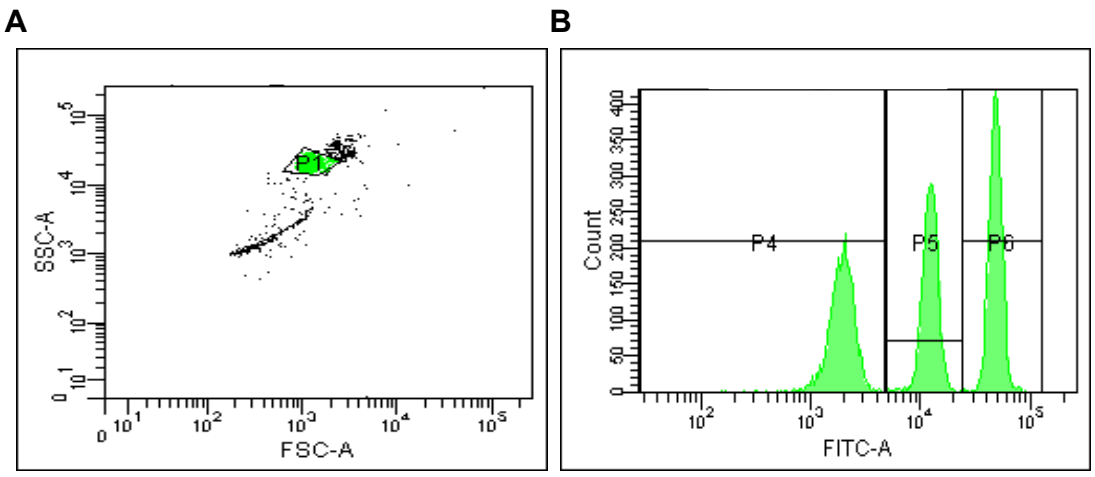

Figure 2.7 Calibration cytogram and gated histogram. (A) FS log versus SS log cytogram. P1 represents the region of calibration beads that were used to calibrate the assay prior to experimentation. (B) Gated fluorescent histogram of calibration beads. P4 measures CD61, P5 measures CD42b and P6 measures CD49b.

2.8.2 Glycoprotein quantification

Sample analysis was performed by generation of a log FSC versus log SSC cytogram and isolating the platelets from other whole blood cells. Each sample was run analysing approximately 10,000 events and the MFI of each peak were recorded (Figure 2.8).

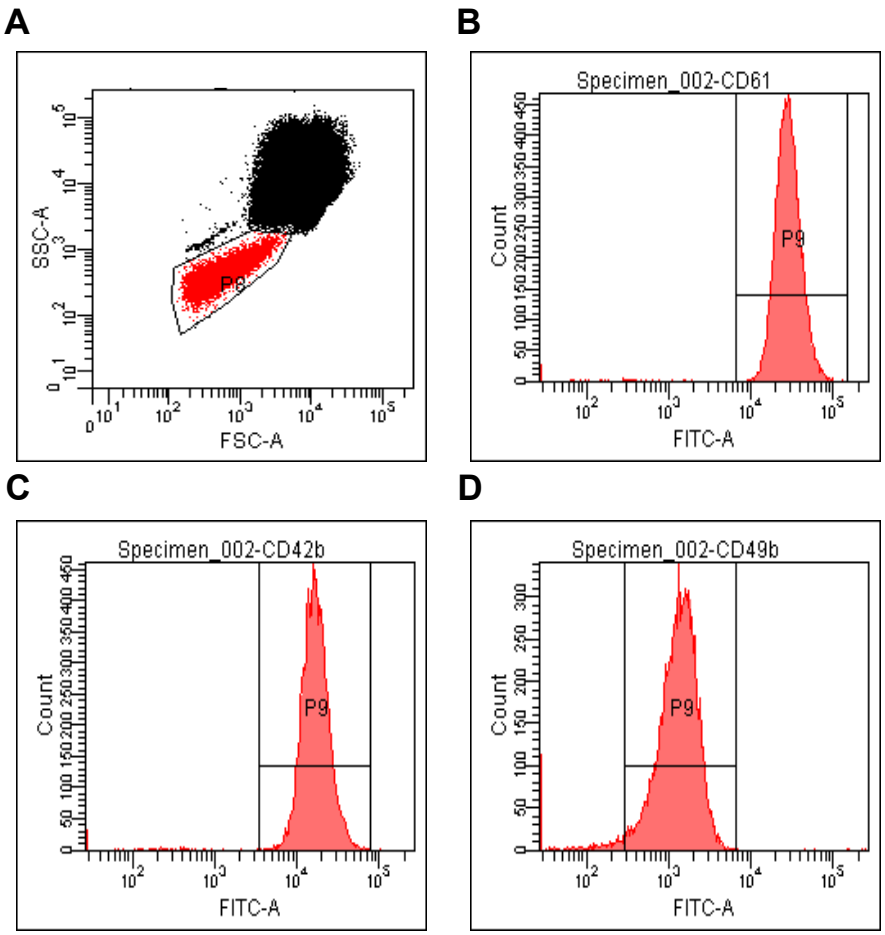

Figure 2.8 Histograms of platelet quantitation. (A) Whole blood cytogram with the platelets gated in red for analysis. (B) Quantification of GpIIIa number. (C) Quantification of GpIb number. (D) Quantification of GpIa number.

2.8.3 Sample analysis

The number of platelet glycoproteins GpIIIa, GpIb and GpIa were determined using a calibration curve by plotting the LOG_{10} of the MFI calibration values for the 3 calibration beads on the x-axis against their corresponding LOG_{10} number of monoclonal antibody molecules on the y-axis. A linear line was drawn through the points and the MFI values calculated for each of the sample tubes were used to interpolate the expression numbers of platelet glycoproteins GpIIIa, GpIb and GpIa from the calibration curve.

2.9 Preparation of polymer surfaces

The University of Ulster's Nanotechnology and Integrated Bioengineering Centre (NIBEC) manufactured the polymer surfaces. The surfaces were developed using a well-known polymer de-mixing technique (Dalby et al., 2002). Two polymers, polystyrene (PS) and polymethylmethacrylate (PMMA) were mixed together in a 50:50 ratio at concentrations of 1 %, 3 % and 5 % (w/v) in chloroform. The polymer mix was then spin coated at 6000 rpm for 60 seconds onto glass coverslips forming different sized nanostructures to enable capture of vWF.

2.9.1 Analysis of polymer surfaces

Blood was perfused over the polymer surfaces at arterial shear 1500 s^{-1} for 5 minutes. An end point image was taken and percentage platelet surface coverage was analysed using MatLab software.

Chapter 3

An assay of dynamic platelet function measuring platelets translocating on VWF

3.1 Introduction

Platelets are crucial in haemostasis but also play a central role in thrombosis. Platelet function testing offers a potential prognostic marker in predicting those who may be of increased risk of cardiovascular events (Tantry et al., 2013). This is supported by platelet function studies which highlight that high platelet reactivity during clopidogrel treatment is associated with an increased risk of post-percutaneous coronary intervention (PCI) thrombotic events (Brar et al., 2011, Parodi et al., 2011). Nevertheless platelet function testing is not routinely performed in clinical practice. The current limitations of platelet function tests include insufficient standardisation (Harrison et al., 2011), a lack of correlation between tests (Sambu and Curzen, 2011) and most importantly, the desire for tests that mimic physiological conditions that platelets experience *in vivo* (Gorog and Fuster, 2013).

During vascular damage, matrix proteins such as collagen are exposed to the flowing blood plasma. Von Willebrand Factor (VWF) binds to this exposed collagen and in doing so, undergoes a conformational change in its structure which facilitates its interaction with circulating platelets in flow (Ruggeri and Mendolicchio, 2007, Ulrichts et al., 2006). Platelets tether to the VWF and platelet translocation (stop/start motion of the platelet) occurs as weak bonds between the VWF and the platelet are formed and broken on the damaged endothelial surface, due to the dynamic forces of the blood. This process results in intracellular signaling which activates the platelet and results in stable platelet adhesion to the damaged surface (Savage et al., 1996, Zhang et al., 2014).

Our research group has previously described a physiological assay of platelet function which measures the movement of platelets on VWF and provides unique insights into the behaviour of platelets *in vivo*, known as the Dynamic Platelet Function Assay (DPFA) (Kent et al., 2010). In brief, the DPFA uses custom-designed parallel plate flow chambers coated with purified human VWF. Whole blood is perfused over the VWF surface under arterial shear conditions (1500 s^{-1}). An Andor camera images platelets as they interact with VWF while a novel platelet tracking software is used to monitor individual platelet movement on VWF. Multiple

parameters of platelet translocation behaviour are derived and are used for the assessment of platelet function in our cohorts of interest. The measured parameters with definitions are shown in the Table 3.1.

Table 3.1 Measured platelet translocation behaviours with definitions

Number	Parameter	Definition
1	Platelet tracks	The number of platelets that interact with VWF
2	Platelet translocation	The number of platelets that travel >1.5 the average radius of the platelet
3	Weighted median speed	The speed a translocating platelet moves in the direction of flow (μm/second)
4	Static platelets	The number of platelets that travel <1.5 the average radius of the platelet
5	Unstable platelet interactions	Platelets that interact with VWF for a period that is greater than 10 frames but less than 490 frames
6	Percentage of platelet surface coverage	Percentage of platelet surface coverage on the final frame (500)

In this chapter, I will discuss:

- How the platelet tracking software (Chapter 2) was validated.
- How platelet count and haematocrit (HCT) influence platelet adhesion to VWF in the DPFA.
- The behaviour of platelets from individual donors assayed repeatedly.
- A normal reference range of platelet function for the assay.

3.2 Results

3.2.1 Validation of the DPFA

3.3.1.1 Validation of platelet tracking software (use of an ideal image set)

The platelet tracking software (Chapter 2) was validated using an ideal image set. The data resulting from this validation study has been submitted for publication (Ralph *et al*., 2015, under review in Transactions on Image Processing, Appendix B). The ideal data sets contained images with known values of platelet translocation behaviour, in addition to a range of different platelet translocation behaviours that were experienced experimentally. The tracking software processed these images and the values generated were compared with the expected values. There were a total of 3 runs per experiment. The ideal data set determined the mean absolute percentage error for 5 of 6 platelet translocation behaviours explored in this thesis. The parameter measuring unstable platelet interactions with VWF was not included, as this parameter was derived post-submission of the manuscript. The results obtained from these experiments are shown in Table 3.2.

Table 3.2 Mean absolute percentage error of measured platelet translocation behaviour versus object count. Increasing object count results in an increase in the mean absolute percentage error.

Platelet behaviour	Mean absolute percentage error							
	Object Count	**50**	**100**	**150**	**200**	**250**	**300**	**350**	**400**
Platelet tracks		0.4	0.7	0.5	0.5	0.8	0.9	1.1	1.6
Platelet translocation		2.1	3.8	8.1	7.6	8.1	13.4	18.3	15.5
Weighted median speed (µm/sec)		0.1	0.1	0.1	0.1	0.1	0.1	0.1	0.1
Static platelets		2.1	3.8	8.1	7.6	8.1	13.4	18.3	15.5
Percentage of platelet surface coverage		5.5	12.0	12.2	12.5	12.2	13.0	13.2	14.1

3.3.1.2 Validation of platelet tracking software (use of a P2Y1 inhibitor)

To further validate the accuracy of the platelet tracking software, a selective $P2Y_1$ inhibitor (MRS2179) was used to assess its effect on platelet translocation behaviour. The $P2Y_1$ receptor has a role in calcium mobilization, platelet shape change (Baurand et al., 2001) and has previously been shown to significantly amplify platelet translocation speeds compared with non-MRS2179-treated controls (Mazzucato et al., 2004). Therefore, blood samples from healthy donors (n=7) were treated with or without 20 µM MRS2179. A significant increase in platelet translocation speed was observed in donors treated with 20 µM MRS2179 compared to non-MRS2179-treated controls (3.1 ± 0.4 µm/sec versus 2.4 ± 0.3 µm/sec; *$p < 0.05$) (Figure 3.1). This demonstrates that the platelet algorithm is sensitive in detecting subtle changes in platelet movement on VWF.

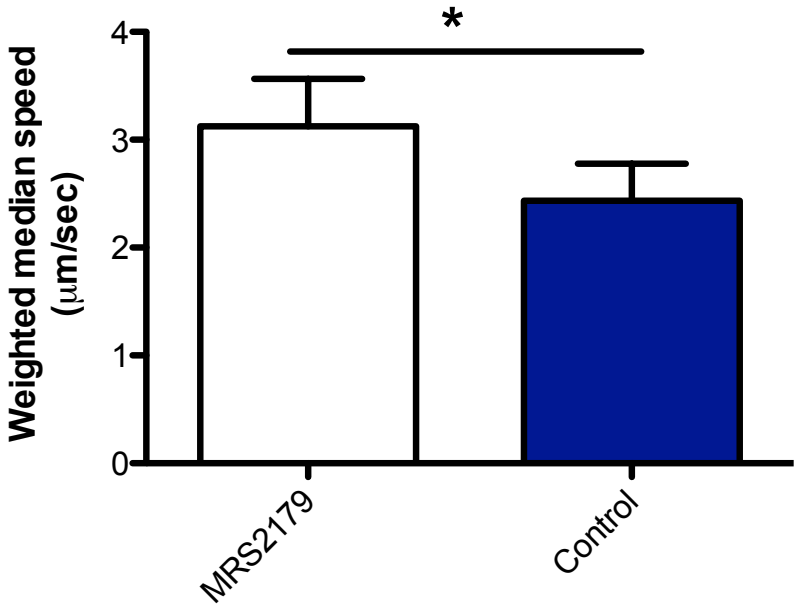

Figure 3.1 $P2Y_1$ inhibition significantly increases platelet translocation speeds on VWF. Blood from 7 healthy donors and treated with 20 μM MRS2179 ($P2Y_1$ inhibitor) for 10 minutes prior to perfusion over VWF at arterial shear. Each donor had a total of 6 runs (3 MRS2179-treated and 3 non-treated controls). Treatment of blood with MRS2179 significantly increased platelet translocation speeds on VWF. A paired student's t test was used to detect statistically significant differences between conditions (*$P < 0.05$). Data is represented as mean ± SEM.

3.2.2 Factors influencing dynamic platelet adhesion

3.2.2.1 Platelet count significantly impacts on platelet adhesion to VWF

Thrombocytopenia in adults has been defined as platelet counts < 150 x 10^3 µL of blood (Gauer and Braun, 2012). To assess the sensitivity of the DPFA to platelet count, blood samples from healthy donors (n=6) with platelet counts within the normal range (150-450 x 10^3 µL of blood) were compared with the same blood samples diluted to platelets counts of < 150 and < 100 x 10^3 µL of blood (Table 3.3). The DPFA data demonstrated that decreasing platelet count resulted in a significant reduction in platelet interaction with VWF (Figure 3.2). Decreasing platelet count resulted in a significant decrease in the number of platelet tracks (273 ± 28 versus 171 ± 8 versus 127 ± 7; slope ***p < 0.0001, R^2 = 0.83) and translocating platelets (208 ± 24 versus 130 ± 5 versus 79 ± 6; slope ***p < 0.0001, R^2 = 0.86). Notably, no significant difference was observed in weighted median speed (3.4 ± 0.6 µm/sec versus 2.9 ± 0.3 µm/sec versus 3.9 ± 0.7 µm/sec, R^2 = 0.02) or in the number of static platelets (53 ± 6 versus 45 ± 6 versus 41 ± 7, R^2 = 0.09). However, the number of unstable platelet interactions (460 ± 18 versus 236 ± 13 versus 173 ± 10; slope ***p < 0.0001, R^2 = 0.71) and the percentage of platelet surface coverage (6.7 ± 0.3 % versus 5.9 ± 0.4 % versus 5.0 ± 0.4 %; slope ***p < 0.0001, R^2 = 0.43) were significantly decreased upon lowering platelet count.

Table 3.3 Significant reductions in platelet count. Platelet counts were significantly reduced (***P < 0.0001, one-way ANOVA) per experiment by diluting platelet counts in JNL buffer and reconstituting back into red blood cells (RBCs). There was no significant difference in blood HCT. All data is represented as mean ± SD.

Healthy normals (N=6)	>150 x 10^3 /µL platelets	<150 x 10^3 µL platelets	<100 x 10^3 µL platelets	P value
Platelet count (x10^3/µl)	199 ± 38	115 ± 12	85 ± 7	**<0.0001*** **
% Hematocrit	36 ± 2	36 ± 2	35 ± 2	0.5705

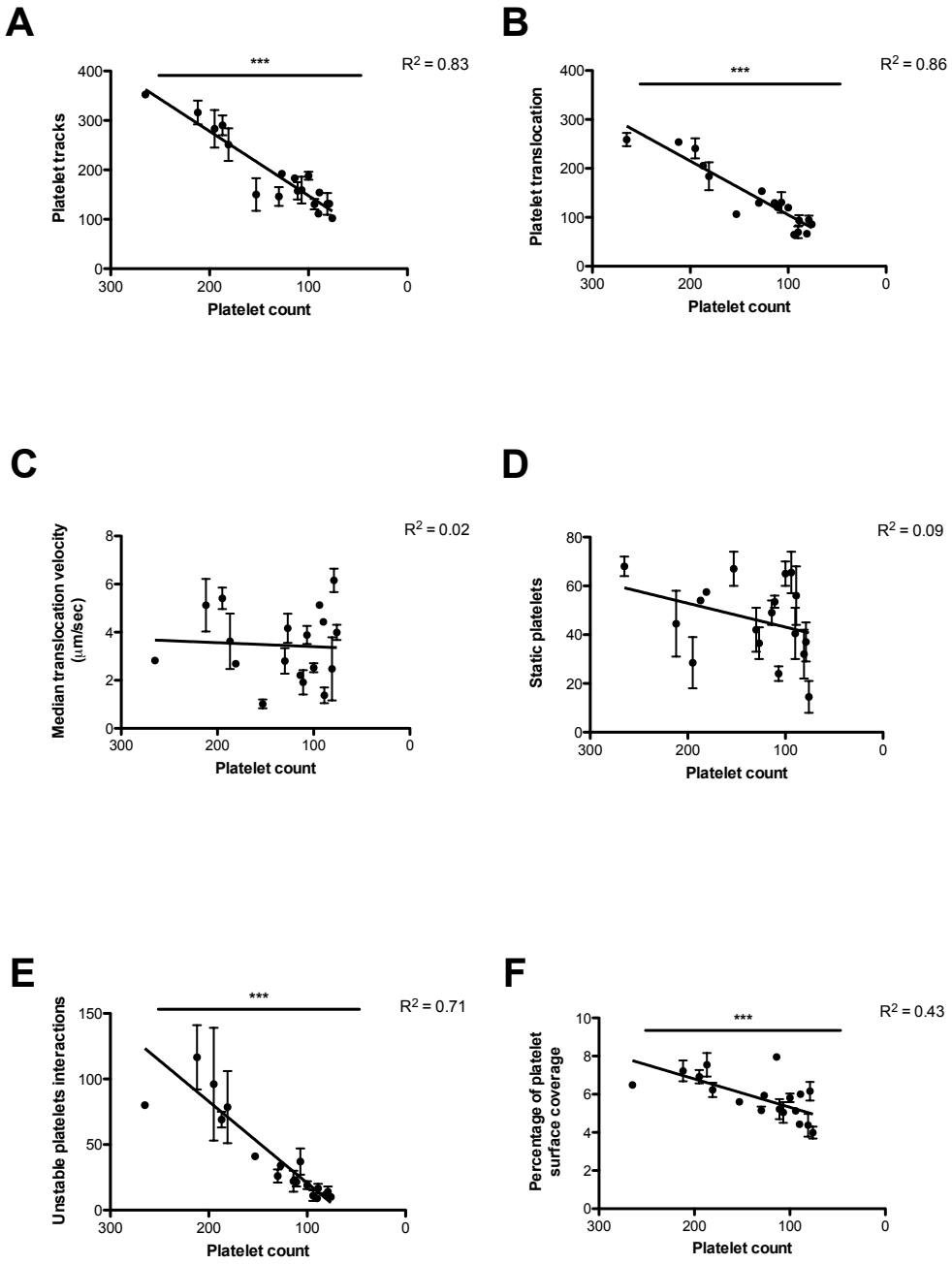

Figure 3.2 Decreasing platelet count significantly reduces platelet interactions with VWF. Platelets isolated from whole blood were diluted in JNL buffer to the desired platelet counts and reconstituted back into RBCs. The blood was then perfused over VWF at arterial shear. Each donor had a duplicate of runs for each condition. Reductions in platelet count significantly reduced platelet translocation behaviour on VWF. A simple linear regression model was used to test the slopes between the platelet count and measured platelet behaviour (***$p < 0.0001$). The R^2 values for the best-fit lines are shown in the graph. Data is represented as mean ± SEM, n = 6.

3.2.2.2 HCT significantly impacts on platelet adhesion to VWF

3.2.2.2.1 RBC collisions reduce the time taken for platelets to pass through the cell-free layer (numerical simulation)

In collaboration with Professor Eric Shaqfeh (Stanford University, California USA), it was demonstrated using numerical simulation models of platelet-wall adhesion, that RBCs play a significant role in determining initial platelet adhesion (Fitzgibbon et al., 2014). The numerical simulation models of platelet-wall adhesion set out to determine whether RBC collisions with platelets have an effect on the time taken for platelets to cross the cell-free layer (CFL). The CFL refers to the Fahraeus–Lindquist layer (F-L), a phenomenon whereby RBCs migrate to the centre of the vessel forcing the platelets to the vascular wall. The model predicted that the time taken for platelets to pass through the F-L was significantly lower in those simulations where RBCs collided with platelets versus those where RBC did not collide with platelets (Figure 3.3).

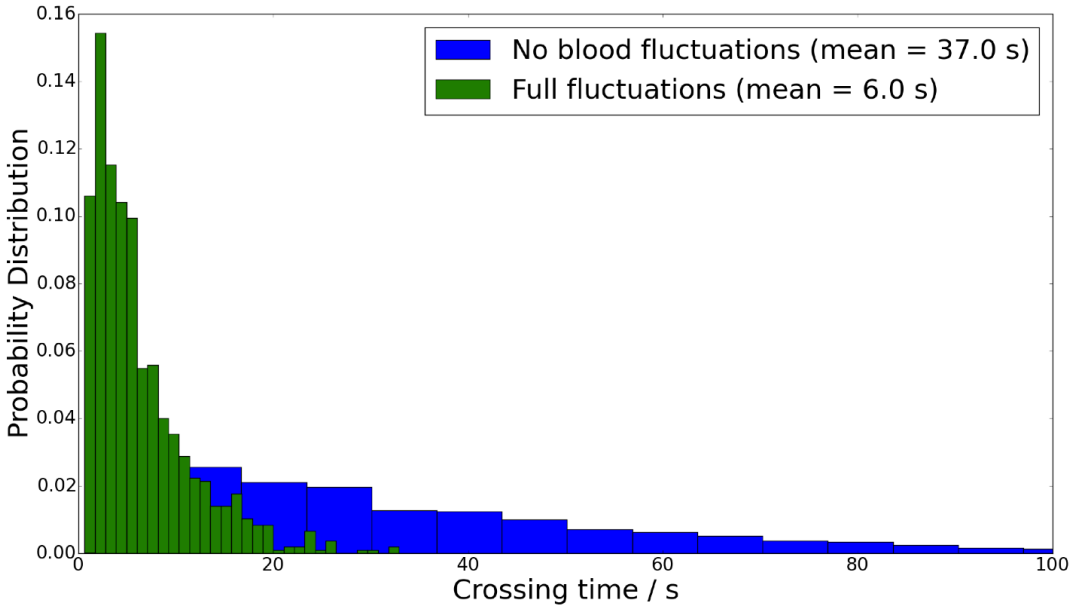

Figure 3.3 Platelets cross the CFL at faster rates in the presence of RBC collisions then in the absence of RBC collisions. The Fahraeus–Lindquist layer (F-L) is set to 4.2 µm in width. The numerical simulation model predicted that in the absence of RBC collisions (no blood fluctuations) with platelets it takes the platelet approximately 37 seconds to cross through the F-L. In the presence of RBC collisions (full fluctuations) with platelets, platelets cross the F-L in approximately 6 seconds.

3.2.2.2.2 Reducing HCT concentrations significantly reduce platelet-VWF interactions (The DPFA)

As demonstrated in Figure 3.3, platelets in the absence of RBC collisions take longer to cross the CFL than in the presence of RBC collisions. Using the DPFA, the effect of reducing HCT levels (which will reduce RBC-platelet collisions) on platelet adhesion to VWF was investigated. The normal haematocrit ranges for healthy adults can vary from laboratory to laboratory but in general is between 35-50 %. Blood samples from healthy donors (n=5) the percentages of HCT ranging from 39-44 % were compared with the same blood sample diluted to HCT concentrations ranging from 21-25 % and 12-17 % (Table 3.4). The DPFA experiments showed that decreasing HCT resulted in a steady decline in platelet interactions with VWF (Figure 3.4). Furthermore, reducing HCT resulted in a significant decrease in the number of platelet tracks (289 ± 48 versus 202 ± 20 versus 92 ± 16; slope ***$p < 0.0001$, R^2 = 0.55) and translocating platelets (220 ± 44 versus 141 ± 22 versus 59 ± 12; slope ***$p < 0.001$, R^2 = 0.55). No significance was observed in weighted median speed (3.0 ± 0.3 µm/sec versus 3.0 ± 0.6 µm/sec versus 2.7 ± 0.9 µm/sec, R^2 = 0.02) with reducing HCT. However, there was a significant decrease in the number of static platelets (66 ± 7 versus 51 ± 6 versus 27 ± 5; slope ***$p < 0.0001$, R^2 = 0.49), unstable platelet interactions (505 ± 93 versus 320 ± 34 versus 130 ± 22; slope **$p < 0.01$, R^2 = 0.33) and in the percentage of platelet surface coverage (7.2 ± 0.6 % versus 5.7 ± 0.1 % versus 3.2 ± 0.4 %; slope ***$p < 0.0001$, R^2 = 0.69) with lowering levels of HCT.

Table 3.4 Significant reductions in HCT. There was no significant difference in platelet count. Blood HCT was significantly reduced (***P < 0.0001, one-way ANOVA) per experiment by diluting HCT in JNL buffer and reconstituting back into platelet rich plasma (PRP). All data is represented as mean ± SD.

Healthy normals (N=5)	39-44% hematocrit	21-25% hematocrit	12-17% hematocrit	P value
Platelet count (x10^3/µl)	190 ± 12	171 ± 38	176 ± 35	0.2599
% Hematocrit	41 ± 2	24 ± 2	15 ± 2	**<0.0001*** **

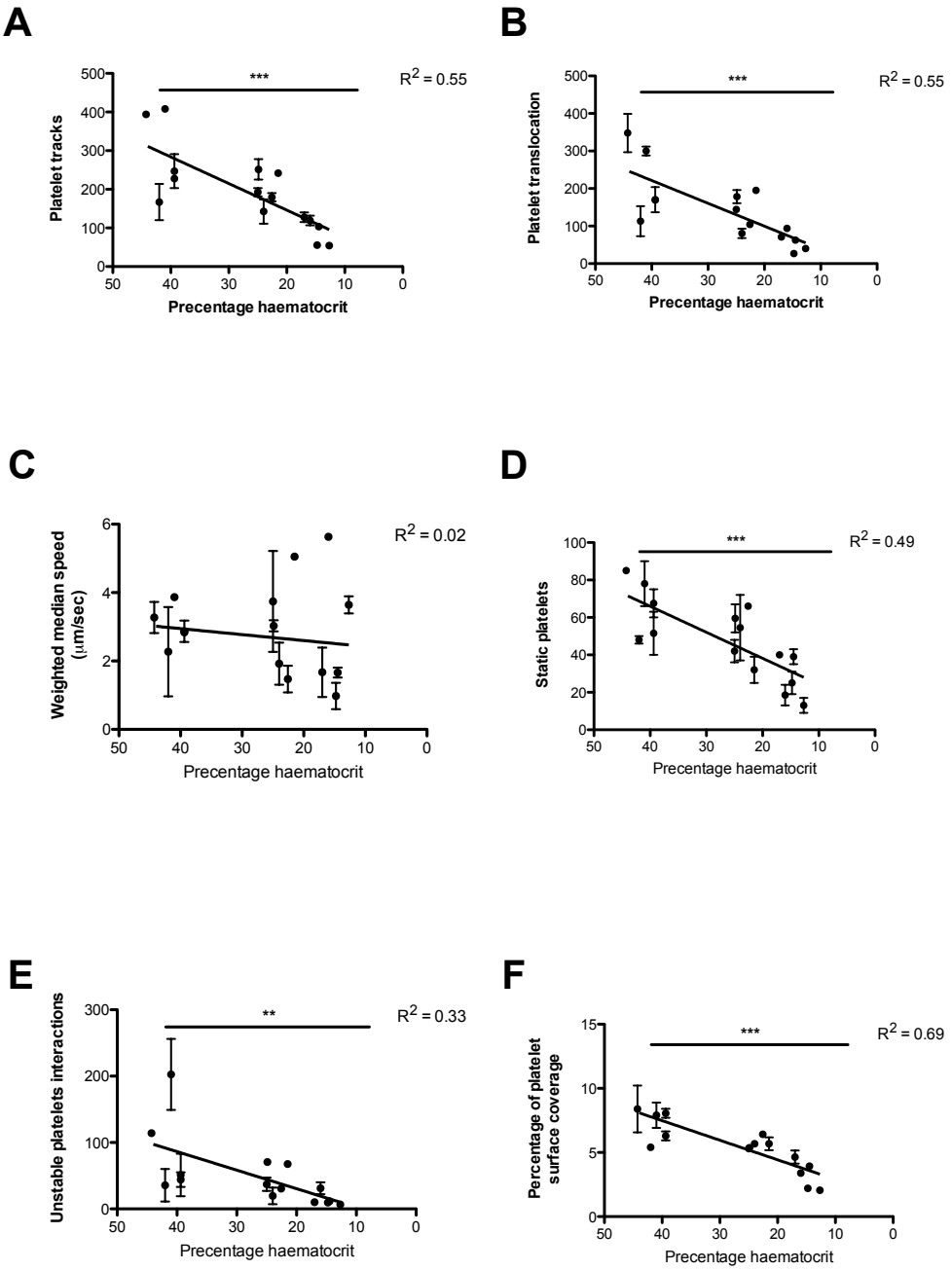

Figure 3.4 Decreasing HCT significantly reduces platelet interactions with VWF. RBCs isolated from whole blood were diluted in JNL buffer to the desired HCT concentration and reconstituted back into PRP. The blood was then perfused over VWF at arterial shear. Each donor had a duplicate of runs for each condition. Reductions in HCT significantly reduced platelet translocation behaviour on VWF. A simple linear regression model was used to test the slopes between the HCT and measured platelet behaviour (**$p < 0.01$ and ***$p < 0.0001$). The R^2 values for the best-fit lines are shown in the graph. Data is represented as mean ± SEM, n = 5.

3.2.3 Repeatability of the DPFA

3.2.3.1 Platelet translocation behaviour on VWF does not change significantly in healthy individuals over time

The long-term repeatability of the DPFA was assessed using 3 healthy donors, testing each in triplicate over 5 consecutive months. No significant change was observed in platelet counts or HCT percentages over time (Table 3.5). Analysis of DPFA data showed there was an insignificant difference in platelet translocation behaviour on VWF such that the number of platelet tracks, translocating platelets, weighted median speed, static platelets, unstable platelets interactions or percentages of platelet surface coverage were not significantly ($p > 0.05$) altered over a duration of 5 months (Figure 3.5).

Table 3.5 No significant change in platelet count or HCT over time. There was no significant change in platelet count or HCT ($P > 0.05$, one-way ANOVA) in healthy donors (n=3) over 5 consecutive months. All data is represented as mean ± SD.

Condition	Month 1	Month 2	Month 3	Month 4	Month 5	P value
Platelet count ($x10^3/\mu l$)	177 ± 33	201 ± 46	211 ± 38	224 ± 83	220 ± 61	0.8422
% Hematocrit	40 ± 1	41 ± 4	39 ± 2	40 ± 3	40 ± 2	0.9777

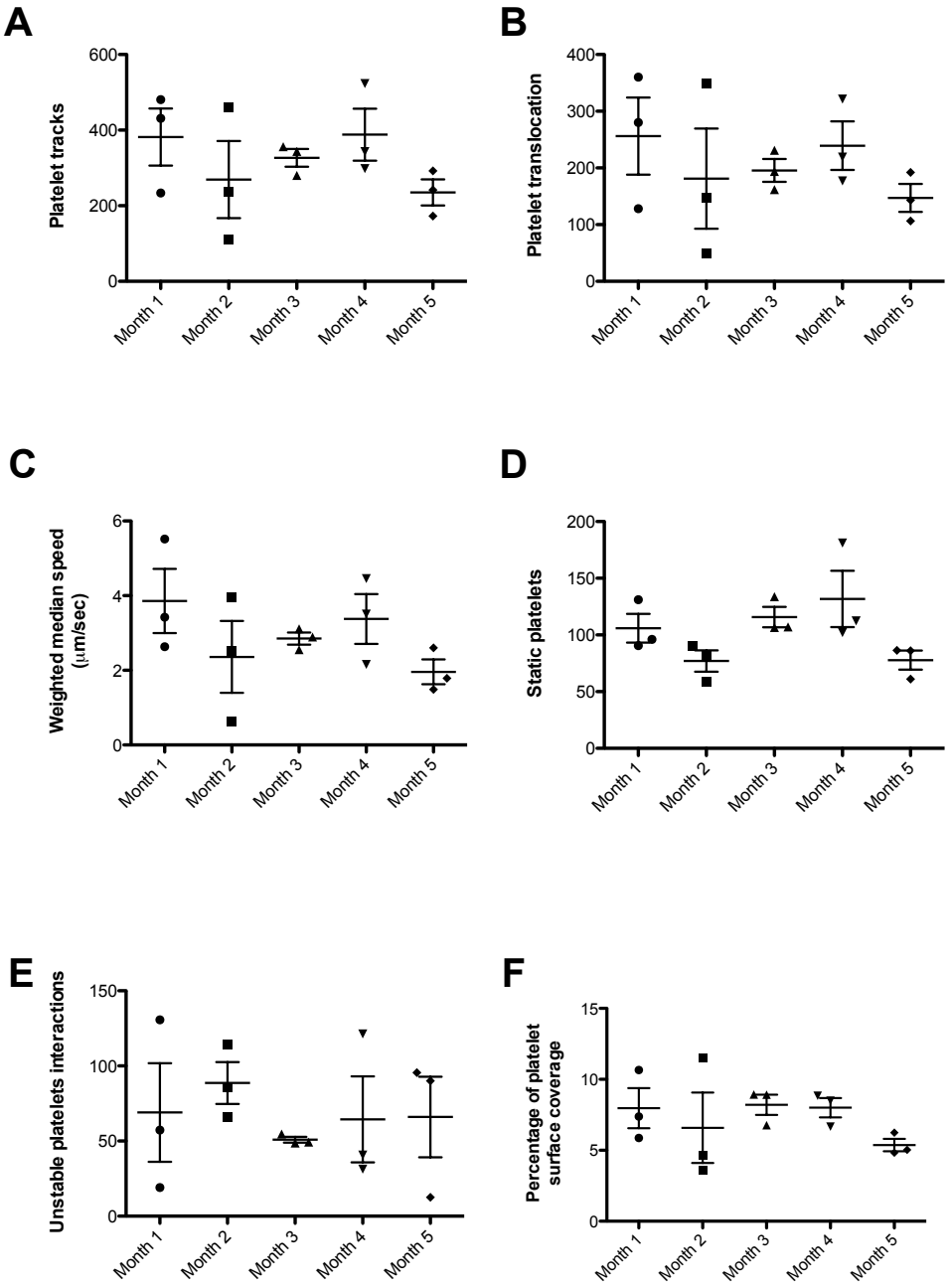

Figure 3.5 There was no significant change in platelet translocation behaviour on VWF in healthy donors over time. Blood from healthy donors (n=3) was perfused over VWF at arterial shear over 5 consecutive months. Each donor had a triplicate of runs. No significant change was observed in platelet translocation behaviour over 5 consecutive months. A one-way ANOVA or Kruskal-wallis test was used where appropriate to detect statistically significant differences between the varying conditions. Data is represented as mean ± SEM.

3.2.4 Normal reference range for healthy donors on the DPFA

A normal reference range for healthy donors was established for the DPFA using 109 healthy volunteers (53 males and 56 females). The donors ranged in age from 19-82 years, and had platelet counts in the range of 120-403 x 10^3 per µL of blood and HCT ranging from 31-46 % (Table 3.6). In order to address the variability of the DPFA related to blood condition and experimental error, each donor's blood was assayed in triplicate. All runs were then analysed, and runs outside the mean ± 2SD were removed before each donor's parameters were averaged over 3 or less eligible runs. This process allowed us to detect and remove the extreme outliers to determine a normal reference range. A normal reference range was then established for each of the six parameters measured in this thesis (Table 3.7). The six parameters for the 109 donors recruited for the normal reference are shown in the scatter plot (Figure 3.6). The normal distribution for these donors is illustrated in Figure 3.7. The effects of age and gender in the assay are discussed in Chapter 4.

Table 3.6 Healthy donor characteristics (Reference range)

Characteristics	Healthy donors (n=109)
Age range (years)	19-82
Number of male donors	53
Number of female donors	56
Platelet count range ($x10^3$µl)	120-403
Haematocrit range (%)	31-46

Table 3.7 Reference range of platelet function for healthy donors on the DPFA. Table shows mean ± SD and the cut-off range (mean ± 2SD) for each of the measured platelet translocation behaviours on the DPFA for healthy donor populations. Normality was assessed using a Shapiro-Wilk test.

Measured platelet translocation behaviours	Healthy donors (n=109)	Cut-off range (mean ± 2SD)
Platelet tracks	357 ± 114	585 - 129
Translocating platelets	245 ± 85	415 - 75
Weighted median speed (μm/sec)	4.4 ± 1.9	8.2 - 0.6
Static platelets	84 ± 33	150 - 18
Unstable platelet interactions	99 ± 55	209 - 0
Percentage of platelet surface coverage	7.9 ± 2.4	12.7 - 3.1

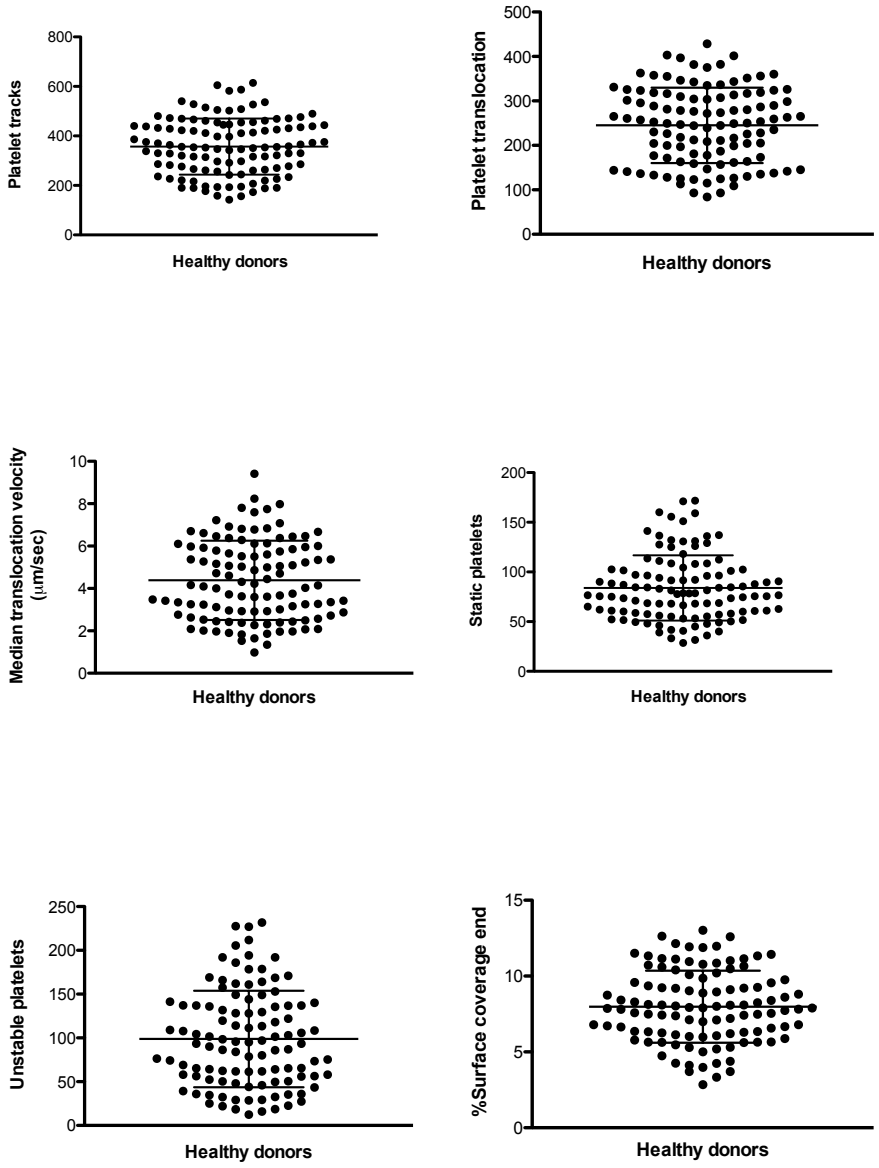

Figure 3.6 Reference range of platelet function for healthy donors on the DPFA. Blood from healthy donors (n=109) was perfused over VWF at arterial shear. Each donor had a triplicate of runs and normal reference range was determined for healthy donor populations. Each dot on the graph represents an individual donor tested on the assay. Data is represented as the mean ± SD.

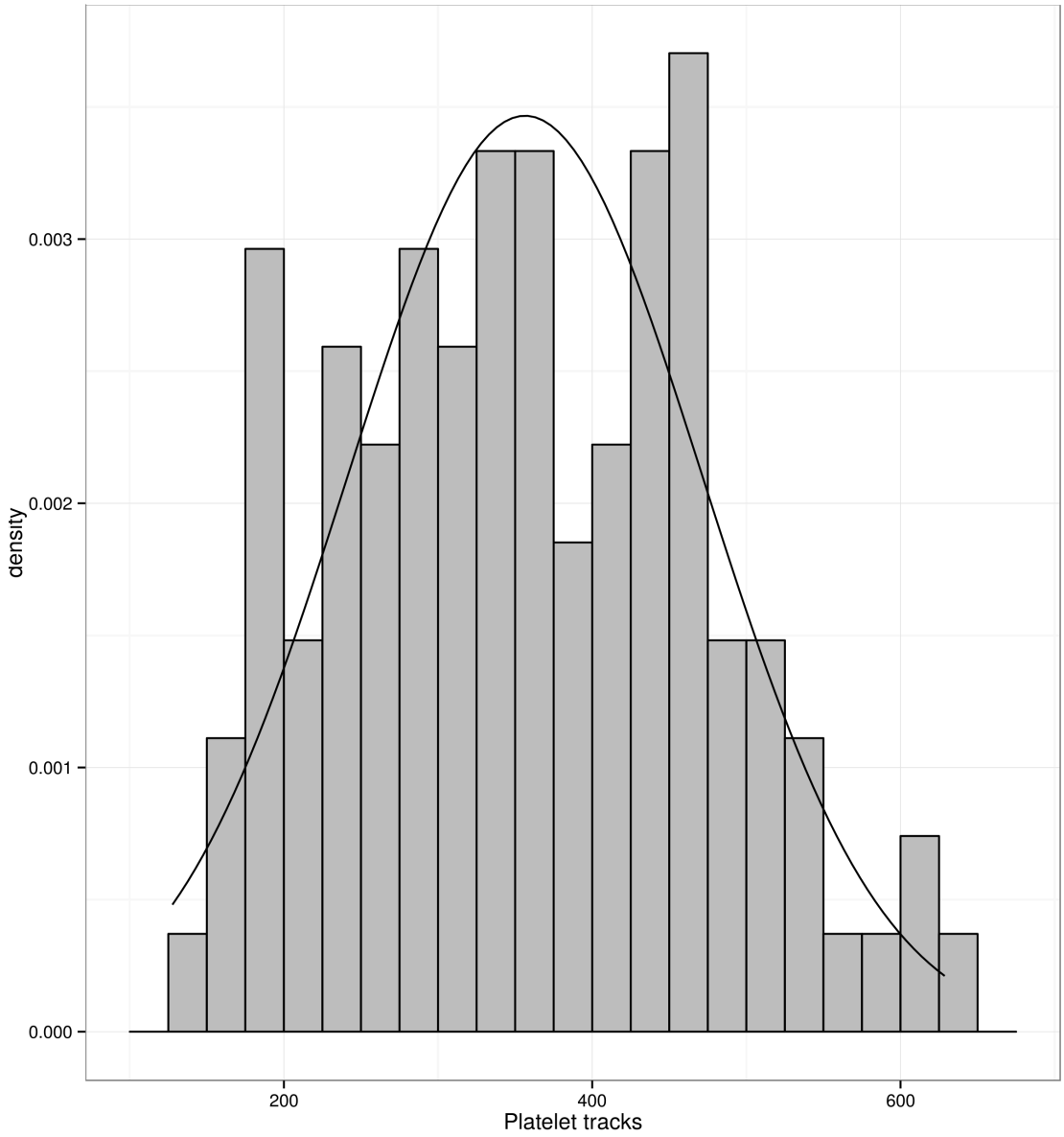

Figure 3.7 Histogram showing a normal distribution for platelets interacting with VWF in healthy donors.

3.2.5 Correlation analysis of DPFA outputs

A Spearman correlation analysis was performed to determine how well each of the measured parameters from DPFA correlated with another. The DPFA parameter outputs taken from healthy donors (n=5) were analysed using a Spearman correlation. It was determined that there was a significant correlation between the number of platelet tracks and the number of platelets that translocated on VWF (*$p < 0.05$). No significant correlations were found between any of the other measured parameters on the DPFA (Table 3.8).

Table 3.8 Spearman correlation analysis of DPFA outputs. Ptracks = Platelet tracks, Ptrans = Platelet translocation, WMS = Weighted median speed, Pstatic = Static platelets, Punstable = Unstable platelet interactions and Psurface = Percentage of platelet surface coverage. * Represents a statistically significant difference ($p < 0.05$).

Parameter	Ptracks	Ptrans	WMS	Pstatic	Punstable	Psurface
Ptracks	-	*	ns	ns	ns	ns
Ptrans	*	-	ns	ns	ns	ns
WMS	ns	ns	-	ns	ns	ns
Pstatic	ns	ns	ns	-	ns	ns
Punstable	ns	ns	ns	ns	-	ns
Psurface	ns	ns	ns	ns	ns	-

3.3 Discussion

In this chapter, an ideal data set (described in Chapter 2) and $P2Y_1$ inhibitor (MRS2179) were used to validate the accuracy of the platelet tracking software. Firstly, the software was validated with the ideal data set. The ideal data set contained images with known values of platelet translocation behaviour. These ideal images were run through the tracking software and the values generated were compared with the expected values. The ideal data set determined the mean absolute percentage error for each of the measured platelet translocation behaviours. The number of merging and separating events is highly correlated with object count. Hence, higher object counts result in greater numbers of merging and separating events, which increase the potential for mistracking of platelets. The tracking software marks the centroid position of each platelet on each frame and it uses this centroid position to track platelet movement. Hence as platelets merge and separate from one another, the centroid position of the platelet moves too, resulting in platelet mistracking. Moreover, movement of the centroid position due to merging and separating is known as artificial movement and this will have an effect on the accuracy of the platelet tracking process. Secondly to validate the platelet tracking process, a selective $P2Y_1$ inhibitor (MRS2179) was used to assess its effect on platelet translocation behaviour. Mazzucato et al., (2004) previously showed that MRS2179 could significantly amplify platelet translocation speeds on VWF compared with non-MRS2179 treated controls. Since velocity is a new measure in our assay, the $P2Y_1$ receptor inhibitor was chosen as opposed to classical antiplatelet agents such as aspirin or experimental inhibitors such as thromboxane blockers, where their effects on platelet translocation on VWF is not known. Using the platelet tracking software it was observed that platelet translocation velocities were also significantly increased upon treatment with MRS2179 versus non-MRS2179 treated controls confirming that the assay was capable of detecting the predicted effects of this drug.

The possible biological factors that can affect dynamic platelet adhesion to VWF including varying platelet counts and varying HCT were investigated. In previous studies, it has been shown that platelet function tests such as the PFA-100 are

sensitive to platelet count and HCT. Platelet count and HCT, when lowered to pathological values, were shown to significantly prolong closure times (CT) in the device, e.g. the time taken for platelets to occlude the aperture completely (Kundu et al., 1996). By investigating the sensitivity of the DPFA to reduced platelet count, a steady decline in platelet translocation behaviour on VWF in those samples with lower platelet counts was observed. Platelet interactions were reduced in those samples with lower platelet counts, as represented by the significant decrease in the numbers of platelet tracks. It has been reported that following surgery HCT was strongly correlated with bleeding times rather than platelet count and that reductions in RBCs resulted in a significant increase in bleeding time (Valeri et al., 2001).

Large-scale numerical simulations of blood flow have shown that platelet margination is significantly influenced by RBCs, such that the RBCs drive the platelets close to the vessel wall (Zhao et al., 2012). In this thesis, using numerical simulation models of platelet wall adhesion, it was demonstrated that the time taken for platelets to pass through the CFL was significantly lower in those simulations where RBC collided with platelets versus those where RBC did not collide with platelets (Fitzgibbon et al., 2014). This was confirmed indirectly in the experiments in which HCT was varied in samples run on the DPFA. The results of these HCT experiments demonstrated that platelet translocation behaviour on VWF steadily declined with a reduction in HCT. This is in agreement with a study by Chen and colleagues that observed that increasing or decreasing the levels of HCT could positively or negatively regulate the adhesion of platelets to VWF (Chen et al., 2013). Previous work of Aarts et al., (1983) investigating platelet adherence to umbilical arteries also demonstrates that RBC size can be of major importance in regulating platelet adherence.

A normal reference range of platelet function for the DPFA was established. The minimum number of participants required to establish a reference interval in a population is 39 (Solberg, 1987). A total of 109 healthy donors were assayed on the DPFA. To account for the possible effect of gender, equal numbers of males and

females were recruited (M=53 and F=56). Generating normal reference ranges are important as they can be used to potentially identify those donors who may be at risk of bleeding or thrombosis.

To conclude, in this chapter the accuracy of the novel platelet tracking software was demonstrated, using custom-developed ideal data sets that determine the mean absolute percentage error for each measured trajectory classifier. Although these errors represent the lower limit of actual error that is associated with real experiments, the assay is still capable of detecting subtle changes in platelet function (explored in more detail in Chapters 4, 5 and 6). The capability of the assay to detect subtle changes in platelet function is demonstrated via the use of the selective purinergic platelet inhibitor MRS2179, which shows significant increases in platelet translocation velocities upon administration (Figure 3.1). The DPFA is sensitive to platelet count and HCT and this should be considered when comparing two cohorts to one another. It was found that the DPFA has suitable repeatability, as there was no significant change in platelet function in 3 healthy donors over the duration of 5 consecutive months. Thus, this assay has the potential to provide unique insights to the behaviour of platelets *in vivo* in healthy and diseased cohorts.

Chapter 4

Age-related changes in platelet function are more profound in females than in males

4.1 Introduction

Age affects most cellular processes but the effect of age on platelet function is unclear. Most studies to date have used non-physiological approaches such as light transmission aggregometry (LTA) or flow cytometry to investigate age-related changes in platelet function (Emery et al., 1995, Knight et al., 1997, Gleerup and Winther, 1995, Jayachandran et al., 2005). These studies have reported that aging results in significant increases in the release of plasma β-thromboglobulin (βTG), plasma platelet factor 4 (PF4), phosphoinositide turnover, platelet aggregation and plasma fibrinogen (Zahavi et al., 1980, Bastyr et al., 1990, Franchini, 2006).

Ideally assays of platelet function should replicate the flow and shear environment that platelets experience *in vivo*. The platelet function analyser, the PFA-100 assesses platelet function under high-shear conditions. The device measures the time taken for platelets to occlude an aperture that is coated with either collagen and epinephrine (CEPI) or collagen and ADP (CADP). The results of the PFA-100 are reported as closure time (CT) (Kundu et al., 1995). A number of studies have used the PFA-100 to assess age-related changes in platelet function. However, the results of these studies are inconsistent. For example Sestito and colleagues, demonstrated an absence of correlation between age and platelet CT (n=62) (Sestito et al., 1999). A PFA-100 study of healthy Koreans (n=120) identified that older Koreans (> 40 years) had platelet CT's that were significantly shorter than those observed in younger populations (Cho et al., 2007).

In this thesis, the Dynamic Platelet Function Assay (DPFA) was employed to comprehensively investigate the effect of age on platelet function in over 100 healthy donors. A total of four platelet translocation behaviours on VWF were measured, relating to the different stages of platelet interaction with VWF. The number of platelets that interact with VWF (platelet tracks); the number of platelets that translocate on the surface (platelet translocation); the number of platelets that interact but do not adhere to the surface (unstable platelet interactions); and the

percentage of platelets that remain stuck to the VWF surface on the final frame (percentage of platelet surface coverage) were assessed.

In this chapter, I will discuss platelet function as measured by the DPFA:

- In older and younger healthy adult populations.
- In older and younger healthy males.
- In older and younger healthy females.

4.2 Results

4.2.1 Evaluation of the effects of aging on platelet function in the DPFA

4.2.1.1 Platelet behaviour on VWF differs between healthy older and younger adults

Older adults were defined as males ≥ 50 years and females ≥ 40 years and younger adults as males < 50 years and females < 40 years. These age cut-offs were chosen because males ≥ 50 have a higher mortality rate from coronary heart disease than younger males (Jousilahti et al., 1999) and in females early menopause can begin at 40 years and is associated with an increased risk for cardiovascular disease (Shuster et al., 2010). A total of 109 subjects were studied (older adults n=44 and younger adults n=65). The characteristics of the donors are shown in table 4.1. The inclusion criteria were: healthy volunteers with no previous history of disease and taking no prescribed medication.

Older adults had a significant reduction in the number of platelet tracks (319 ± 15 versus 384 ± 15; **p < 0.01), translocating platelets (222 ± 11 versus 265 ± 11; **p < 0.01) and numbers of unstable platelet interactions (69 ± 6 versus 118 ± 8; ***p < 0.0001) with VWF. In older adults there was a significant increase in the percentage of platelet surface coverage (8.6 ± 0.3 % versus 7.5 ± 0.2 %; *p < 0.05) compared with the younger adults (Figure 4.1).

Table 4.1 Donor characteristics

	n number	Age	Platelet count ($x10^3/\mu L$)	Haematocrit (%)
Males < 50 years	33	19-36	154-258	34-43
Males ≥ 50 years	20	50-82	121-248	35-45
Females < 40 years	32	21-38	120-387	20-46
Females ≥ 40 years	24	42-70	168-285	31-44
Total	**109**	-	-	-

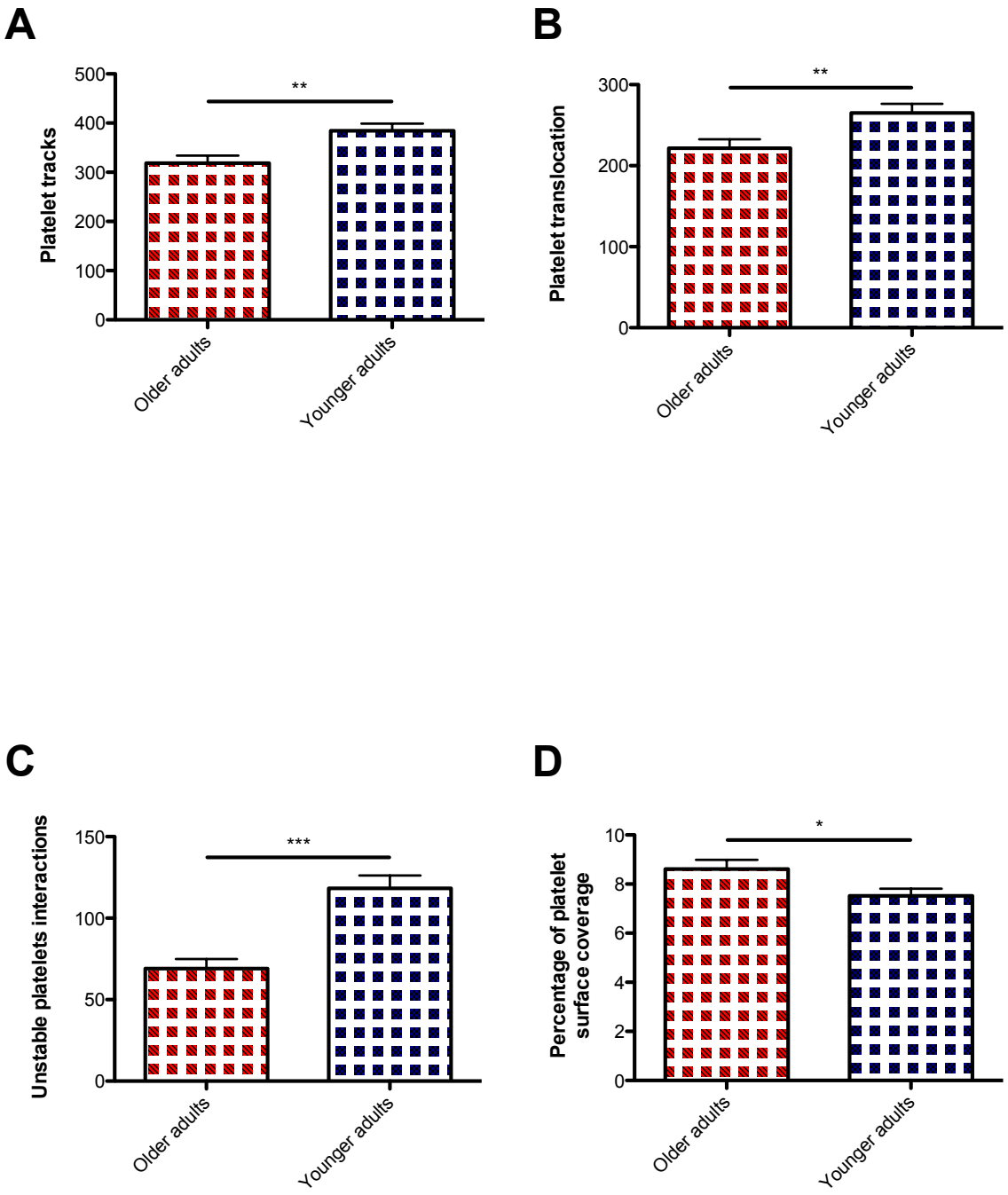

Figure 4.1 Platelet behaviour on VWF differs between healthy older and younger adults. Blood taken from 44 older adults and 65 younger adults was perfused over VWF at arterial shear. Platelet translocation behaviour on VWF was measured. Platelets from older donors adhered more to VWF compared to younger donors (*p < 0.05, **p < 0.01 and ***p < 0.0001). An unpaired and unpaired Welch's t-test was used were appropriate to detect statistical significance. Data is represented as the mean ± SEM.

4.2.2 Evaluation of the effects of gender and age on platelet function in the DPFA

Having demonstrated that platelet translocation behaviour was significantly different between older and younger adults, the effect of age in males and females was compared. Platelet behaviour was compared in males ≥ 50 years and males < 50 years (n=20 and n=33 respectively) and females ≥ 40 years and females < 40 years (n=24 and n=32 respectively).

4.2.2.1 Older and younger males

In older males (≥ 50 years) compared with males < 50 years, there was no significant difference in the number of platelet tracks (308 ± 22 versus 354 ± 21) or in platelet translocation (211 ± 15 versus 236 ± 15). However, males ≥ 50 years compared with males < 50 years had a significant decrease in the number of unstable platelet interactions (81 ± 12 versus 116 ± 11; *p < 0.05) with VWF and a significant increase in the percentage of platelet surface coverage (8.2 ± 0.4 % versus 7.0 ± 0.3 %; *p < 0.05) (Figure 4.2).

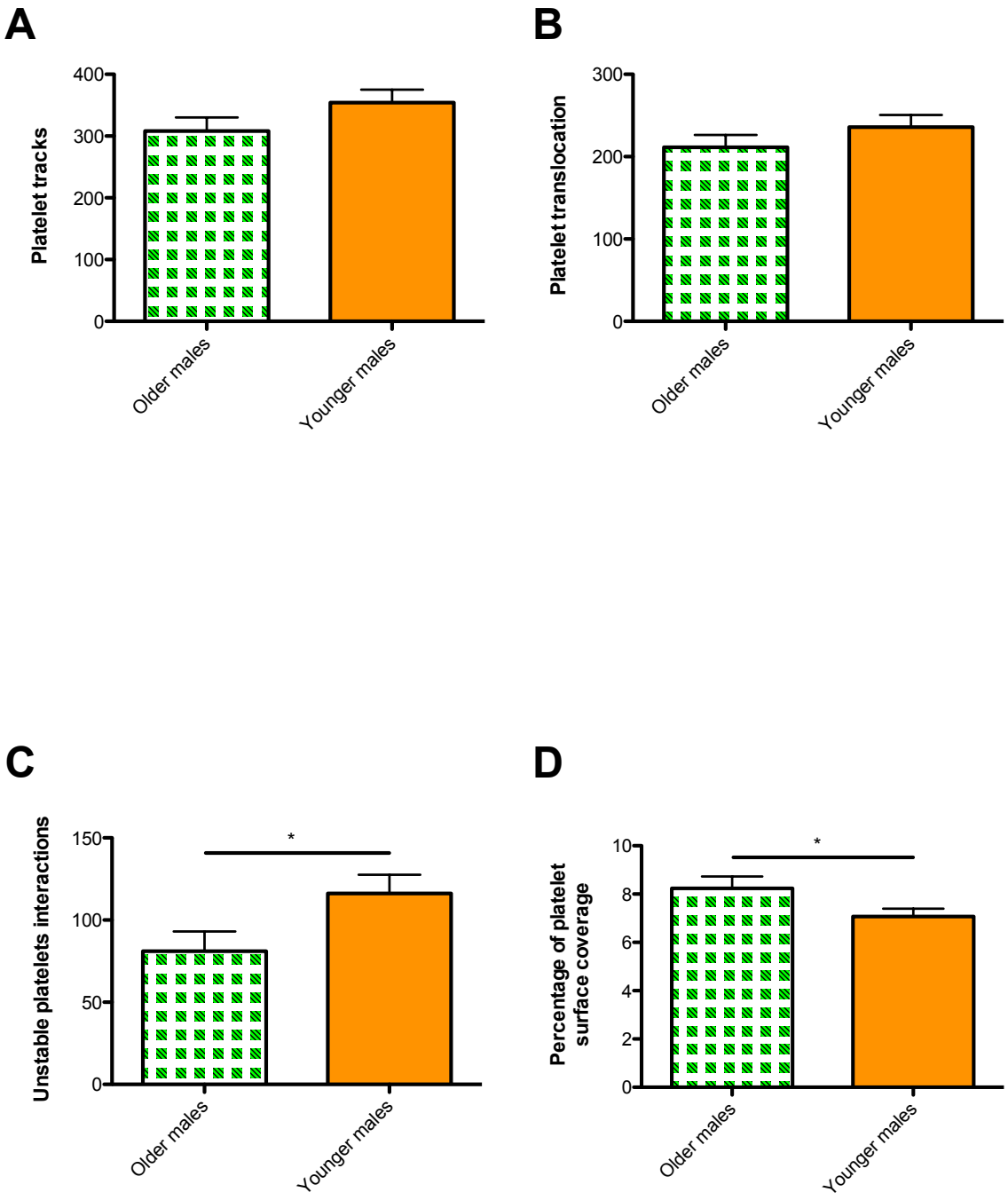

Figure 4.2 Platelet behaviour on VWF differs between healthy older and younger males. Blood taken from 20 older males and 33 younger males was perfused over VWF at arterial shear. Platelet translocation behaviour on VWF was measured. Platelets from older males adhered more to VWF compared to younger males (*$p < 0.05$). An unpaired and unpaired Welch's t-test was used where appropriate to detect statistical significance. Data is represented as the mean ± SEM.

4.2.2.2 Older and younger females

Older females (≥ 40 years) compared with younger females < 40 years had a significant reduction in the number of platelet tracks (323 ± 21 versus 426 ± 20; **p<0.01), platelet translocation (228 ± 16 versus 290 ± 14 **p < 0.01) and number of unstable platelet interactions (65 ± 6 versus 123 ± 11; ***p < 0.0001). There was no significant difference in the percentage of platelet surface coverage (8.8 ± 0.5 % versus 7.8 ± 0.4 %) between the two groups (Figure 4.3).

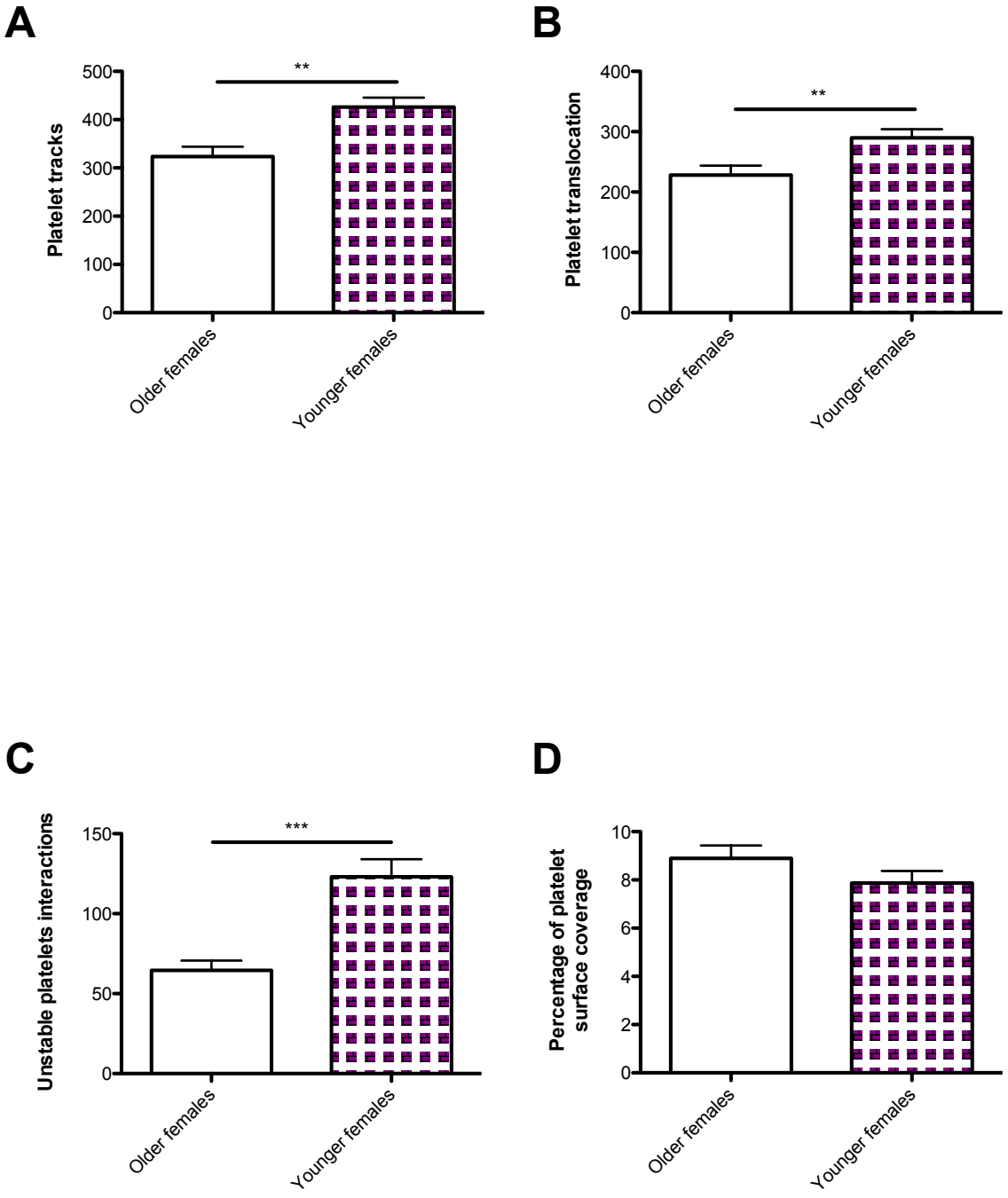

Figure 4.3 Platelet behaviour on VWF differs between healthy older and younger females. Blood taken from 24 older females and 32 younger females was perfused over VWF at arterial shear. Platelet translocation behaviour on VWF was measured. Platelets from older females adhered more to VWF compared to younger females (**$p < 0.01$ and ***$p < 0.0001$). An unpaired and unpaired Welch's t-test was used where appropriate to detect statistical significance. Data is represented as the mean ± SEM.

4.3 Discussion

The results of this chapter demonstrates that age has a significant effect on platelet translocation behaviour on VWF. Aging, results in enhanced platelet adherence to VWF (increases in platelet surface coverage and decreases in unstable platelet interactions with VWF) with this effect being more profound in females than in males.

Previous studies have reported that platelet activation increases with age. For example, Bastyr et al., (1990) demonstrated increased platelet phospholipid content, suggesting increases in transmembrane signalling with age. It has also been shown that age is associated with an increase in platelet aggregability (Gleerup and Winther, 1995). Reilly and FitzGerald, (1986) showed that bleeding times were significantly reduced in older subjects. In this thesis, the DPFA was used to assess platelet function in real time and to characterise platelet behavior in a cohort of normal individuals. Overall the results were consistent with the concept that age was associated with more reactive platelets. This was readily apparent in the surface coverage of VWF where there was greater platelet adhesion in the older cohort. These increases in platelet surface coverage in the older cohorts are unlikely to be a result of increased plasma levels of VWF. Although, plasma levels of VWF in this study were not measured, it was previously demonstrated by Wu and co-workers that plasma levels of VWF have no significant effect on platelet adhesion to glass surfaces coated with immobilised VWF (Wu et al., 1996). Also, the DPFA measures the initial interaction of platelets with VWF (first 16.7 seconds), therefore it is unlikely that increases fibrinogen levels would increase platelet adhesion to the VWF surface in older donors because the assay measures single platelets rather than the formation of platelet aggregates. The older population had significantly less platelets interacting with VWF that did not adhere to the surface as defined by a reduction in unstable platelet interactions with VWF. This element of the study has identified that there was greater platelet adherence in the older population. This also demonstrates the advantage of measuring multiple parameters of platelet behaviour on VWF. A reduction in platelet interactions with VWF could be interpreted as a reduction in the activity of the platelets, but using the DPFA's other measure outputs, it is evident

that there are less platelet's that unstably adhere to the VWF surface which results in a significant increase in platelet surface coverage on VWF in older individuals.

The results of this study suggest that the effect of aging on platelet translocation behaviour on VWF was more pronounced in females than in males. This may be related to the potential influence of sex hormones such as testosterone and estrogen. Previous studies of platelet function have suggested that testosterone and estrogen can have a regulatory role in platelet function (Tarantino et al., 1994, Ajayi et al., 1995, Campelo et al., 2012). Testosterone has been shown to significantly enhance platelet thromboxane A_2 receptor density and heighten platelet aggregation responses to arachidonic acid (Ajayi et al., 1995). Platelets express the estrogen receptor β (Khetawat et al., 2000, Nealen et al., 2001) and deletion of the estrogen receptor β in aged female mice results in the amplification in the thrombogenicity of platelets (Jayachandran et al., 2010). The results conveyed in this thesis show more pronounced change in platelet translocation behaviour on VWF in older females when compared to that of older males and this may be reflective of a reduction in estrogen levels experienced in females rather than the gradual decline of testosterone levels in males associated with aging. This is recommended as an area for future research. In this thesis, no significant differences in platelet count or HCT were observed between the measured groups. This is in contrast to a Scandinavian study of platelet counts in males and females that demonstrated that females have greater platelet counts than males (Bain, 1985). Males however, have been demonstrated to have higher HCT than females (Zeng et al., 2001). It is unknown why there were no observed differences in platelet count and HCT, between males and females in this thesis. However, it must be acknowledged that measures of platelet count and HCT can vary widely between individuals and that these values can differ from laboratory to laboratory. In this thesis, males had platelet counts ranging from 121-258 and HCT 34-45 % (Table 4.1). Females had platelet counts ranging from 120-387 and HCT 20-46 % (Table 4.1). Significant differences between genders are seen in large population studies and while this group of over a 100 normal donors is large it is not large enough to provide differences in these values.

There is a paucity of studies on the influence of age on platelet adhesion to vascular proteins. Significantly this study demonstrates, for the first time, that aging has a significant impact on platelet adhesion to VWF under arterial shear conditions; resulting in enhanced platelet adherence to VWF. This novel DPFA with its multi-parameter analysis of platelet translocation behaviour on VWF is capable of detecting subtle changes in platelet function. These-age related alterations in platelet function may contribute to the increased incidence of thrombotic events seen with aging.

Chapter 5

Platelet translocation behaviour in very low birth weight (VLBW) preterm and full-term neonates

5.1 Introduction

A fetus has platelet counts within the normal adult range by 22 weeks of gestation (Sola-Visner, 2012). The incidence of haemorrhage in preterm neonates is higher than that of full-term neonates, in particular intraventricular haemorrhage (IVH) (Ballabh, 2010). IVH is multifactorial but platelet dysfunction in preterm neonates may be a contributing factor to these increased incidences of bleeding. Michelson and colleagues found that platelet hyporeactivity in preterms neonates was maximal on days 3 to 4 of life, which coincides with the peak in IVH incidence (Michelson, 1998). This finding is indirectly related to a more recent study in adults that showed that reduced platelet activity is associated with increased incidence of IVH (Naidech et al., 2009).

It is unclear whether platelet function is significantly different between very low birth weight (VLBW) preterm and full-term neonates as there are limited studies on platelet function in neonates. The majority of studies have been conducted in either cord blood or in full-term neonates, due to the availability of larger circulating volumes of blood (Sola-Visner, 2012, Ferrer-Marin et al., 2013). Despite having platelet counts similar to adults, the evidence suggests that platelets from neonates are hyporesponsive. Platelet hyporesponsiveness in neonates has been demonstrated by measuring P-selectin expression, which reflects alpha granule secretion. Neonates display reduced expression compared to blood samples from adults (Israels et al., 2003, Sitaru et al., 2005, Rajasekhar et al., 1997). Platelet hyporeactivity is greater in those VLBW preterm neonates at the lowest gestational ages (Sola-Visner, 2012, Ucar et al., 2005, Sitaru et al., 2005). Notwithstanding this observed neonatal platelet hyporeactivity, platelet function analyser, PFA-100 studies on neonate platelets, show that neonates have shorter closure times (CT) than adults (Israels et al., 2001, Boudewijns et al., 2003). Cone and plate studies also demonstrate that neonates have improved platelet adhesion to extracellular matrix (ECM) compared with adults. Nevertheless, preterm neonates display decreased platelet adhesion when compared to full-term neonates (Linder et al., 2002, Levy-Shraga et al., 2006). A study by Del Vecchio et al, using a device designed for

neonates to detect template bleeding times determined that preterms had prolonged bleeding times compared to full-term neonates (Del Vecchio et al., 2008).

Though there are relatively few platelet studies in preterm neonates, the evidence suggests that platelet hyporeactivity is more pronounced in those VLBW preterm neonates at the lowest gestational ages (those ≤ 32 weeks gestation). In addition, platelet translocation behaviour on VWF under arterial shear conditions has never been characterised before in neonate populations. Hence, the DPFA's low blood volume requirement (< 100 µL) made it possible to investigate changes in platelet translocation behaviour on VWF in neonates. Only 1 mL of blood was required from each neonate per experiment.

In this chapter, I will investigate platelet function in

- Preterm and full-term neonates.
- Preterm and preterm neonates with lower platelet counts.
- Preterm and preterm neonates with lower haematocrit (HCT).

5.2 Results

5.2.1 Study populations

A total of 26 preterm neonates ≤ 32 weeks gestation and 13 full-term neonates were recruited during the course of the study. The mean (± SD) gestational age of the preterm and full-term neonates was 27 ± 2 and 40 ± 1 weeks respectively. The mean birth weight was 1.0 ± 0.3 kg and 3.6 ± 0.5 kg for preterm and full-term neonates respectively. The neonatal demographics are shown in table 5.1. Clinical outcomes of the neonates included level of resuscitation in the delivery room, culture proven or clinically suspected sepsis treated with antibiotics at least for 5 days, duration of mechanical ventilation, respiratory distress syndrome (RDS), chronic lung disease (CLD) defined as supplementation of oxygen needed at 36 weeks' post menstrual age (Shennan et al., 1988), necrotising enterocolitis (NEC) defined using Bell's staging criteria (Walsh and Kliegman, 1986), patent ductus arteriosus (PDA), duration of parenteral nutrition, retinopathy of prematurity (ROP), intraventricular hemorrhage (IVH) defined by Papile's classification (Papile et al., 1978), periventricular leucomalacia (PVL), length of NICU stay, discharge weight and mortality.

Table 5.1 Preterm and full-term neonatal demographics. There was no significant reduction in platelet count between preterm and full-term neonates. However, preterm neonates had a significant reduction in hematocrit (*$p < 0.05$).

Demographics	**Preterms (n=26)**	**Full-terms (n=13)**
Gestation (weeks)	27±2	40 ± 1
Birth weight (kg)	1.0 ± 0.3	3.6 ± 0.5
Male	12	10
Female	14	3
Platelet count ($x10^3/\mu L$)	151 ± 65	188 ± 43
Haematocrit (%)	*39 ± 8	46 ± 2
Spontaneous Vaginal Delivery	11	6
Assisted Vaginal Delivery (forceps, ventouse)	0	4
Caesarean Section	15	3
Apgar at 1 min	5.4	8.3
Apgar at 5 min	7.6	9.0

5.2.2 VLBW preterms display significantly altered platelet function on VWF compared to full-term neonates

Platelets from VLBW preterm neonates (n=15) with platelet counts > 104 x 10^3 per µl of blood and HCT 41 ± 1 % exhibited significantly different platelet translocation behaviour on VWF when compared with full-term neonates (n=13). Preterm neonates had a significant increase in platelet tracks (333 ± 29 versus 224 ± 13; ** $p < 0.01$), platelet translocation (230 ± 21 versus 156 ± 7; **$p < 0.01$) and weighted median speed (4.2 ± 0.3 µm/sec versus 2.7 ± 0.2 µm/sec; **$p < 0.01$). No statistically significant differences were seen in the numbers of static platelets (78 ± 8 versus 60 ± 7). Preterms though had significantly increased numbers of unstable platelet interactions (168 ± 22 versus 58 ± 5; ***$p < 0.0001$) with VWF but no significant change in the percentage of platelet surface coverage (6.0 ± 0.4 % versus 5.4 ± 0.3 %) (Figure 5.1). No correlations were found with the clinical outcomes and the behaviour of platelets on VWF.

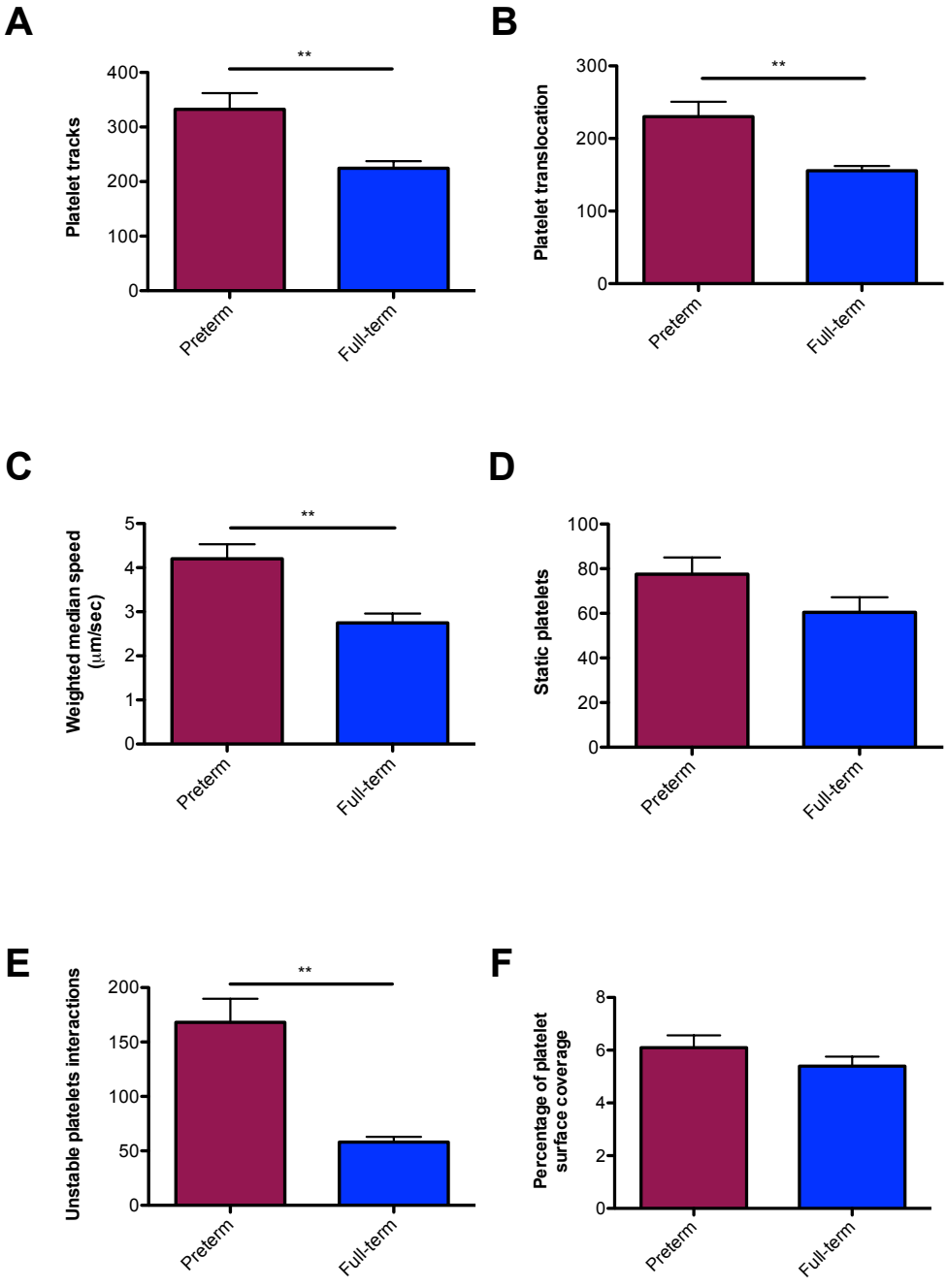

Figure 5.1 Platelets from VLBW preterm neonates display significantly altered platelet translocation behaviour on VWF. Blood from 15 preterms and 13 full-term neonates was perfused over VWF at arterial shear. Platelet translocation behaviour on VWF was measured. Platelets from preterm neonates displayed altered platelet translocation behaviour on VWF (*$p < 0.05$, **$p < 0.01$ and ***$p < 0.0001$). An unpaired t-test and unpaired t-test with Welch's correction were used where appropriate to detect statistically significant differences between the groups. Data is represented as mean ± SEM.

5.2.3 VLBW preterm neonates increased numbers of GPIb on the surface of their platelets compared to full-term neonates

Platelets interact with VWF under arterial shear conditions via their GPIbα receptors, which subsequently result in the activation of the integrin αIIbβ3 and adhesion of the platelet at the site of vascular damage (Savage et al., 1996, Zhang et al., 2014). It was observed using the DPFA that preterm neonates had greater numbers of platelets interacting but not adhering to VWF (Figure 5.1A and F). Therefore, in a subset of preterm (n=4) and full-term neonates (n=6), GPIb receptor count (CD42b) and GPIIIa (CD61) were measured (Figure 5.2). Platelets from preterm neonates had a significant increase in the number of GPIb on the surface of their platelets (48,000 ± 3868 versus 38,689 ± 1724; *$p < 0.05$). There was no significance difference in GPIIIa expression between VLBW preterms and full-term neonates (52,892 ± 3331 versus 53,208 ± 4436).

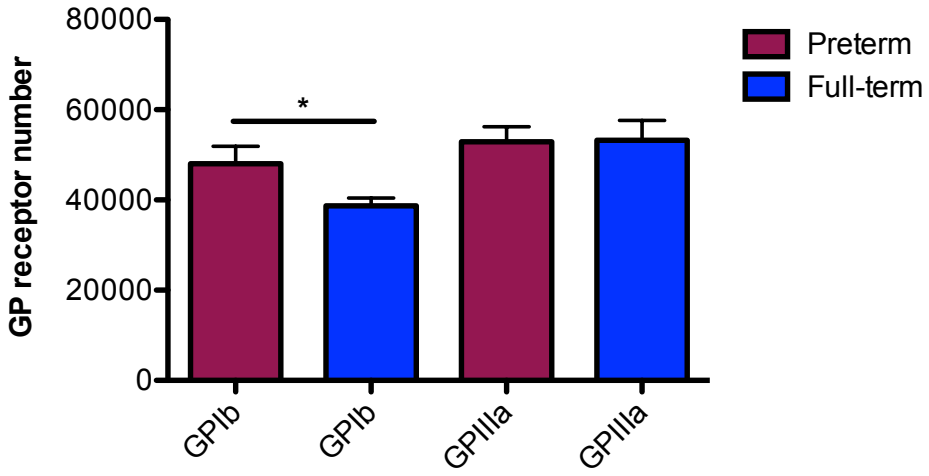

Figure 5.2 VLBW preterm neonates have increased levels of GPIb on their platelet surface. A BIOCYTEX platelet GP screen kit was used to quantify platelet receptor counts of GPIb and GPIIIa in blood samples from 4 preterms and 6 full-term neonates. The GPIb and GPIIIa were quantified using FITC-labelled CD42b and CD61 antibodies respectively. Preterm neonates had increased levels of GPIb (*$p < 0.05$). An unpaired t-test was used where appropriate to detect statistically significant differences between the groups. Data is represented as mean ± SEM.

5.2.4 VLBW preterm neonates with lower platelet counts have significantly reduced platelet interaction with VWF compared with preterms with higher platelet counts

IVH is a multifactorial process that occurs in preterm neonates with thrombocytopenia but repeatedly occurs in preterm neonates with normal platelet counts too (Sola-Visner, 2012). Thrombocytopenia is a common manifestation in preterm neonates (Gunnink et al., 2014). A six-year study of 47,291 neonates found that neonates in the lower reference range (5^{th} percentile; ≤ 32 weeks gestation) had platelet counts at 104 x 10^3 per µL of blood (Wiedmeier et al., 2009). This thesis, using the DPFA, examined the effect of platelet counts < 104 x 10^3 per µL of blood, on platelet behaviour on VWF in preterm neonates. Preterm neonates with platelet counts < 104 x 10^3 per µL of blood and HCT of 44 ± 3 (n=5) were compared with preterm neonates with platelet counts > 104 x 10^3 per µL of blood and HCT of 41 ± 1 (n=15). Platelet translocation behaviour was drastically reduced in those preterms at lower platelets counts (< 104 x 10^3 per µL of blood). Preterm neonates with lower platelet counts had a significant decrease in the numbers of platelet tracks (110 ± 24 versus 333 ± 29; ***p < 0.0001) and platelet translocation (71 ± 19 versus 230 ± 21; ***p < 0.0001). No significant difference was found in weighted median speed (3.5 ± 1.1 µm/sec versus 4.2 ± 0.3 µm/sec) in those preterms with lower platelet counts. However, preterm neonates with lower platelet counts displayed significantly reduced numbers of static platelets (31 ± 6 versus 78 ± 8; **p < 0.01), numbers of unstable platelet interactions (57 ± 18 versus 168 ± 22; *p < 0.05) with VWF and a reduction in the percentage of platelet surface coverage (2.5 ± 0.3 % versus 6.0 ± 0.4 %; ***p < 0.0001) (Figure 5.3).

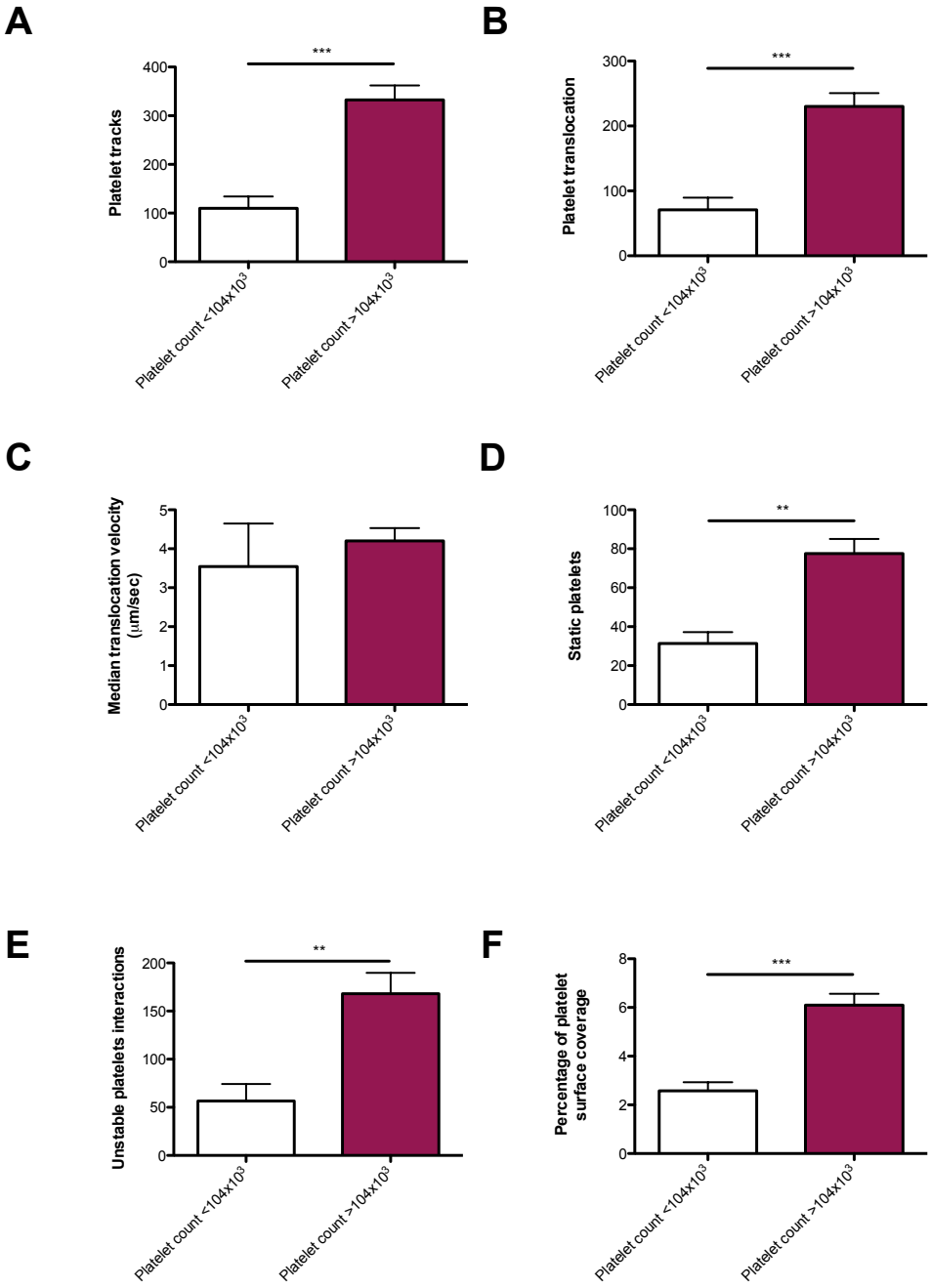

Figure 5.3 VLBW preterm neonates with lower platelet counts have significantly reduced platelet interactions with VWF. Blood from 5 preterm neonates with platelet counts < 104 x 10^3 µL of blood and 15 preterms with platelet counts > 104 x 10^3 µL of blood were perfused over VWF at arterial shear. Preterm neonates with platelet counts < 104 x 10^3 µL of blood displayed reduced platelet interactions with VWF (*p < 0.05, **p < 0.01 and ***p < 0.0001). An unpaired t-test and unpaired t-test with Welch's correction were used where appropriate to detect statistically significant differences between the groups. Data is represented as mean ± SEM.

5.2.5 Preterm neonates with HCT have significantly reduced platelet interactions with VWF compared with preterms with higher HCT.

Anaemia is common in preterm neonates in neonatal intensive care for a number of reasons including: decreasing red blood cell production, blood loss and increased red blood cell destruction (Aher et al., 2008). During the first week of life preterm neonates with anaemia (HCT < 28%) have a prolonged rate of bleeding (Sola et al., 2001). Therefore the effect of HCT in preterm neonates was assessed on the DPFA. Preterm neonates were identified with a platelet count of 177 ± 39 x 10^3 and an average HCT of 28% (n=6) and these were compared to preterms with a platelet count of 164 ± 44 x 10^3 and an HCT averaging 41% (n=15). Statistical analysis of the data confirmed that platelets from preterm neonates with lower HCT exhibited significantly reduced platelet translocation behaviour on VWF when compared preterm neonates with higher HCT. Preterm neonates with lower HCT had a significant decrease in the numbers of platelet tracks (162 ± 25 versus 333 ± 29; **p < 0.01), platelet translocation (99 ± 19 versus 230 ± 21; **p < 0.01) and weighted median speed (2.4 ± 0.2 µm/sec versus 4.2 ± 0.3 µm/sec; **p < 0.01). There was trend towards reduced numbers of static platelets (52 ± 8 versus 78 ± 8) in those preterms with lower HCT but this was not statistically significant. However, preterm neonates with lower HCT displayed a reduction in the numbers of unstable platelet interactions (60 ± 22 versus 168 ± 22; ***p < 0.0001) with VWF and a decrease in the percentage of platelet surface coverage (3.7 ± 0.4 % versus 6.0 ± 0.4 %; **p < 0.01) (Figure 5.4).

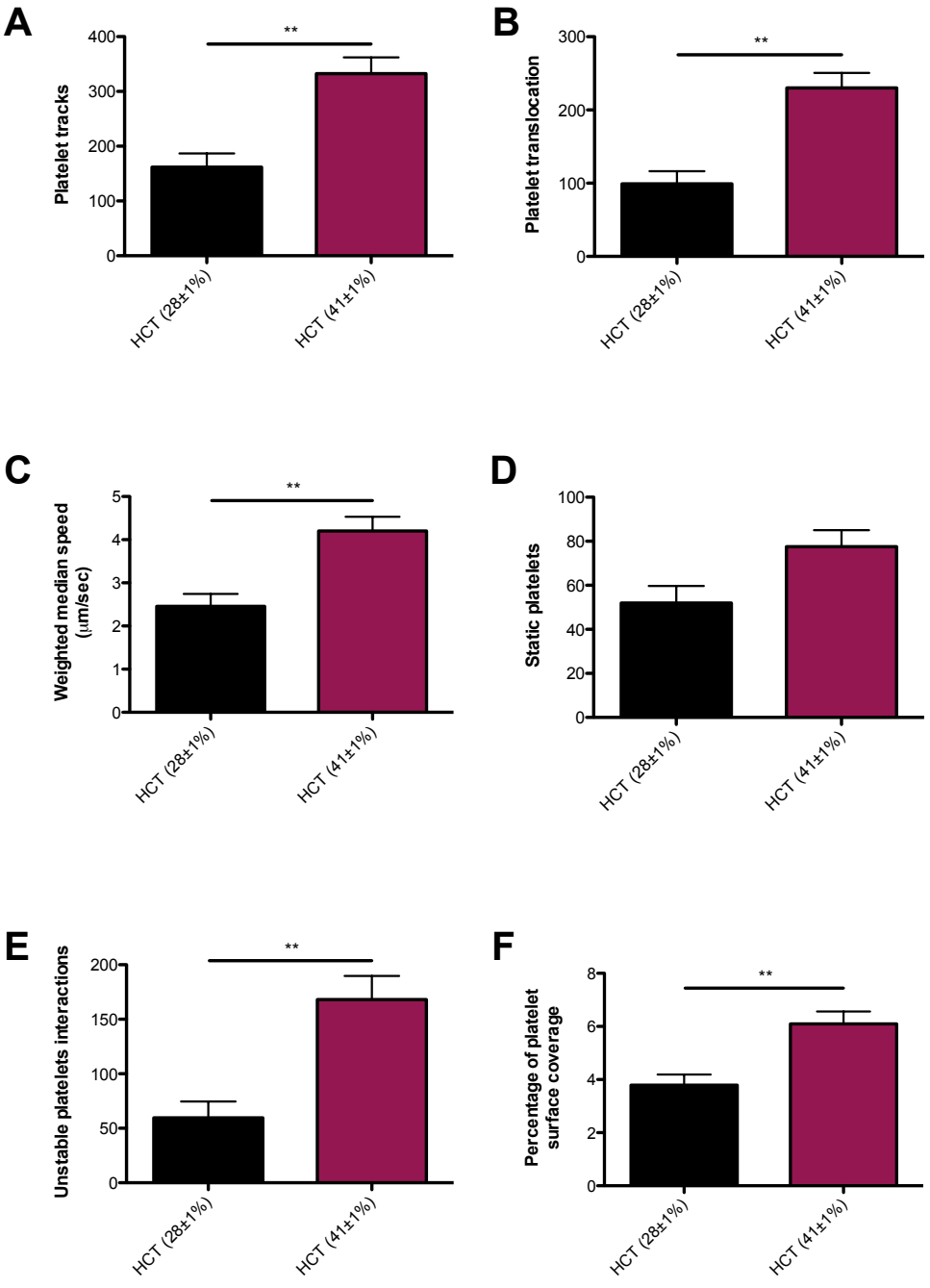

Figure 5.4 Preterm neonates with lower HCT have significantly reduced platelet interactions with VWF. Blood from 6 preterm neonates with lower HCT and 15 preterms with higher HCT was perfused over VWF at arterial shear. Preterm neonates with lower HCT had significantly reduced platelet interaction with VWF (*$p < 0.05$, **$p < 0.01$ and ***$p < 0.0001$). An unpaired t-test and unpaired t-test with Welch's correction were used where appropriate to detect statistically significant differences between the groups. Data is represented as mean ± SEM.

5.3 Discussion

Platelet function in neonates is not well understood. In this chapter, platelet function was investigated in VLBW preterm and full-term neonates using the DPFA and in smaller subset of preterm and full-term neonates, using flow cytometry. The DPFA was used to assess platelet translocation behaviour on VWF. Platelet membrane glycoproteins GPIb (CD42b) and GPIIIa (CD61) were also quantified which are responsible for platelet adhesion to VWF (Savage et al., 1996). The major findings were that: (1) preterm neonates have significantly different platelet translocation behaviour on VWF; (2) preterm neonates have greater expression numbers of GPIb receptor on their platelet surface; (3) preterm neonates with lower platelet or HCT display reduced platelet interaction with VWF.

VLBW preterms are at a higher risk of bleeding than full-term neonates (Sola-Visner, 2012). Platelet dysfunction may contribute to an increased incidence of bleeding in this group (Michelson, 1998). Platelet activation studies have confirmed that neonates are hyporesponsive to agonists such as epinephrine, ADP and thrombin compared with healthy adults (Israels et al., 2003). The evidence suggests that preterms have more pronounced platelet hyporesponsiveness than full-term neonates. This is consistent with studies demonstrating that preterm neonates have decreased platelet adhesion and prolonged bleeding times compared to full-term neonates (Boudewijns et al., 2003, Levy-Shraga et al., 2006, Del Vecchio et al., 2008). Inhibition of platelet function using cyclooxygenase inhibitors, indomethacin and ibuprofen, has previously been demonstrated, using ultrasound examinations, to increase bleeding incidence in preterm neonates with patent ductus arteriosus (PDA) (Brunner et al., 2013).

VWF plays a crucial role in mediating the initial platelet adhesion at the site of vascular injury which ceases bleeding (Chen and Lopez, 2005). It was therefore investigated whether platelet interactions with VWF were significantly different between VLBW preterms and full-term neonates under flow conditions. There are relatively few studies examining platelet adhesion to vascular proteins under conditions of flow in neonates. Cone and plate studies demonstrate that preterms

have decreased platelet adhesion to extracellular matrix (ECM) to that of full-term neonates (Linder et al., 2002, Levy-Shraga et al., 2006). Although, these assays provide useful information on platelet function, they rely on a single end point analysis rather than direct measurement of platelet interaction in 'real-time'. Therefore, through the use of the DPFA it was possible to assess multiple parameters of platelet translocation behaviour and characterise platelet profiles for both preterm and full-term neonates.

Assessment of platelet translocation behaviour on VWF in preterm and full-term neonates demonstrated that preterm neonates displayed altered platelet function. Interestingly, it was identified that platelets from preterm neonates exhibited increased numbers of platelet tracks, platelet translocation, platelet translocation velocities and unstable platelet interactions with VWF. The increased numbers of platelet tracks in preterm infants was likely to be a consequence of increased numbers of GPIb on the platelet surface which would facilitate platelet interaction with immobilised VWF. However, in a subset of preterm and full-term neonates (n = 5 and n =6 respectively), no significant difference in mean platelet volume was observed (9.6 ± 0.8 versus 9.0 ± 0.8). Therefore, it is unlikely that the platelet size significantly influenced the receptor numbers of GPIb measured in this thesis. Despite preterm neonates having increased numbers of platelets interacting with VWF, as measured by the number of platelet tracks, neither the percentage of platelet surface coverage nor the numbers of static platelets on VWF were significantly greater in preterm neonate cohorts. There was a significant increase observed in the numbers of unstable platelet interactions (e.g. those that interact with VWF but do not adhere). Both of the above findings combined may imply that the adhesiveness of platelets to VWF is decreased in preterm neonates. Platelets need to activate integrin αIIbβ3 for platelets to adhere to VWF (Savage et al., 1996) and this reduced adherence may be related to impaired αIIbβ3 function. This hypothesis is supported by PAC-1 binding studies (PAC-1 binds activated αIIbβ3) in platelets from VLBW preterm neonates stimulated with thrombin receptor agonist peptide (TRAP), showed reduced binding efficiency of PAC-1 to αIIbβ3 (Sitaru et al., 2005). The reduced activation of αIIbβ3 may explain why platelet translocation

velocities are significantly increased in preterm neonates. In chapter 3, it was demonstrated using the DPFA that MRS2179 (selective $P2Y_1$ inhibitor) leads to significant increases in platelet translocating velocities. MRS2179 inhibits platelet shape change and calcium mobilisation, thus impairing the ability of platelets to activate (Baurand et al., 2001). The increased platelet translocating velocities may be reflective of the more pronounced platelet hyporeactivity observed in preterm populations. RBC's as measured by mean corpuscular volume were also found to be significantly larger in preterm infants than those in full-term neonates (107.3 ± 5.5 versus 101.7 ± 4.7, **$p < 0.01$). The size of the RBCs may potentially play a role in alternating how platelets behave on VWF but this warrants further investigation in the future.

Preterm neonates with lower platelet counts or lower HCT exhibited significantly reduced platelet translocation behaviour on VWF in comparison to preterm neonates with higher platelet counts or HCT. This finding is consistent with the data presented in chapter 3 which demonstrated that a reduction in platelet or HCT count significantly impairs platelet adhesion to VWF. Reductions in HCT have previously been demonstrated to inhibit platelet adhesion to VWF (Chen et al., 2013). In this thesis, it was observed that platelet interactions with VWF were decreased in those preterms with lower platelet or HCT count. Also, it was observed that the number of unstable platelet interactions was decreased in those preterms with lower platelet or HCT. This reduction is likely to be caused by the reductions in the numbers of platelets interacting with the surface. This is further validated by the significant decrease observed in platelet surface coverage in those preterms with lower platelet or HCT count.

As shown in this thesis, preterm neonates display increased numbers of platelets interacting with VWF compared to full-term neonates. This may be a compensatory mechanism to counteract the pronounced hyporeactivity in preterm neonate populations. This compensatory mechanism is not possible in those neonates with lower platelet or HCT and therefore may help explain why bleeding risk in those preterms with thrombocytopenia and anaemia, is significantly greater than in those

preterms with normal platelet and HCT count (Sola-Visner, 2012). Such results complement the findings by Sola et al., (2001) highlighting that those preterm neonates with the lower HCT (< 28%) experience the longest bleeding times.

This work presented in this thesis demonstrates, for the first time, that VLBW preterm neonates have significantly different platelet translocation behaviour on VWF compared with full-term neonates. Preterm neonate platelets display reduced adherence to VWF with a significant increase in platelet translocating velocity. To counteract this more pronounced hyporeactivity observed in preterm neonates and reduced platelet adherence to VWF, preterm neonates may increase the numbers of platelets that interact with VWF (platelet tracks). These differences in platelet function may contribute to the higher incidences of bleeding observed in preterm neonate populations.

Chapter 6

Platelet translocation behaviour in pregnancy and utero-placental disease

6.1 Introduction

The role of platelets in haemostasis and thrombosis is well established. More recently it has been identified that platelets serve as potential mediators in the formation of a normally functioning placenta (Sato et al., 2005, Bodis et al., 2014, Sato et al., 2010). It has been reported that alterations in platelet-mediated placentation may contribute to the development of utero-placental conditions including intrauterine growth restriction (IUGR) (Norris et al., 1994, Mullers, 2015), pregnancy induced hypertension (PIH) (Morrison et al., 1985) and preeclampsia (PET) (Stubbs et al., 1986, Janes and Goodall, 1994, Norris et al., 1993). Moderate success has been reported with the use of anti-platelet therapy in preventing recurrent utero-placental disease (Askie et al., 2007).

Pregnancies complicated by growth restriction and hypertension pose a significant risk to both mother and fetus, and these conditions contribute significantly to maternal morbidity, mortality and the sequelae of prematurity (National Clinical Practice Guideline No.29, 2014). Additionally, the link between the later development of cardiovascular disease and a history of either fetal growth restriction or hypertension in pregnancy is well established (Smith et al., 2014).

PIH is defined by hypertension of ≥ 140/90 occurring after 20 weeks gestational age, and when proteinuria is present, PET ensues (NICE guideline No. 62, 2006). It is the defective and shallow placentation occurring in early pregnancy that is thought to result in a spectrum of utero-placental conditions. It may either uniquely effect the fetal-placental interface resulting in IUGR; the materno-placental interface with resulting PIH and PET, and in some cases both (Mullers 2015, personal communication, Rotunda hospital Dublin).

There is no single biomarker currently in existence with sufficient power to predict the development of IUGR, PIH and PET conditions early in pregnancy. Therapy such as aspirin could be prescribed to potentially encourage healthy placentation and thus prevent short and long-term complications for both mother and fetus. In an effort to characterise platelet behavior in pregnancy and develop a screening tool,

previous authors have embarked on a number of studies investigating platelet function in pregnancy (Morrison et al., 1985, Horn, 1991, Norris et al., 1993, Norris et al., 1994, Nicolini et al., 1994, Nadar and Lip, 2004, Gatti et al., 1994, Star et al., 1997, Can et al., 2010). The results of these studies are inconsistent, not least due to a lack of standardisation of the methodology of platelet function testing used (Cattaneo et al., 2013). More recently, a modified version of light transmission aggregometry (LTA) was used to assess platelet function in normal pregnancy and the common pregnancy conditions IUGR, PIH and PET by our collaborating research team at the Rotunda hospital Dublin (Burke et al., 2013). This assay uses a 96-well plate to examine platelet reactivity in response to multiple sub-maximal concentrations of agonists. When compared with aged-matched non-pregnant controls, platelet reactivity was found to be significantly reduced in first trimester normal pregnancies, increasing as gestational age advanced. When investigating platelet function in pregnancies complicated with either hypertensive conditions or fetal growth restriction, platelet reactivity was found to be significantly reduced compared to that of healthy third trimester pregnant controls (Mullers, 2015). However, LTA does not replicate the flow and shear environment that platelets are exposed to *in vivo*. Therefore, the Dynamic Platelet Function Assay (DPFA) was employed to comprehensively investigate platelet function under arterial shear conditions in both normal pregnancies and pregnancies complicated by placental disease.

In this chapter, I will discuss platelet function in:

- Age-matched females who are not pregnant with those in the third trimester of a healthy pregnancy.
- Healthy pregnancy and pregnancy with IUGR.
- Healthy pregnancy and pregnancy with PIH.
- Healthy pregnancy and pregnancy with PET.

6.2 Results

6.2.1 Study populations

The study enrolled a total of 32 females who were not pregnant, 21 third trimester healthy pregnancies, 23 third trimester pregnancies with IUGR, 16 third trimester pregnancies PIH and 27 third trimester pregnancies with PET. Haematocrits (HCT) were significantly reduced in the pregnancy groups in comparison to non-pregnant controls ($p < 0.01$**). There was a trend towards a decreased platelet count in pregnancy but this was found to note be statistically significant. The demographics of the study populations are outlined in Table 6.1

Table 6.1 Demographics of study populations

Demographics		No pregnancy n = 32	Healthy pregnancy Control n = 21	Intra-uterine growth restriction n = 23	Pregnancy-induced hypertension n = 16	Pre-eclampsia n = 27
Age (years)		21-38	19-47	19-47	17-37	20-43
Platelet count (x10^3 per µL)		215 (120-387)	171 (107-266)	156 (99-223)	157 (118-234)	141 (64-277)
HCT (%)		38 (20-46)	31 (26-45)*	31 (25-38)*	30 (22-37)*	32 (16-48)*
Nulliparous (%)		-	36% (8/22)	45% (10/23)	44% (7/16)	70% (19/27)
BMI		-	25.2 (19-34)	26 (18-40)	29 (22-36)	29 (20.5-40)
Caucasian ethnicity (%)		-	91% (20/22)	96% (22/23)	94% (15/16)	85% (23/27)
IVF pregnancy (%)		-	5% (1/22)	9% (2/22)	0%	11% (3/27)
History of IUGR (%)		-	0%	26% (6/23)	6% (1/16)	7% (2/27)
History of PIH/PET (%)		-	0%	9% (2/23)	44% (7/16)	19% (5/27)
History of essential HTN (%)		-	0%	0%	13 % (3/13)	26% (7/27)
Smokers (%)		-	9% (2/22)	22% (5/23)	6% (1/16)	11% (3/27)
GA at diagnosis (Wks, days)		-	N/A	30+2 (20-39+6)	37+1 (32-40+6)	36+1 (28-40+6)
Antihypertensive medication (%)		-	0%	4% (1/23)	69% (11/16)	60% (16/27)
GA at blood draw (Wks, days)		-	36+1 (28-40+7)	34+2 (27-39+6)	37+2(33-40+6)	36+2 (29-40+6)
GA at delivery (Wks, days)		-	40+2 (37-41+6)	37+2 (30-39+6)	39+3 (36-40+7)	37+2 (29-40+6)
Birth weight (g)		-	3610 (3010-4400)	2100 (1090-2970)	3309 (2040-4860)	2827 (1008-4410)
Estimated blood loss (mls)		-	345 (150-1150)	339 (150-800)	330 (200-700)	412 (200-800)
Blood group:	**O-**	-	9% (2/22)	13% (3/23)	6% (1/16)	4% (1/27)
	O+	-	55% (12/22)	35% (8/23)	38% (6/16)	33% (9/27)
	B-	-	0%	13% (3/23)	6% (1/16)	7% (2/27)
	B+	-	5% (1/22)	4% (1/23)	0%	19% (5/27)
	A-	-	5% (1/22)	4% (1/23)	0%	4% (1/27)
	A+	-	27% (6/22)	22% (5/23)	38% (6/16)	30% (8/27)
	AB-	-	0%	0%	6% (1/16)	0%
	AB+	-	0%	9% (2/23)	6% (1/16)	4% (1/27)

***** Pregnancy was within the normal ranges for the healthy donors, however, on average pregnancy resulted in a significant decrease in HCT

6.2.2 Platelet function in healthy pregnancy

Platelets from females who were not pregnant (n=32) exhibited significantly different platelet translocation behaviour on VWF when compared with healthy females in the third trimester of pregnancy (n=21). In particular, it was observed that healthy pregnant females had a significant decrease in the number of platelet tracks (271 ± 20 versus 426 ± 20; ***p < 0.0001), platelet translocation (165 ± 10 versus 290 ± 14; ***p < 0.0001) and a reduction in weighted median speeds (2.4 ± 0.2 µm/sec versus 4.8 ± 0.4 µm/sec; ***p < 0.0001). However, when comparing the results of healthy pregnant females to non-pregnant females, no significant differences were observed in the number of static platelets (91 ± 8 versus 93 ± 6) or in the numbers of unstable platelet interactions (93 ± 14 versus 123 ± 11) on VWF. Nonetheless, it was identified that pregnant females had a significant decrease in the percentage of platelet surface coverage (5.5 ± 0.3 % versus 7.9 ± 0.5 %; ***p < 0.0001) (Figure 6.1).

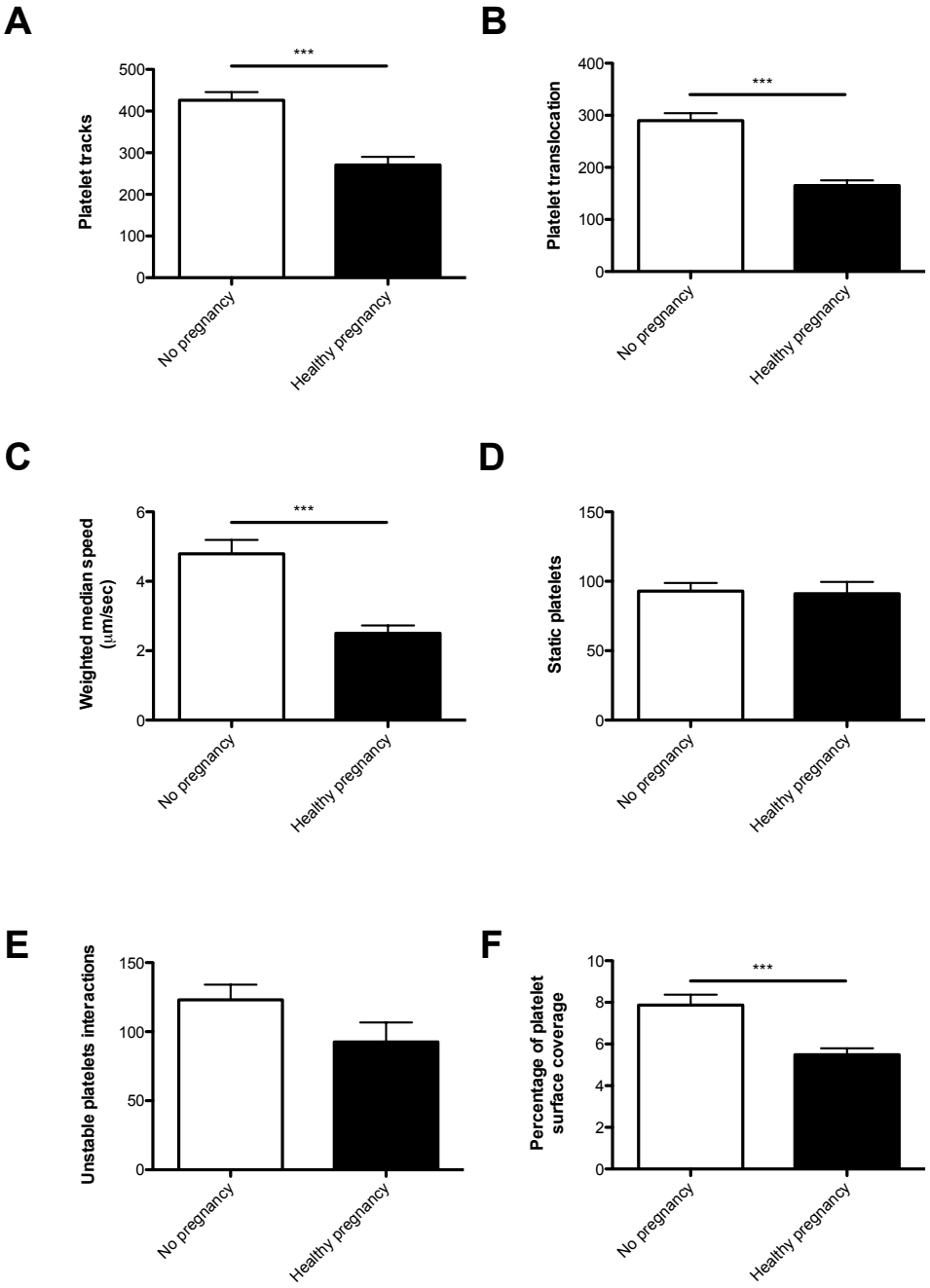

Figure 6.1 Platelet function in non-pregnant and pregnant females. Blood from 32 non pregnant females and 21 pregnant females in the third trimester of pregnancy was perfused over VWF at arterial shear. Pregnant females showed a significant change in platelet translocation behaviour on VWF (*$p < 0.05$, **$p < 0.01$ and ***$p < 0.0001$). An unpaired t-test and unpaired t-test with Welch's correction was used where appropriate to detect statistically significant differences between the groups. Data is represented as mean ± SEM.

6.2.3 Platelet function in pregnancy with IUGR

In pregnancy with IUGR (n=23) when compared with healthy pregnancy (n=21) there were no significant differences in the number of platelet tracks (238 ± 21 versus 271 ± 20), platelet translocation (160 ± 15 versus 165 ± 10) or in weighted median speeds (2.3 ± 0.1 μm/sec versus 2.5 ± 0.2 μm/sec). However, in pregnancy with IUGR there was a significant reduction in the numbers of static platelets (68 ± 6 versus 91 ± 8; *$p < 0.05$). Notably in pregnancy with IUGR there were no significant differences in either the numbers of unstable platelet interactions (72 ± 8 versus 93 ± 14) with VWF or in the percentage of platelet surface coverage (4.9 ± 0.3 % versus 5.4 ± 0.3 %) (Figure 6.2).

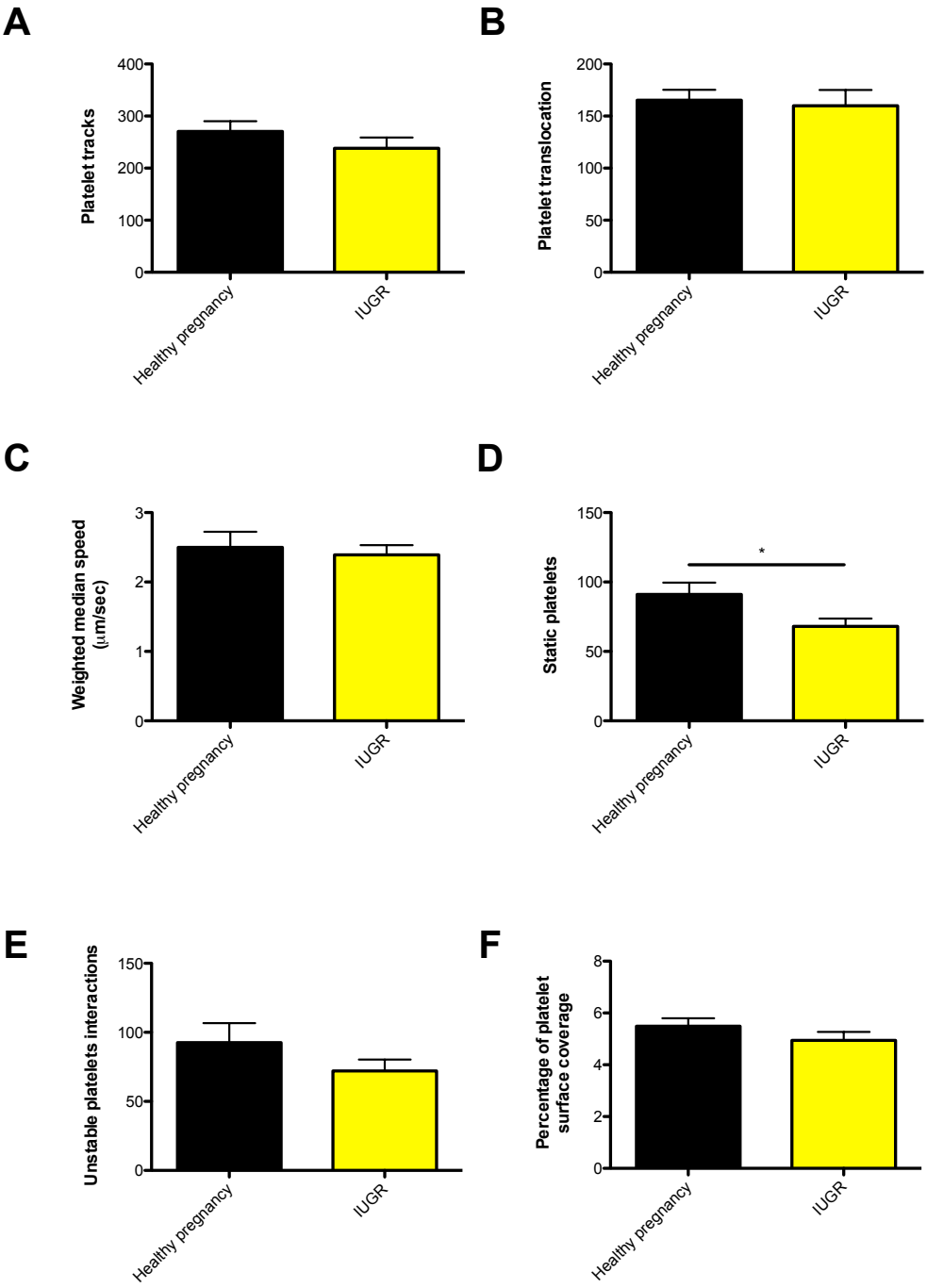

Figure 6.2 Platelet function in pregnant females with IUGR. Blood from 21 pregnant females with no IUGR and 23 pregnant females with IUGR was perfused over VWF at arterial shear. Pregnancy with IUGR resulted in a significant reduction in the number of platelets that stably adhere to VWF (*$p < 0.05$). An unpaired t-test and unpaired t-test with Welch's correction was used where appropriate to detect statistically significant differences between the groups. Data is represented as mean ± SEM.

6.2.4 Platelet function in pregnancy with PIH

In pregnancy with PIH (n=16) when compared with healthy pregnancy (n=21) there was significantly reduced platelet translocation behaviour on VWF. Notably when comparing pregnancy with PIH with healthy pregnancy there were significant reductions in the number of platelet tracks (208 ± 18 versus 271 ± 20; *$p < 0.05$) and platelet translocation (133 ± 12 versus 165 ± 10; *$p < 0.05$) on VWF. No significant difference was observed in weighted median speeds (2.2 ± 0.2 µm/sec versus 2.5 ± 0.2 µm/sec) on VWF between PIH and healthy pregnancy. However, pregnancy with PIH compared to healthy pregnancy, demonstrated a significant decrease in the number of static platelets (59 ± 5 versus 91 ± 8; **$p < 0.05$) and in the number of unstable platelet interactions (52 ± 7 versus 93 ± 14; *$p < 0.05$). There was no significant reduction in the percentage of platelet surface coverage (4.8 ± 0.3 versus 5.4 ± 0.3 %) in pregnancy with PIH (Figure 6.3).

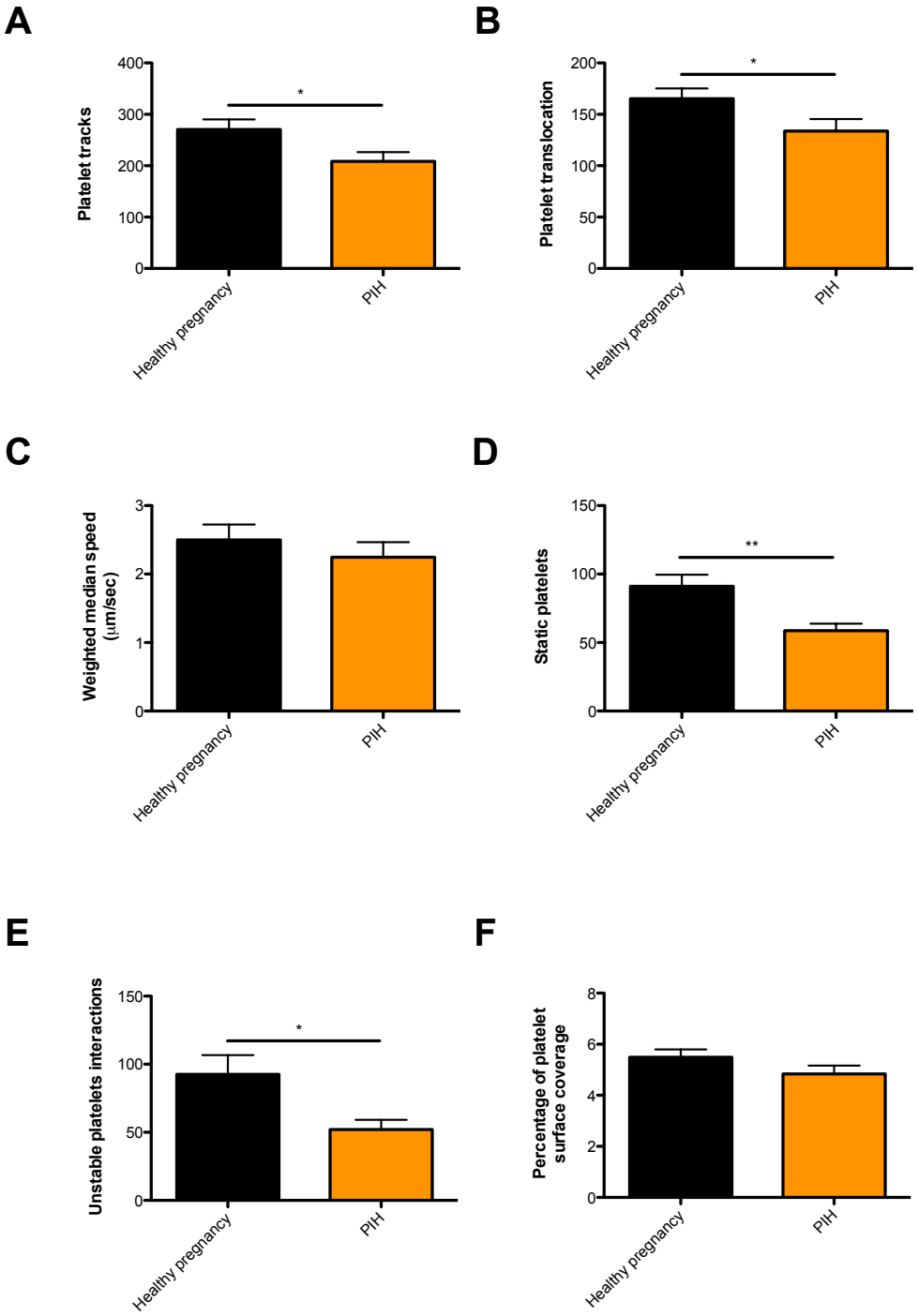

Figure 6.3 Platelet function in females with PIH. Blood from 21 females with no PIH and 16 pregnant females with PIH was perfused over VWF at arterial shear. Pregnancy with PIH resulted in a significant reduction in platelet translocation behaviour on VWF (*$p < 0.05$ and **$p < 0.01$). An unpaired t-test and unpaired t-test with Welch's correction was used where appropriate to detect statistically significant differences between the groups. Data is represented as mean ± SEM.

6.2.5 Platelet function in pregnancy with PET

In pregnancy with PET (n=27) when compared with healthy pregnancy (n=21) there was a significantly reduced platelet translocation behaviour on VWF. Also in pregnancy with PET when compared with healthy pregnancy there was a significant reduction in the number of platelet tracks (187 ± 10 versus 271 ± 20; **p < 0.01) and platelet translocation (117 ± 8 versus 165 ± 10; **p < 0.01). No significant change was observed in weighted median speeds (μm/sec 2.3 ± 0.2 versus 2.5 ± 0.2 μm/sec) in PET versus healthy pregnancy. However, in pregnant females with PET there was a significant decrease in the number of static platelets (61 ± 5 versus 91 ± 8; **p < 0.05) and the number of unstable platelet interactions (59 ± 7 versus 93 ± 14; *p < 0.05) with VWF. In pregnancy with PET there was a trend towards a decreased percentage of platelet surface coverage (4.7 ± 0.3 versus 5.4 ± 0.3 %) in PET, but this was not statistically significant (Figure 6.4).

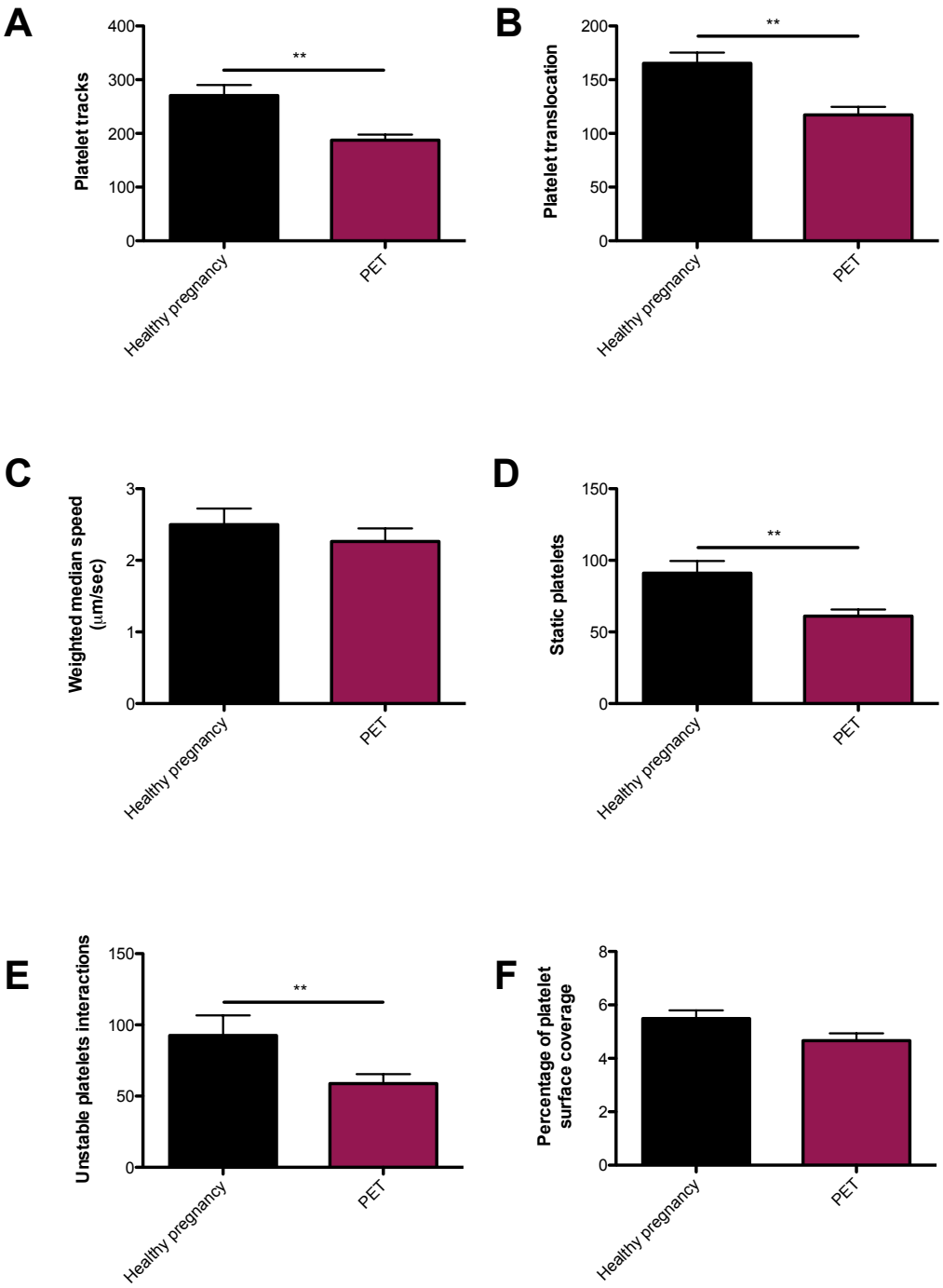

Figure 6.4 Platelet function in females with PET. Blood from 27 pregnant females with PET and 21 pregnant females with healthy pregnancy was perfused over VWF at arterial shear. Pregnancy with PET resulted in a significant reduction in platelet translocation behaviour on VWF (*$p < 0.05$ and **$p < 0.01$). An unpaired t-test and unpaired t-test with Welch's correction were used where appropriate to detect statistically significant differences between the groups. Data is represented as mean ± SEM.

6.3 Discussion

In this chapter, the results demonstrate that platelet function significantly changes during pregnancy. Pregnancy results in an increase in platelet reactivity as demonstrated by a significant reduction in platelet translocation speeds on VWF compared with non-pregnant controls. In utero-placental diseases such as IUGR, PIH and PET, platelet translocation behaviour on VWF is significantly altered compared to normal healthy pregnant controls. These changes in platelet function maybe reflective of platelet impairment, which was found to be greatest for those pregnancies complicated by PET.

The literature reports on a number of platelet studies, with overall inconsistent results. There are some studies that suggest platelet reactivity increases during pregnancy (Gerbasi et al., 1990, Holmes et al., 2002). Fitzgerald et al., (1987) Indicated that platelet-derived thromboxane is increased in pregnancy. Robb et al., (2010) demonstrated that pregnancy resulted in an increase in the platelet activation marker P-selectin. More recently, using the LTA 96-well plate assay, Burke et al., (2013) established that platelet reactivity was significantly reduced in the first trimester of pregnancy compared with non-pregnant controls and subsequently increased during the second and third trimester of pregnancy in comparison with non-pregnant controls. Building on in this initial body of work, the purpose of this element of the thesis was to apply the DPFA to pregnancy subjects, to describe platelet behavior in-vivo, as evidenced by multiple platelet parameters, and to assess a more physiological aspect of platelet function in healthy third trimester pregnant females compared with age-matched non-pregnant controls. The results demonstrated that in pregnancy, there is a significant reduction in platelet interactions with VWF as shown by significantly less platelet tracks. This is most likely due to an expected reduction in HCT in pregnancy compared with non-pregnant controls (Table 6.1). As part of the normal physiological changes in pregnancy, haemodilution reduces the concentration of red blood cells in circulation (Faupel-Badger et al., 2007). As shown in chapter 3, reducing HCT impairs platelet adhesion to VWF. Interestingly, in this thesis it was observed that platelet translocation speeds were significantly reduced in pregnancy which maybe reflective

of enhanced platelet reactivity. It is reasonable to suggest that the enhanced platelet reactivity reduces the time taken for platelets to adhere to VWF, thereby reducing platelet translocation speeds. This is further validated with the observation that despite having a dramatic reduction in the number of platelets interacting with VWF, there were no significant differences in either the number of static or unstable platelet interactions with VWF between both groups.

As previously described, Burke et al., (2013) demonstrated decreased platelet reactivity compared to non-pregnant controls in the first trimester of healthy pregnancy. It has been speculated that such reduced platelet reactivity may facilitate a fundamental spiral artery invasion, without the unwanted coagulation cascade (Mullers 2014, personal communication Rotunda Hospital Dublin). Maternal spiral artery invasion is a vital step in the development of a healthy placenta, with complications in this process believed to result in IUGR and PET (Lyall et al., 2013). Platelet hyperreactivity has previously being reported in PET in early placentation with utero-placental disease (Janes and Goodall, 1994). This finding supports the role of low dose aspirin in preventing defective placentation in early pregnancy (Bujold et al., 2010). Platelet activation may well be increased early in pregnancies destined to develop with utero-placental disease, unfortunately longitudinal studies from first trimester through to third trimester are considerably lacking and are warranted.

A further number of studies have concluded that platelet reactivity is reduced in pregnancies with established IUGR, PIH and PET (Peracoli et al., 2008, O'Brien et al., 1986, Norris et al., 1993, Norris et al., 1994, Mullers, 2015). These studies were carried out in the third trimester of pregnancy and assessed platelet function by measuring TGF-beta levels (Peracoli et al., 2008) or agonist-induced platelet aggregation (O'Brien et al., 1986, Norris et al., 1993, Norris et al., 1994, Mullers, 2015). The finding of platelet hyporeactivity has been suggested to reflect granule depletion, and this may directly describe a platelet release reaction for these conditions (O'Brien et al., 1986).

A number of authors have concluded that platelet activation is increased in these conditions such as IUGR, PIH and PET (Konijnenberg et al., 1997, Morrison et al., 1985, Sheu et al., 2002, Janes and Goodall, 1994) citing the clinical condition of vasoactive substance release in hypertensive disease in pregnancy to explain these results. Further to this, a number of authors correlated both measures of platelet activation with platelet functional assays, and felt that while markers of platelet activation may be increased, this may represent a platelet releasate reaction, culminating in overall reduced platelet function in utero-placental disease (Peracoli et al., 2008, Morrison et al., 1985, Norris et al., 1994). As previously discussed, studies of platelet function in pregnancy to date are fraught with inconsistencies in the methodology used to assess platelet function, and are therefore difficult to compare. Furthermore, the platelet aggregation studies cited here have used either a limited number of agonists, or maximal concentrations of agonists, and were not designed to assess platelet function under shear conditions.

In this thesis, using a near-physiological assay of platelet function under arterial shear, it has been demonstrated that platelet behavior is significantly altered across a range of platelet interactions on VWF in utero-placental disease. Pregnancy with IUGR was associated with a significant reduction in the number of static platelets (i.e. those platelets that travel less than 1.5 times the average radius of the platelet). Pregnancies with PIH and PET resulted in multiple changes in platelet translocation behaviour on VWF, such as reductions in platelet tracks, translocating platelets, static and unstable platelet interactions with VWF. These changes in platelet function were more pronounced in the PET group, which is not surprising considering PET represents a more severe clinical form of utero-placental disease. These changes in platelet function may be representative of a gross platelet function impairment.

Overall the results of this study are consistent with the concept that pregnancy results in a significant increase in platelet reactivity which is compensated by a significant reduction in HCT. Utero-placental disease is associated with an

impairment in platelet function. This impairment is most apparent in those pregnant females with PET.

In this thesis, third trimester pregnancies were selected as utero-placental disease was well established. Utero-placental disease can often be challenging to diagnose early in pregnancy. Therefore, this chapter set out to determine whether the DPFA could pick up subtle changes in platelet function in known cases of placental disease. However, to predict development of these conditions (IUGR, PIH, PET), platelet function should be assessed early in pregnancy. As a next logical step, it is proposed that applying this assay in a large cohort across the three trimesters of pregnancy, with the view to refining a screening tool that will identify cases that will ultimately benefit from early intervention with antiplatelet therapy.

Chapter 7

Development of a synthetic surface to capture VWF from human plasma

7.1 Introduction

Von Willebrand Factor (VWF) circulates in human plasma at concentrations of approximately 10 μg/mL (Mannucci, 1998) However, the concentration of VWF in human plasma can differ significantly between individuals (Franchini et al., 2014), with deficiencies resulting in the onset of von Willebrand disease (VWD). VWD is the most common bleeding disorder globally, affecting 1% of the population (James and Goodeve, 2011). The gold standard test for diagnosing VWD is measurement of VWF activity via platelet agglutination in the presence of the antibiotic Ristocetin (VWF:RCo) (Roberts, 2014). There are 4 types of VWD (Type I, Type II, Type III and acquired VWD). The conventional tests are regarded as being inaccurate and can often lead to the misdiagnosis of patients; in particular diagnosis of Type I VWD (Roberts, 2014). Type I VWD is the most common form of VWD and accounts for 75 % of patients diagnosed with the disease. Type I VWD results in minor bleeding due to the production of insufficient amounts of VWF (Sadler, 2003). Type I VWD can be challenging to diagnose, for example, individuals who are blood group O (lowest VWF levels) are sometimes diagnosed as having Type I VWD but have normal VWF levels for their blood group (Branchford and Di Paola, 2012, Gill et al., 1987*)*. The same is also possible for individuals who are blood group AB (highest levels of VWF) who are classed as normal but in reality have Type I VWD (Gill et al., 1987, Branchford and Di Paola, 2012).

There are currently no diagnostic tests available to assess how VWF behaves in the vasculature under shear conditions. Although the Dynamic Platelet Function Assay (DPFA) is capable of detecting subtle changes in platelet function, a limitation of the assay is that it does not use autologous VWF to measure platelet function. An element of this thesis was to demonstrate the proof of concept for development of a novel synthetic surface that mimics collagen, and which is capable of capturing donor-specific VWF from blood plasma as a means of recruiting platelets from the same donor in an autologous manner.

In this chapter, I will:

- Identify a feature size in a topographically-defined surface that captures VWF
- Determine whether platelet adhesion on this surface is dependent on the capture of VWF in the first instance
- Determine if increased concentrations of VWF result in more platelet adhesion

7.2 Results

7.2.1 Optimisation of polymer surfaces for capture of VWF from flowing blood

Previous work by Minelli et al., (2008) demonstrated that a surface coated with de-mixed solution of poly(methyl methacrylate) PMMA / polystyrene had the ability to capture VWF in a microfluidic device, through an unknown mechanism from flowing blood. The scope of the first part of this experimental work was to replicate a topographically-defined surface which could facilitate the capture of VWF under arterial shear. Polymer solutions comprised of 1%, 3% and 5% (w/v) PMMA and polystyrene micro-beads were resuspended in chloroform at a ratio of 50:50 prior to spin-coating onto glass coverslip surfaces. These were subsequently allowed to air-dry, which resulted in the formation of nanostructures of different sizes. Larger concentrations of polymer solution were predicted to produce larger nanostructures. Platelet adhesion to each of the 1%, 3% and 5% polymer de-mixing solutions under arterial shear flow was assessed (Figure 7.1). There was no significant difference in platelet adhesion to either of the polymer solutions selected for analysis. However, a 3% polymer de-mixing concentration had on average the best platelet adhesion (n=7; 5.5% versus 9.9% versus 7.4%).

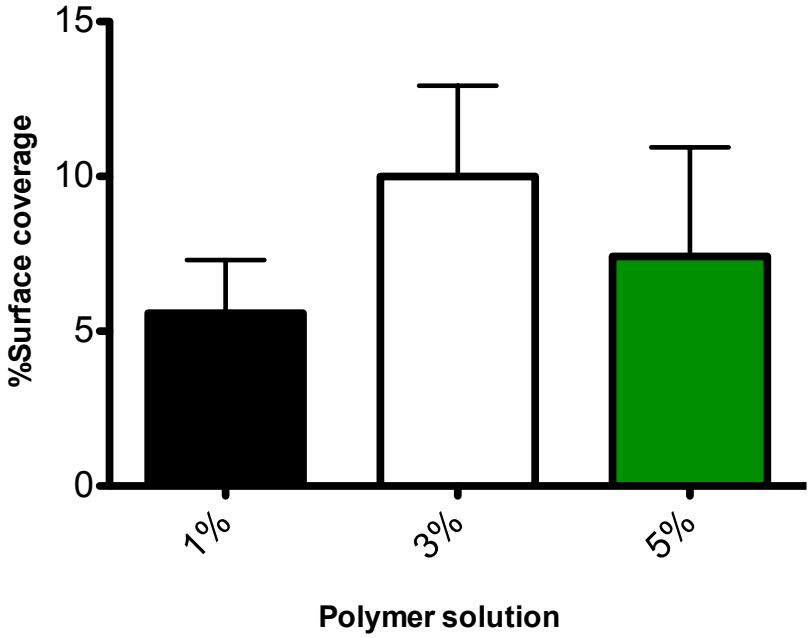

Figure 7.1 The 3 % de-mixing polymer solution has the greatest platelet adhesion. Blood from 7 healthy donors was perfused over each of the polymer de-mixing surfaces 1%, 3% and 5% under arterial shear conditions. A single end-point image was taken after 5 minutes of perfusion of blood. The 3% polymer surface on average had the greatest platelet adhesion. A Kruskal-Wallis test was used to detect statistically-significant differences across the varying polymer concentrations. Data is represented as mean ± SEM.

7.2.2 The polymer surface captures platelets from flowing blood via the A1-VWF platelet-GPIbα interaction

Further experimentation was carried out on the 3% (w/v) polymer surface based on the observation that this surface on average captured the greatest numbers of platelets. Furthermore, the scope of subsequent experiments was to determine whether the interactions of platelets with the polymer surface were VWF-platelet specific. To determine this, blood from 3 healthy donors was perfused over the polymer surface in the presence and absence of the GPIbα-specific antibody AK2. AK2 binds to the GPIbα, thereby blocking the platelets interaction with the A1 domain of VWF. It was observed that platelet adhesion to the surface was inhibited in those samples treated with antibody AK2 (Figure 7.2a). To further check the specificity of the surface to capture VWF under arterial shear conditions, a VWF-A1 specific antibody CR1 was used. CR1 has previously been demonstrated to block the A1 domain of VWF (Dong et al., 2001). Blocking this domain should prevent platelet adhesion to the polymer surface. Blood from 3 healthy donors was then perfused over the polymer surface, with or without the VWF-A1 specific antibody CR1. Platelet adhesion to the surface was inhibited in those samples treated with antibody CR1 (Figure 7.2b).

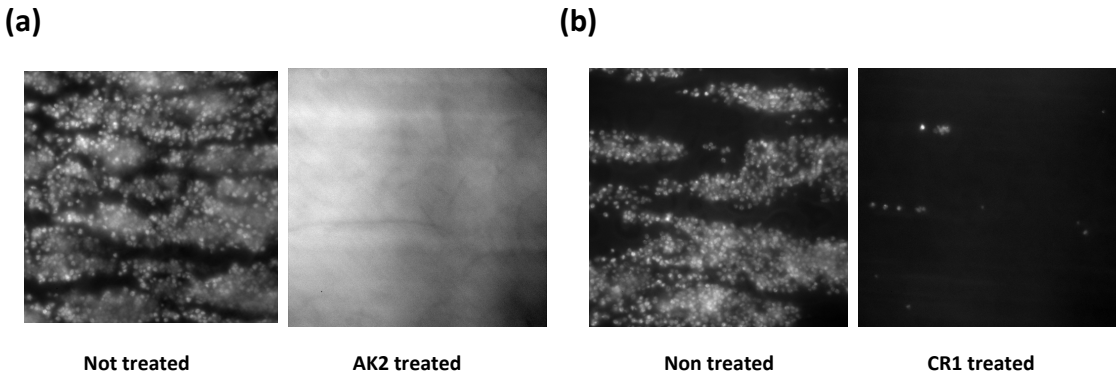

Figure 7.2 Whole blood treated with antibodies that block the platelet VWF receptor GPIbα or A1-VWF prevents platelet adhesion to the polymer surface. Blood from 3 healthy donors treated in the presence and absence of AK2 or CR1 was perfused over the polymer surface under arterial shear conditions. A single end-point image was taken after 5 minutes of perfusion of blood. (a) Representative images of treatment of blood with or without 25 μg/ml of platelet VWF receptor antibody GPIbα AK2 (n=3). (b) Representative images of treatment of blood with or without 25 μg/ml A1-VWF CR1 antibody (n=3).

7.2.3 The polymer surface is sensitive to an increased concentration of VWF

The concentration of VWF can significantly differ between individuals (Franchini et al., 2014). Therefore, the task was to determine whether the polymer surface was sensitive to an increased concentration of VWF. Purified human VWF was added to blood from 10 healthy donors prior to perfusion over the polymer surface and compared with a non-treated control sample (Figure 7.3). Assessment of platelet adhesion to the surface showed that those samples pre-treated with purified human VWF had significantly increased platelet adhesion to the surface in comparison with non-treated control samples (35 ± 8% versus 11 ± 5%; **$p < 0.01$).

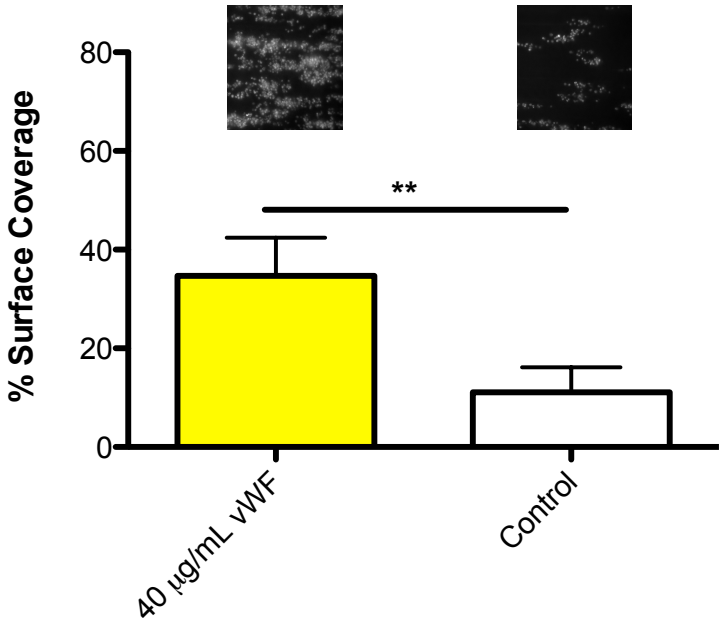

Figure 7.3 Increasing the concentration of VWF in blood increases platelet adhesion to the polymer surface. Blood from 10 healthy volunteers was preincubated with 40 µg/mL of purified human VWF and compared to an untreated blood samples from the same donor. The percentage of platelet surface coverage was measured for each end-point image, after 5 minutes of blood perfusion over the surface. Platelet adhesion to the surface was significantly increased with the addition of purified VWF (**$p < 0.01$). A paired t-test was used to detect statistically-significant differences between the conditions. Data is represented as mean ± SEM.

7.3 Discussion

During vascular damage, vascular matrix proteins such as collagen are exposed to flowing blood. The first step in this process is the adhesion of VWF to the exposed collagen, followed by adhesion of the platelets to the surface. Collagen is commonly used as a substrate for platelet function studies. However, the use of collagen as a research tool for assessing platelet function is problematic. Firstly, there are many sources (e.g. human, equine and murine) and types (type I, II, III etc.) of collagen and it is currently unclear which is optimal for use in an experimental setup. Secondly, collagen surfaces lack uniformity, resulting in variable platelet adhesion.

In this chapter, a principle objective was to demonstrate a proof of concept to develop a novel synthetic surface that mimics collagen and is capable of capturing donor-specific VWF from blood. This approach was based on the published work by Minelli et al., (2008) who demonstrated that a surface coated with de-mixed solution of PMMA/polystyrene captured VWF from flowing blood in a microfluidic device. To develop the nano-surface, a well-known polymer de-mixing technique 'spin coating' was used (Dalby et al., 2002). Different concentrations of polymer solution (1%, 3% and 5% w/v) were tested to determine the optimum feature sizes for platelet capture. Larger concentrations of polymer solution were predicted to provide nanostructures of greater height and depth. Interestingly, Minelli et al., (2008) had noted in their experiments, that those surfaces with larger feature size and depth favoured the greatest capture of VWF. Although no significant differences in platelet capture were observed, we did observe that the 3% polymer mix captured on average the greatest number of platelets. It was determined that this interaction between platelets and the polymer surface was VWF-platelet specific through the use of two control experiments implementing blocking antibodies. Treatment of whole blood prior to perfusion over the polymer surface with either AK2 antibody (which functions to inhibit GPIbα) or CR1 antibody (which blocks the A1 domain of VWF) prevented platelet adhesion to the surface. The efficiency of these antibodies in blocking platelet adhesion to immobilized VWF surfaces under flow conditions has been verified previously. Wu et al., (1996) previously demonstrated with the use of immobilised VWF, that treatment of whole blood with AK2, inhibited platelet

adhesion to VWF under flow conditions. Dong et al., (2001) subsequently showed that the CR1 antibody could also inhibit platelet adhesion to VWF under flow-based conditions. The addition of purified VWF to blood *in vitro* significantly enhanced platelet adhesion to the surface. This observation correlates well with a study on fibrillar type I collagen which demonstrated that increased concentrations of VWF were associated with enhanced platelet adhesion (Neeves et al., 2013).

The preliminary data reported in this PhD study is encouraging and demonstrates the proof of concept for development of a novel synthetic surface that mimics collagen and is capable of capturing donor specific VWF from blood plasma for investigation of platelet interactions with autologous VWF. Identifying a functional difference in the VWF interaction with platelets may be of imperative clinical importance in the helping to identify those people who are at increased risk of bleeding or thrombosis.

Chapter 8

General discussion

Ideally, platelet function should be assayed under flow and shear conditions that occur *in vivo*. Currently, the only clinically validated assay of platelet function is the platelet function analyser, the PFA-100. The PFA-100 assesses platelet function under high-shear conditions. However, the assay suffers from a number of limitations, including its insensitivity to detect mild bleeding disorders (Quiroga et al., 2004) and its reliability on a single end point analysis rather than direct measurement of platelet interaction in 'real-time'. Previously, Prof Kenny's RCSI research group had developed the Dynamic Platelet Function Assay (DPFA), that used a novel parallel plate flow chambers coated with purified human VWF and custom-designed platelet tracking software (Kent et al., 2010, Lincoln et al., 2010). The custom-designed platelet tracking software was capable of deriving novel parameters of platelet function that related to the biological activity of platelets *in vivo*. However, the reliability and the clinical relevance of the measured parameters of the DPFA were unclear and there were errors in its platelet tracking process. A primary objective of this thesis was to investigate the above issues through validation and clinical evaluation of the DPFA.

Firstly, as outlined in chapter 3, with the support of software engineers, the probability function detailed in Lincoln et al., (2010) was replaced with a less directional distance weighting method (Ralph *et al.*, 2015, under review in Transactions on Image Processing, Appendix B). Implementation of a distance weighting method allowed for the identification of individual platelets, which were part of a platelet group and to track them as they merged and split from the group. Merging and splitting of platelets increased the potential for platelet fragmentation. Platelet fragmentation occurs where a single platelet track is recorded smaller set of tracks. Thus, stitching together the fragmented tracks to form a full track, enhanced the ability of the tracking software to accurately measure platelet function.

The accuracy of the distance weighting method to track platelet function was validated computationally using an ideal data set and biologically using a $P2Y_1$ receptor inhibitor MRS2179. The ideal data set determined the percentage systematic error for each measured parameter of platelet behaviour and also

revealed that higher object counts resulted in greater numbers of merging and separating platelet events. Merging and separating of platelets increased the potential for mistracking. Despite this potential for mistracking, the DPFA was still capable of detecting subtle changes in platelet function. This was demonstrated through the use of MRS2179. Platelets treated in the presence of the $P2Y_1$ receptor inhibitor had significantly amplified platelet translocation speeds on VWF and this confirmed the results of previously published data (Mazzucato et al., 2004). This finding verified the ability of the assay to determine drug effect. The DPFA was sensitive to HCT which matched predicted results generated by computer simulation models of dynamic platelet-wall adhesion (Fitzgibbon et al., 2014). This finding demonstrated the importance of RBC platelet interactions in determining initial platelet adhesion and the capability of the DPFA to diagnose altered platelet function. A reference range of platelet function was determined for the assay evaluating a total of 109 healthy donors. This is well above the number of donors required which is 39 (Solberg, 1987).

In chapter 4, the effect of age and gender on platelet function was investigated. The results demonstrated that both age and gender play a significant role in altering the behaviour of platelets. The data showed that platelets become more active with age, with this effect being more profound for females than in males. Despite having reduced numbers of platelets interacting with VWF, platelets from older donors had significant increases in the platelet surface coverage. This was due to increased adherence of platelets to VWF as measured by a significant reduction in the numbers of unstable platelet interactions with VWF. These more profound changes in platelet function associated with aging in females may be related to sex hormones. Both estrogen and testosterone have been shown to affect platelet function (Jayachandran et al., 2010, Ajayi et al., 1995). Estrogen levels fall rapidly in older females as opposed to the rather gradual decline of testosterone levels in older males. This may explain why alterations in platelet function are more extensive in females than in males. This is recommended as an area for future research.
Overall, the results generated by the DPFA are consistent with the concept that age is associated with more reactive platelets (Bastyr et al., 1990, Gleerup and Winther,

1995, Reilly and FitzGerald, 1986). This finding demonstrates the power of the DPFA to detect subtle alterations in platelet function related to aging.

The DPFA can quantify platelet function in < 100 µL of blood, thereby making it suitable for research in cohorts where blood availability is a limiting factor. In chapter 5, platelet function in very low birth weight (VLBW) preterms and full-term infants was investigated. Studies in the neonatal area are restricted due to small circulating blood volumes (80 mL/kg). Utilising the DPFA, it was demonstrated that VLBW preterm infants had significantly different platelet translocation behaviour on VWF compared with full-term infants. In particular, it was found that VLBW preterm infants displayed decreased platelet adhesiveness to VWF with an accompanying increase in platelet translocation speeds and unstable platelet interactions with VWF. A possible explanation may relate to reduced PAC-1 binding (binds activated αIIbβ3) in VLBW preterm infants (Sitaru et al., 2005). Platelets need to activate αIIbβ3 in order to adhere to immobilised VWF (Savage et al., 1996). Therefore, reduced activation of αIIbβ3 would reduce adherence of platelets to VWF, leading to increases in platelet translocation speeds and numbers of unstable platelet interactions with VWF. Notably VLBW preterm infants identified with either low platelet count (<104 x 10^3 µL of blood) or HCT (28%) displayed significantly reduced platelet translocation behaviour on VWF. This result matched the behaviour of platelets presented in chapter 3 which demonstrated that reducing platelet count or HCT significantly inhibited platelet adhesion to VWF.

Overall, the results of the DPFA experiments with neonates were consistent with previous studies of platelet function which report that VLBW preterm infants have impaired platelet function (Boudewijns et al., 2003, Levy-Shraga et al., 2006, Del Vecchio et al., 2008). These differences in platelet function may contribute to the higher incidences of bleeding observed in preterm infant populations. This evidence further validates the use of the DPFA to distinguish changes in platelet function.

Platelets have been identified to serve as potential mediators in the formation of a normally functioning placenta (Sato et al., 2005, Bodis et al., 2014, Sato et al., 2010). Alterations in platelet-mediated placentation may contribute to the development of

utero-placental diseases (Norris et al., 1994, Mullers, 2015, Morrison et al., 1985, Stubbs et al., 1986, Janes and Goodall, 1994, Norris et al., 1993). In chapter 6, the DPFA was used to assess platelet function changes in healthy pregnancy and in pregnancy with utero-placental disease. The results of the DPFA suggested that healthy pregnant females in the third trimester had more reactive platelets than healthy females who were not pregnant. More reactive platelets are concurrent with decreases in platelet translocation speeds on VWF in pregnant females. In this thesis, it hypothesised that decreases in HCT may compensate for this hyperreactive state. This may explain why pregnant females had significant reductions in the numbers of platelets interacting with VWF. Pregnancy with utero-placental disease was associated with impairment in platelet function. This impairment was more profound in utero-placental disease with PET. This is interesting as PET represents a more severe clinical form of utero-placental disease in comparison to IUGR or PIH. This finding demonstrates the ability of the DPFA to extricate small changes in platelet function. It is proposed that future studies should apply this assay in a large cohort across the three trimesters of pregnancy, as these studies are considerably lacking and are warranted.

Finally, in chapter 7, the future of the DPFA was explored. One of the limitations of the assay is that is does not use autologous VWF to measure platelet function. Previous work by Minelli et al., (2008) demonstrated that a surface coated with de-mixed poly(methyl methacrylate) PMMA / polystyrene had the ability to capture VWF from flowing blood in a microfluidic device through an unknown mechanism. As our research group did not have the expertise to design such a surface, we collaborated with the Nanotechnology and Integrated BioEngineering Centre (NIBEC) in Ulster University Jordanstown. The preliminary work presented in this thesis is encouraging. It was demonstrated that the polymer surface was capable of capturing VWF from flowing blood, followed by platelet adhesion to the polymer surface. Platelet interactions with the polymer surface were shown to be GPIα / VWF specific through the use of blocking antibodies AK2 (which functions to block GPIbα) and CR1 (which blocks the A1 domain of VWF). The surface was also sensitive to increased concentrations of VWF, verified through the addition of purified VWF to blood *in*

vitro, which significantly enhanced platelet adhesion to the surface. The DPFA with a polymer surface that can capture VWF from blood plasma to assess platelet function would be extremely powerful in future research work.

There are many advantages to the DPFA that have been discussed in this thesis including the use of whole blood, low sample volumes (< 100 µL), a shear environment and the measurement of multiple behaviours of platelets translocating on VWF in real-time. A major limitation of the assay relates to the assay surface, which is only coated with VWF, so therefore only focuses on two platelet receptor interactions. Firstly, the platelet GPIbα interaction with VWF that results in the characteristic tethering and rolling of platelets, followed by activation of αIIbβ3 for stable platelet adhesion. However, *in vivo* collagen plays a key step in the platelet activation process through engagement with platelet receptor GPVI. The result is powerful activation signals causing αIIbβ3 activation, release of platelets agonists such as ADP and subsequent platelet thrombus formation. More recently, de Witt et al., (2014) demonstrated the use of a multi-surface and multi-parameter flow assay that could characterise platelet thrombus formation in healthy subjects and those with platelet function deficiencies. The major advantage of de Witt et al., (2014) assay in comparison to DPFA presented in this thesis was the ability to pick up multiple receptor abnormalities. The assay incorporates multiple surfaces such as collagens, peptides and laminin to name a few as opposed to just VWF measured in this thesis. However, the process is labour intensive, involves multiple staining procedures, manual analysis and because the assay incorporates multiple proteins, there likely is a considerable expense in running the assay. In contrast to this, DPFA involves a single staining procedure, prior to a flow run and a custom designed platelet-tracking software, which provides rapid analysis of cohorts of interest (< 5 minutes). Morgan et al., (2013) developed 3D enclosed perfusable microvessels manufactured in bioremodelable hydrogel (collagen type I). The major of advantages of this system in contrast to the DPFA include the ability to visualise a 3D microenvironment *in vitro*, not only the capability to study models of thrombosis but also to study models of tumor angiogenesis, wound healing and diabetes. The limitations of assay described by Morgan et al., (2013) include a complicated

manufacturing procedure, therefore limits its throughput and microvessel reproducibility at lateral dimensions below 50 µm.

In conclusion, this thesis, took a previously described DPFA Lincoln et al., (2010), addressed the issues in its tracking process through refinement and validation of the accuracy of its parameter outputs. The DPFA was evaluated clinically, using blood samples from adults, neonates and females with healthy pregnancy and pregnancies complicated with utero-placental disease. The DPFA was shown to be capable of detecting subtle changes in platelet function in these clinical cohorts. These changes in platelet function were cognizant to the behaviours of platelets *in vivo*. It is recommended that future work should seek to enhance and further understand the assays outputs.

References

AARTS, P. A., BOLHUIS, P. A., SAKARIASSEN, K. S., HEETHAAR, R. M. & SIXMA, J. J. 1983. Red blood cell size is important for adherence of blood platelets to artery subendothelium. *Blood,* 62**,** 214-7.

AHER, S., MALWATKAR, K. & KADAM, S. 2008. Neonatal anemia. *Seminars in fetal & neonatal medicine,* 13**,** 239-47.

AJAYI, A. A., MATHUR, R. & HALUSHKA, P. V. 1995. Testosterone increases human platelet thromboxane A2 receptor density and aggregation responses. *Circulation,* 91**,** 2742-7.

ANDREWS, R. K. & BERNDT, M. C. 2013. Bernard-Soulier syndrome: an update. *Seminars in thrombosis and hemostasis,* 39**,** 656-62.

ANDREWS, R. K., GARDINER, E. E., SHEN, Y., WHISSTOCK, J. C. & BERNDT, M. C. 2003. Glycoprotein Ib-IX-V. *The international journal of biochemistry & cell biology,* 35**,** 1170-4.

ASKIE, L. M., DULEY, L., HENDERSON-SMART, D. J. & STEWART, L. A. 2007. Antiplatelet agents for prevention of pre-eclampsia: a meta-analysis of individual patient data. *Lancet,* 369**,** 1791-8.

AUTON, M., SOWA, K. E., BEHYMER, M. & CRUZ, M. A. 2012. N-terminal flanking region of A1 domain in von Willebrand factor stabilizes structure of A1A2A3 complex and modulates platelet activation under shear stress. *The Journal of biological chemistry,* 287**,** 14579-85.

AUTON, M., SOWA, K. E., SMITH, S. M., SEDLAK, E., VIJAYAN, K. V. & CRUZ, M. A. 2010. Destabilization of the A1 domain in von Willebrand factor dissociates the A1A2A3 tri-domain and provokes spontaneous binding to glycoprotein Ibalpha and platelet activation under shear stress. *The Journal of biological chemistry,* 285**,** 22831-9.

BAIN, B. J. 1985. Platelet count and platelet size in males and females. *Scandinavian journal of haematology,* 35**,** 77-9.

BAL DIT SOLLIER, C., BERGE, N., BOVAL, B., DUBAR, M. & DROUET, L. 2010. Differential sensitivity and kinetics of response of different ex vivo tests

monitoring functional variability of platelet response to clopidogrel. *Thrombosis and haemostasis,* 104**,** 571-81.

BALLABH, P. 2010. Intraventricular hemorrhage in premature infants: mechanism of disease. *Pediatric research,* 67**,** 1-8.

BASTYR, E. J., 3RD, KADROFSKE, M. M. & VINIK, A. I. 1990. Platelet activity and phosphoinositide turnover increase with advancing age. *The American journal of medicine,* 88**,** 601-6.

BAURAND, A., RABOISSON, P., FREUND, M., LEON, C., CAZENAVE, J. P., BOURGUIGNON, J. J. & GACHET, C. 2001. Inhibition of platelet function by administration of MRS2179, a P2Y1 receptor antagonist. *European journal of pharmacology,* 412**,** 213-21.

BERNDT, M. C., SHEN, Y., DOPHEIDE, S. M., GARDINER, E. E. & ANDREWS, R. K. 2001. The vascular biology of the glycoprotein Ib-IX-V complex. *Thrombosis and haemostasis,* 86**,** 178-88.

BLIDEN, K. P., DICHIARA, J., TANTRY, U. S., BASSI, A. K., CHAGANTI, S. K. & GURBEL, P. A. 2007. Increased risk in patients with high platelet aggregation receiving chronic clopidogrel therapy undergoing percutaneous coronary intervention: is the current antiplatelet therapy adequate? *Journal of the American College of Cardiology,* 49**,** 657-66.

BLOCK, S. M. 1992. Making light work with optical tweezers. *Nature,* 360**,** 493-5.

BODIS, J., PAPP, S., VERMES, I., SULYOK, E., TAMAS, P., FARKAS, B., ZAMBO, K., HATZIPETROS, I. & KOVACS, G. L. 2014. "Platelet-associated regulatory system (PARS)" with particular reference to female reproduction. *Journal of ovarian research,* 7**,** 55.

BORN, G. V. 1962. Aggregation of blood platelets by adenosine diphosphate and its reversal. *Nature,* 194**,** 927-9.

BOUDEWIJNS, M., RAES, M., PEETERS, V., MEWIS, A., CARTUYVELS, R., MAGERMAN, K. & RUMMENS, J. L. 2003. Evaluation of platelet function on cord blood in 80 healthy term neonates using the Platelet Function Analyser (PFA-100); shorter in vitro bleeding times in neonates than adults. *European journal of pediatrics,* 162**,** 212-3.

BRANCHFORD, B. R. & DI PAOLA, J. 2012. Making a diagnosis of VWD. *Hematology / the Education Program of the American Society of Hematology. American Society of Hematology. Education Program,* 2012**,** 161-7.

BRAR, S. S., TEN BERG, J., MARCUCCI, R., PRICE, M. J., VALGIMIGLI, M., KIM, H. S., PATTI, G., BREET, N. J., DISCIASCIO, G., CUISSET, T. & DANGAS, G. 2011. Impact of platelet reactivity on clinical outcomes after percutaneous coronary intervention. A collaborative meta-analysis of individual participant data. *Journal of the American College of Cardiology,* 58**,** 1945-54.

BREET, N. J., VAN WERKUM, J. W., BOUMAN, H. J., KELDER, J. C., RUVEN, H. J., BAL, E. T., DENEER, V. H., HARMSZE, A. M., VAN DER HEYDEN, J. A., RENSING, B. J., SUTTORP, M. J., HACKENG, C. M. & TEN BERG, J. M. 2010. Comparison of platelet function tests in predicting clinical outcome in patients undergoing coronary stent implantation. *JAMA : the journal of the American Medical Association,* 303**,** 754-62.

BRUNNER, B., HOECK, M., SCHERMER, E., STREIF, W. & KIECHL-KOHLENDORFER, U. 2013. Patent ductus arteriosus, low platelets, cyclooxygenase inhibitors, and intraventricular hemorrhage in very low birth weight preterm infants. *The Journal of pediatrics,* 163**,** 23-8.

BUJOLD, E., ROBERGE, S., LACASSE, Y., BUREAU, M., AUDIBERT, F., MARCOUX, S., FOREST, J. C. & GIGUERE, Y. 2010. Prevention of preeclampsia and intrauterine growth restriction with aspirin started in early pregnancy: a meta-analysis. *Obstetrics and gynecology,* 116**,** 402-14.

BURKE, N., FLOOD, K., MURRAY, A., COTTER, B., DEMPSEY, M., FAY, L., DICKER, P., GEARY, M. P., KENNY, D. & MALONE, F. D. 2013. Platelet reactivity changes significantly throughout all trimesters of pregnancy compared with the nonpregnant state: a prospective study. *BJOG : an international journal of obstetrics and gynaecology,* 120**,** 1599-604.

CAMPELO, A. E., CUTINI, P. H. & MASSHEIMER, V. L. 2012. Testosterone modulates platelet aggregation and endothelial cell growth through nitric oxide pathway. *The Journal of endocrinology,* 213**,** 77-87.

CAN, M. M., KAYMAZ, C., CAN, E., TANBOGA, I. H., API, O., KARS, B., CEREN TOKGOZ, H., TURKYILMAZ, E., AKGUN, T., SONMEZ, K., SAGLAM, M., TURAN, C., UNAL,

O. & SEREBRUANY, V. 2010. Whole blood platelet aggregation failed to detect differences between preeclampsia and normal pregnancy. *Platelets,* 21**,** 496-7.

CANOBBIO, I., BALDUINI, C. & TORTI, M. 2004. Signalling through the platelet glycoprotein Ib-V-IX complex. *Cellular signalling,* 16**,** 1329-44.

CARDINAL, D. C. & FLOWER, R. J. 1980. The electronic aggregometer: a novel device for assessing platelet behavior in blood. *Journal of pharmacological methods,* 3**,** 135-58.

CATTANEO, M., CERLETTI, C., HARRISON, P., HAYWARD, C. P., KENNY, D., NUGENT, D., NURDEN, P., RAO, A. K., SCHMAIER, A. H., WATSON, S. P., LUSSANA, F., PUGLIANO, M. T. & MICHELSON, A. D. 2013. Recommendations for the Standardization of Light Transmission Aggregometry: A Consensus of the Working Party from the Platelet Physiology Subcommittee of SSC/ISTH. *Journal of thrombosis and haemostasis : JTH*.

CHEN, H., ANGERER, J. I., NAPOLEONE, M., REININGER, A. J., SCHNEIDER, S. W., WIXFORTH, A., SCHNEIDER, M. F. & ALEXANDER-KATZ, A. 2013. Hematocrit and flow rate regulate the adhesion of platelets to von Willebrand factor. *Biomicrofluidics,* 7**,** 64113.

CHEN, J. & LOPEZ, J. A. 2005. Interactions of platelets with subendothelium and endothelium. *Microcirculation,* 12**,** 235-46.

CHO, Y. U., CHI, H. S., JANG, S. & PARK, C. J. 2007. [Reconfirmation of preanalytical variables and establishment of reference intervals of platelet function analyzer-100 closure times in Korean adults]. *The Korean journal of laboratory medicine,* 27**,** 318-23.

CRUZ, M. A., YUAN, H., LEE, J. R., WISE, R. J. & HANDIN, R. I. 1995. Interaction of the von Willebrand factor (vWF) with collagen. Localization of the primary collagen-binding site by analysis of recombinant vWF A domain polypeptides. *The Journal of biological chemistry,* 270**,** 19668.

DALBY, M. J., RIEHLE, M. O., JOHNSTONE, H. J., AFFROSSMAN, S. & CURTIS, A. S. 2002. Polymer-demixed nanotopography: control of fibroblast spreading and proliferation. *Tissue engineering,* 8**,** 1099-108.

DE WITT, S. M., SWIERINGA, F., CAVILL, R., LAMERS, M. M., VAN KRUCHTEN, R., MASTENBROEK, T., BAATEN, C., COORT, S., PUGH, N., SCHULZ, A., SCHARRER, I., JURK, K., ZIEGER, B., CLEMETSON, K. J., FARNDALE, R. W., HEEMSKERK, J. W. & COSEMANS, J. M. 2014. Identification of platelet function defects by multi-parameter assessment of thrombus formation. *Nature communications,* 5**,** 4257.

DEL VECCHIO, A., LATINI, G., HENRY, E. & CHRISTENSEN, R. D. 2008. Template bleeding times of 240 neonates born at 24 to 41 weeks gestation. *Journal of perinatology : official journal of the California Perinatal Association,* 28**,** 427-31.

DOGGETT, T. A., GIRDHAR, G., LAWSHE, A., SCHMIDTKE, D. W., LAURENZI, I. J., DIAMOND, S. L. & DIACOVO, T. G. 2002. Selectin-like kinetics and biomechanics promote rapid platelet adhesion in flow: the GPIb(alpha)-vWF tether bond. *Biophysical journal,* 83**,** 194-205.

DONG, J. F., BERNDT, M. C., SCHADE, A., MCINTIRE, L. V., ANDREWS, R. K. & LOPEZ, J. A. 2001. Ristocetin-dependent, but not botrocetin-dependent, binding of von Willebrand factor to the platelet glycoprotein Ib-IX-V complex correlates with shear-dependent interactions. *Blood,* 97**,** 162-8.

DONG, J. F., MOAKE, J. L., NOLASCO, L., BERNARDO, A., ARCENEAUX, W., SHRIMPTON, C. N., SCHADE, A. J., MCINTIRE, L. V., FUJIKAWA, K. & LOPEZ, J. A. 2002. ADAMTS-13 rapidly cleaves newly secreted ultralarge von Willebrand factor multimers on the endothelial surface under flowing conditions. *Blood,* 100**,** 4033-9.

DOPHEIDE, S. M., MAXWELL, M. J. & JACKSON, S. P. 2002. Shear-dependent tether formation during platelet translocation on von Willebrand factor. *Blood,* 99**,** 159-67.

EMERY, J. D., LEIFER, D. W., MOURA, G. L., SOUTHERN, P., MORRISSEY, J. H. & LAWRENCE, J. B. 1995. Whole-blood platelet aggregation predicts in vitro and in vivo primary hemostatic function in the elderly. *Arteriosclerosis, thrombosis, and vascular biology,* 15**,** 748-53.

ESMON, C. T. 2009. Basic mechanisms and pathogenesis of venous thrombosis. *Blood reviews,* 23**,** 225-9.

FAHRAEUS, R. A. L., T 1931. The viscosity of blood in narrow capillary tubes. *American Journal of Physiology,* 96**,** 562-568.

FAUPEL-BADGER, J. M., HSIEH, C. C., TROISI, R., LAGIOU, P. & POTISCHMAN, N. 2007. Plasma volume expansion in pregnancy: implications for biomarkers in population studies. *Cancer epidemiology, biomarkers & prevention : a publication of the American Association for Cancer Research, cosponsored by the American Society of Preventive Oncology,* 16**,** 1720-3.

FERNANDEZ, M. F., GINSBERG, M. H., RUGGERI, Z. M., BATLLE, F. J. & ZIMMERMAN, T. S. 1982. Multimeric structure of platelet factor VIII/von Willebrand factor: the presence of larger multimers and their reassociation with thrombin-stimulated platelets. *Blood,* 60**,** 1132-8.

FERRER-MARIN, F., STANWORTH, S., JOSEPHSON, C. & SOLA-VISNER, M. 2013. Distinct differences in platelet production and function between neonates and adults: implications for platelet transfusion practice. *Transfusion,* 53**,** 2814-21; quiz 2813.

FITZGERALD, D. J., MAYO, G., CATELLA, F., ENTMAN, S. S. & FITZGERALD, G. A. 1987. Increased thromboxane biosynthesis in normal pregnancy is mainly derived from platelets. *American journal of obstetrics and gynecology,* 157**,** 325-30.

FITZGIBBON, S., COWMAN, J., RICCO, A. J., KENNY, D. & SHAQFEH, E. S. 2014. Examining platelet adhesion via Stokes flow simulations and microfluidic experiments. *Soft Matter,* 11**,** 355-67.

FRANCHINI, M. 2006. Hemostasis and aging. *Critical reviews in oncology/hematology,* 60**,** 144-51.

FRANCHINI, M., CRESTANI, S., FRATTINI, F., SISSA, C. & BONFANTI, C. 2014. ABO blood group and von Willebrand factor: biological implications. *Clinical chemistry and laboratory medicine : CCLM / FESCC,* 52**,** 1273-6.

FUKUDA, K., DOGGETT, T., LAURENZI, I. J., LIDDINGTON, R. C. & DIACOVO, T. G. 2005. The snake venom protein botrocetin acts as a biological brace to promote dysfunctional platelet aggregation. *Nature structural & molecular biology,* 12**,** 152-9.

FURLAN, M., ROBLES, R., SOLENTHALER, M., WASSMER, M., SANDOZ, P. & LAMMLE, B. 1997. Deficient activity of von Willebrand factor-cleaving protease in

chronic relapsing thrombotic thrombocytopenic purpura. *Blood,* 89**,** 3097-103.

GATTI, L., TENCONI, P. M., GUARNERI, D., BERTULESSI, C., OSSOLA, M. W., BOSCO, P. & GIANOTTI, G. A. 1994. Hemostatic parameters and platelet activation by flow-cytometry in normal pregnancy: a longitudinal study. *International journal of clinical & laboratory research,* 24**,** 217-9.

GAUER, R. L. & BRAUN, M. M. 2012. Thrombocytopenia. *American family physician,* 85**,** 612-22.

GERBASI, F. R., BOTTOMS, S., FARAG, A. & MAMMEN, E. F. 1990. Changes in hemostasis activity during delivery and the immediate postpartum period. *American journal of obstetrics and gynecology,* 162**,** 1158-63.

GILL, J. C., ENDRES-BROOKS, J., BAUER, P. J., MARKS, W. J., JR. & MONTGOMERY, R. R. 1987. The effect of ABO blood group on the diagnosis of von Willebrand disease. *Blood,* 69**,** 1691-5.

GLEERUP, G. & WINTHER, K. 1995. The effect of ageing on platelet function and fibrinolytic activity. *Angiology,* 46**,** 715-8.

GOROG, D. A. & FUSTER, V. 2013. Platelet function tests in clinical cardiology: unfulfilled expectations. *Journal of the American College of Cardiology,* 61**,** 2115-29.

GOURIER, C., JEGOU, A, HUSSON, J AND PINCET 2008. A Nanospring Named Erythrocyte. The Biomembrane Force Probe. *Cellular and Molecular Bioengineering,* 1**,** 263-275.

GUNNINK, S. F., VLUG, R., FIJNVANDRAAT, K., VAN DER BOM, J. G., STANWORTH, S. J. & LOPRIORE, E. 2014. Neonatal thrombocytopenia: etiology, management and outcome. *Expert review of hematology,* 7**,** 387-95.

HABERICHTER, S. L., JOZWIAK, M. A., ROSENBERG, J. B., CHRISTOPHERSON, P. A. & MONTGOMERY, R. R. 2002. The von Willebrand factor propeptide (VWFpp) traffics an unrelated protein to storage. *Arteriosclerosis, thrombosis, and vascular biology,* 22**,** 921-6.

HAJDENBERG, J. 2004. Template bleeding time and PFA-100 have low sensitivity to screen patients with hereditary mucocutaneous hemorrhages: comparative

study of 148 patients--a rebuttal. *Journal of thrombosis and haemostasis : JTH,* 2**,** 2282-3; author reply 2283-5.

HARRISON, P. 2009. Assessment of platelet function in the laboratory. *Hamostaseologie,* 29**,** 25-31.

HATO, T., GINSBERG M.H. AND SHATTIL S.J. 2002. Integrin αIIbβ3. *In:* MICHELSON, A. D. (ed.) *Platelets.* Elsevier science (USA).

HOLMES, V. A., WALLACE, J. M., GILMORE, W. S., MCFAUL, P. & ALEXANDER, H. D. 2002. Soluble P-selectin levels during normal pregnancy: a longitudinal study. *BJOG : an international journal of obstetrics and gynaecology,* 109**,** 997-1002.

HORN, E. H. 1991. Platelets in normal and hypertensive pregnancy. *Platelets,* 2**,** 183-95.

HUANG, R. H., WANG, Y., ROTH, R., YU, X., PURVIS, A. R., HEUSER, J. E., EGELMAN, E. H. & SADLER, J. E. 2008. Assembly of Weibel-Palade body-like tubules from N-terminal domains of von Willebrand factor. *Proceedings of the National Academy of Sciences of the United States of America,* 105**,** 482-7.

HUIZINGA, E. G., TSUJI, S., ROMIJN, R. A., SCHIPHORST, M. E., DE GROOT, P. G., SIXMA, J. J. & GROS, P. 2002. Structures of glycoprotein Ibalpha and its complex with von Willebrand factor A1 domain. *Science,* 297**,** 1176-9.

HUSSEIN, H. M., EMIRU, T., GEORGIADIS, A. L. & QURESHI, A. I. 2013. Assessment of platelet inhibition by point-of-care testing in neuroendovascular procedures. *AJNR. American journal of neuroradiology,* 34**,** 700-6.

HWANG, H. G. & SCHULMAN, S. 2013. Respiratory review of 2013: pulmonary thromboembolism. *Tuberculosis and respiratory diseases,* 75**,** 89-94.

ISRAELS, S. J., CHEANG, T., MCMILLAN-WARD, E. M. & CHEANG, M. 2001. Evaluation of primary hemostasis in neonates with a new in vitro platelet function analyzer. *The Journal of pediatrics,* 138**,** 116-9.

ISRAELS, S. J., RAND, M. L. & MICHELSON, A. D. 2003. Neonatal platelet function. *Seminars in thrombosis and hemostasis,* 29**,** 363-72.

JACKSON, S. P. 2007. The growing complexity of platelet aggregation. *Blood,* 109**,** 5087-95.

JACKSON, S. P. 2011. Arterial thrombosis--insidious, unpredictable and deadly. *Nature medicine,* 17**,** 1423-36.

JACKSON, S. P., NESBITT, W. S. & WESTEIN, E. 2009. Dynamics of platelet thrombus formation. *Journal of thrombosis and haemostasis : JTH,* 7 Suppl 1**,** 17-20.

JAMES, P. D. & GOODEVE, A. C. 2011. von Willebrand disease. *Genetics in medicine : official journal of the American College of Medical Genetics,* 13**,** 365-76.

JANES, S. L. & GOODALL, A. H. 1994. Flow cytometric detection of circulating activated platelets and platelet hyper-responsiveness in pre-eclampsia and pregnancy. *Clinical science,* 86**,** 731-9.

JAYACHANDRAN, M., KARNICKI, K., MILLER, R. S., OWEN, W. G., KORACH, K. S. & MILLER, V. M. 2005. Platelet characteristics change with aging: role of estrogen receptor beta. *The journals of gerontology. Series A, Biological sciences and medical sciences,* 60**,** 815-9.

JAYACHANDRAN, M., PRESTON, C. C., HUNTER, L. W., JAHANGIR, A., OWEN, W. G., KORACH, K. S. & MILLER, V. M. 2010. Loss of estrogen receptor beta decreases mitochondrial energetic potential and increases thrombogenicity of platelets in aged female mice. *Age,* 32**,** 109-21.

JOUSILAHTI, P., VARTIAINEN, E., TUOMILEHTO, J. & PUSKA, P. 1999. Sex, age, cardiovascular risk factors, and coronary heart disease: a prospective follow-up study of 14 786 middle-aged men and women in Finland. *Circulation,* 99**,** 1165-72.

JU, L., DONG, J. F., CRUZ, M. A. & ZHU, C. 2013. The N-terminal flanking region of the A1 domain regulates the force-dependent binding of von Willebrand factor to platelet glycoprotein Ibalpha. *The Journal of biological chemistry,* 288**,** 32289-301.

KENT, N. J., BASABE-DESMONTS, L., MEADE, G., MACCRAITH, B. D., CORCORAN, B. G., KENNY, D. & RICCO, A. J. 2010. Microfluidic device to study arterial shear-mediated platelet-surface interactions in whole blood: reduced sample volumes and well-characterised protein surfaces. *Biomedical microdevices,* 12**,** 987-1000.

KHETAWAT, G., FARADAY, N., NEALEN, M. L., VIJAYAN, K. V., BOLTON, E., NOGA, S. J. & BRAY, P. F. 2000. Human megakaryocytes and platelets contain the estrogen receptor beta and androgen receptor (AR): testosterone regulates AR expression. *Blood,* 95**,** 2289-96.

KIM, J., ZHANG, C. Z., ZHANG, X. & SPRINGER, T. A. 2010. A mechanically stabilized receptor-ligand flex-bond important in the vasculature. *Nature,* 466**,** 992-5.

KNIGHT, C. J., PANESAR, M., WRIGHT, C., CLARKE, D., BUTOWSKI, P. S., PATEL, D., PATRINELI, A., FOX, K. & GOODALL, A. H. 1997. Altered platelet function detected by flow cytometry. Effects of coronary artery disease and age. *Arteriosclerosis, thrombosis, and vascular biology,* 17**,** 2044-53.

KONIJNENBERG, A., STOKKERS, E. W., VAN DER POST, J. A., SCHAAP, M. C., BOER, K., BLEKER, O. P. & STURK, A. 1997. Extensive platelet activation in preeclampsia compared with normal pregnancy: enhanced expression of cell adhesion molecules. *American journal of obstetrics and gynecology,* 176**,** 461-9.

KROLL, M. H., HELLUMS, J. D., MCINTIRE, L. V., SCHAFER, A. I. & MOAKE, J. L. 1996. Platelets and shear stress. *Blood,* 88**,** 1525-41.

KULKARNI, S., DOPHEIDE, S. M., YAP, C. L., RAVANAT, C., FREUND, M., MANGIN, P., HEEL, K. A., STREET, A., HARPER, I. S., LANZA, F. & JACKSON, S. P. 2000. A revised model of platelet aggregation. *The Journal of clinical investigation,* 105**,** 783-91.

KUNDU, S. K., HEILMANN, E. J., SIO, R., GARCIA, C., DAVIDSON, R. M. & OSTGAARD, R. A. 1995. Description of an in vitro platelet function analyzer--PFA-100. *Seminars in thrombosis and hemostasis,* 21 Suppl 2**,** 106-12.

KUNDU, S. K., HEILMANN, E.J., SIO, R., GARCIA, C. AND OSTGAARD, R.A. 1996. Characterization of an In Vitro Platelet Function Analyzer, PFA-100™. *Clinical and applied Thrombosis/Hemostasis,* 2**,** 241-249.

LANKHOF, H., VAN HOEIJ, M., SCHIPHORST, M. E., BRACKE, M., WU, Y. P., IJSSELDIJK, M. J., VINK, T., DE GROOT, P. G. & SIXMA, J. J. 1996. A3 domain is essential for interaction of von Willebrand factor with collagen type III. *Thrombosis and haemostasis,* 75**,** 950-8.

LENTING, P. J., PEGON, J. N., GROOT, E. & DE GROOT, P. G. 2010. Regulation of von Willebrand factor-platelet interactions. *Thrombosis and haemostasis,* 104**,** 449-55.

LEVY-SHRAGA, Y., MAAYAN-METZGER, A., LUBETSKY, A., SHENKMAN, B., KUINT, J., MARTINOWITZ, U. & KENET, G. 2006. Platelet function of newborns as tested

by cone and plate(let) analyzer correlates with gestational Age. *Acta haematologica,* 115**,** 152-6.

LI, C., MARTIN, S. E. & ROTH, G. J. 1995. The genetic defect in two well-studied cases of Bernard-Soulier syndrome: a point mutation in the fifth leucine-rich repeat of platelet glycoprotein Ib alpha. *Blood,* 86**,** 3805-14.

LINCOLN, B., RICCO, A. J., KENT, N. J., BASABE-DESMONTS, L., LEE, L. P., MACCRAITH, B. D., KENNY, D. & MEADE, G. 2010. Integrated system investigating shear-mediated platelet interactions with von Willebrand factor using microliters of whole blood. *Analytical biochemistry,* 405**,** 174-83.

LINDER, N., SHENKMAN, B., LEVIN, E., SIROTA, L., VISHNE, T. H., TAMARIN, I., DARDIK, R., LUBIN, D., SAVION, N. & VARON, D. 2002. Deposition of whole blood platelets on extracellular matrix under flow conditions in preterm infants. *Archives of disease in childhood. Fetal and neonatal edition,* 86**,** F127-30.

LOU, J., YAGO, T., KLOPOCKI, A. G., MEHTA, P., CHEN, W., ZARNITSYNA, V. I., BOVIN, N. V., ZHU, C. & MCEVER, R. P. 2006. Flow-enhanced adhesion regulated by a selectin interdomain hinge. *The Journal of cell biology,* 174**,** 1107-17.

LUCITT, M. B., O'BRIEN, S., COWMAN, J., MEADE, G., BASABE-DESMONTS, L., SOMERS, M., KENT, N., RICCO, A. J. & KENNY, D. 2013. Assaying the efficacy of dual-antiplatelet therapy: use of a controlled-shear-rate microfluidic device with a well-defined collagen surface to track dynamic platelet adhesion. *Analytical and bioanalytical chemistry,* 405**,** 4823-34.

LUO, S. Z., MO, X., AFSHAR-KHARGHAN, V., SRINIVASAN, S., LOPEZ, J. A. & LI, R. 2007. Glycoprotein Ibalpha forms disulfide bonds with 2 glycoprotein Ibbeta subunits in the resting platelet. *Blood,* 109**,** 603-9.

LYALL, F., ROBSON, S. C. & BULMER, J. N. 2013. Spiral artery remodeling and trophoblast invasion in preeclampsia and fetal growth restriction: relationship to clinical outcome. *Hypertension,* 62**,** 1046-54.

MA, Y. Q., QIN, J. & PLOW, E. F. 2007. Platelet integrin alpha(IIb)beta(3): activation mechanisms. *Journal of thrombosis and haemostasis : JTH,* 5**,** 1345-52.

MADABHUSHI, S. R., SHANG, C., DAYANANDA, K. M., RITTENHOUSE-OLSON, K., MURPHY, M., RYAN, T. E., MONTGOMERY, R. R. & NEELAMEGHAM, S. 2012.

von Willebrand factor (VWF) propeptide binding to VWF D'D3 domain attenuates platelet activation and adhesion. *Blood,* 119**,** 4769-78.

MANCUSO, D. J., TULEY, E. A., WESTFIELD, L. A., WORRALL, N. K., SHELTON-INLOES, B. B., SORACE, J. M., ALEVY, Y. G. & SADLER, J. E. 1989. Structure of the gene for human von Willebrand factor. *The Journal of biological chemistry,* 264**,** 19514-27.

MANNUCCI, P. M. 1998. von Willebrand factor: a marker of endothelial damage? *Arteriosclerosis, thrombosis, and vascular biology,* 18**,** 1359-62.

MARSHALL, B. T., LONG, M., PIPER, J. W., YAGO, T., MCEVER, R. P. & ZHU, C. 2003. Direct observation of catch bonds involving cell-adhesion molecules. *Nature,* 423**,** 190-3.

MARTI, T., ROSSELET, S. J., TITANI, K. & WALSH, K. A. 1987. Identification of disulfide-bridged substructures within human von Willebrand factor. *Biochemistry,* 26**,** 8099-109.

MARTIN, C., MORALES, L. D. & CRUZ, M. A. 2007. Purified A2 domain of von Willebrand factor binds to the active conformation of von Willebrand factor and blocks the interaction with platelet glycoprotein Ibalpha. *Journal of thrombosis and haemostasis : JTH,* 5**,** 1363-70.

MARTIN, K., MEADE, G., MORAN, N., SHIELDS, D. C. & KENNY, D. 2003. A palmitylated peptide derived from the glycoprotein Ib beta cytoplasmic tail inhibits platelet activation. *Journal of thrombosis and haemostasis : JTH,* 1**,** 2643-52.

MATLAB 2011. Version 7.12.0. *The MathWorks Inc.* Natick, Massachusetts:.

MAXWELL, M. J., DOPHEIDE, S. M., TURNER, S. J. & JACKSON, S. P. 2006. Shear induces a unique series of morphological changes in translocating platelets: effects of morphology on translocation dynamics. *Arteriosclerosis, thrombosis, and vascular biology,* 26**,** 663-9.

MAZZUCATO, M., COZZI, M. R., PRADELLA, P., RUGGERI, Z. M. & DE MARCO, L. 2004. Distinct roles of ADP receptors in von Willebrand factor-mediated platelet signaling and activation under high flow. *Blood,* 104**,** 3221-7.

MEHRBOD, M., TRISNO, S. & MOFRAD, M. R. 2013. On the activation of integrin alphaIIbbeta3: outside-in and inside-out pathways. *Biophysical journal,* 105**,** 1304-15.

MENDOLICCHIO, G. L. & RUGGERI, Z. M. 2005. New perspectives on von Willebrand factor functions in hemostasis and thrombosis. *Seminars in hematology,* 42**,** 5-14.

MERKEL, R., NASSOY, P., LEUNG, A., RITCHIE, K. & EVANS, E. 1999. Energy landscapes of receptor-ligand bonds explored with dynamic force spectroscopy. *Nature,* 397**,** 50-3.

MICHELSON, A. D. 1998. Platelet function in the newborn. *Seminars in thrombosis and hemostasis,* 24**,** 507-12.

MICHELSON, A. D. 2007. Platelets. *In:* MICHELSON, A. D. (ed.) *Platelets.* 2nd ed. Worcester Elsevier.

MINELLI, C., KIKUTA, A., TSUD, N., BALL, M. D. & YAMAMOTO, A. 2008. A micro-fluidic study of whole blood behaviour on PMMA topographical nanostructures. *Journal of nanobiotechnology,* 6**,** 3.

MORALES, L. D., MARTIN, C. & CRUZ, M. A. 2006. The interaction of von Willebrand factor-A1 domain with collagen: mutation G1324S (type 2M von Willebrand disease) impairs the conformational change in A1 domain induced by collagen. *Journal of thrombosis and haemostasis : JTH,* 4**,** 417-25.

MORGAN, J. P., DELNERO, P. F., ZHENG, Y., VERBRIDGE, S. S., CHEN, J., CRAVEN, M., CHOI, N. W., DIAZ-SANTANA, A., KERMANI, P., HEMPSTEAD, B., LOPEZ, J. A., CORSO, T. N., FISCHBACH, C. & STROOCK, A. D. 2013. Formation of microvascular networks in vitro. *Nature protocols,* 8**,** 1820-36.

MORRISON, R., CRAWFORD, J., MACPHERSON, M. & HEPTINSTALL, S. 1985. Platelet behaviour in normal pregnancy, pregnancy complicated by essential hypertension and pregnancy-induced hypertension. *Thrombosis and haemostasis,* 54**,** 607-11.

MULLERS, S., BURKE, N., COWMAN, J., KEARNEY, M., FLOOD, K., O' CONNER, H., DICKER, P., TULLY, E., GEARY, M., KENNY, D. AND MALONE F. 2015. Platelet function in intra-uterine growth restriction: altered platelet behaviour as a

cause or a consequence of utero-placental disease. *American journal of obstetrics and gynecology,* 212**,** S125-S126.

NADAR, S. & LIP, G. Y. 2004. Platelet activation in the hypertensive disorders of pregnancy. *Expert opinion on investigational drugs,* 13**,** 523-9.

NAIDECH, A. M., BENDOK, B. R., GARG, R. K., BERNSTEIN, R. A., ALBERTS, M. J., BLECK, T. P. & BATJER, H. H. 2009. Reduced platelet activity is associated with more intraventricular hemorrhage. *Neurosurgery,* 65**,** 684-8; discussion 688.

NEALEN, M. L., VIJAYAN, K. V., BOLTON, E. & BRAY, P. F. 2001. Human platelets contain a glycosylated estrogen receptor beta. *Circulation research,* 88**,** 438-42.

NEEVES, K. B., ONASOGA, A. A., HANSEN, R. R., LILLY, J. J., VENCKUNAITE, D., SUMNER, M. B., IRISH, A. T., BRODSKY, G., MANCO-JOHNSON, M. J. & DI PAOLA, J. A. 2013. Sources of variability in platelet accumulation on type 1 fibrillar collagen in microfluidic flow assays. *PloS one,* 8**,** e54680.

NESBITT, W. S., KULKARNI, S., GIULIANO, S., GONCALVES, I., DOPHEIDE, S. M., YAP, C. L., HARPER, I. S., SALEM, H. H. & JACKSON, S. P. 2002. Distinct glycoprotein Ib/V/IX and integrin alpha IIbbeta 3-dependent calcium signals cooperatively regulate platelet adhesion under flow. *The Journal of biological chemistry,* 277**,** 2965-72.

NICHOLSON, N. S., PANZER-KNODLE, S. G., HAAS, N. F., TAITE, B. B., SZALONY, J. A., PAGE, J. D., FEIGEN, L. P., LANSKY, D. M. & SALYERS, A. K. 1998. Assessment of platelet function assays. *American heart journal,* 135**,** S170-8.

NICOLINI, U., GUARNERI, D., GIANOTTI, G. A., CAMPAGNOLI, C., CROSIGNANI, P. G. & GATTI, L. 1994. Maternal and fetal platelet activation in normal pregnancy. *Obstetrics and gynecology,* 83**,** 65-9.

NIIYA, K., HODSON, E., BADER, R., BYERS-WARD, V., KOZIOL, J. A., PLOW, E. F. & RUGGERI, Z. M. 1987. Increased surface expression of the membrane glycoprotein IIb/IIIa complex induced by platelet activation. Relationship to the binding of fibrinogen and platelet aggregation. *Blood,* 70**,** 475-83.

NORRIS, L. A., GLEESON, N., SHEPPARD, B. L. & BONNAR, J. 1993. Whole blood platelet aggregation in moderate and severe pre-eclampsia. *British journal of obstetrics and gynaecology,* 100**,** 684-8.

NORRIS, L. A., SHEPPARD, B. L., BURKE, G. & BONNAR, J. 1994. Platelet activation in normotensive and hypertensive pregnancies complicated by intrauterine growth retardation. *British journal of obstetrics and gynaecology,* 101**,** 209-14.

NOWAK, A. A., CANIS, K., RIDDELL, A., LAFFAN, M. A. & MCKINNON, T. A. 2012. O-linked glycosylation of von Willebrand factor modulates the interaction with platelet receptor glycoprotein Ib under static and shear stress conditions. *Blood,* 120**,** 214-22.

NURDEN, A. T. 2006. Glanzmann thrombasthenia. *Orphanet journal of rare diseases,* 1**,** 10.

O'BRIEN, W. F., SABA, H. I., KNUPPEL, R. A., SCERBO, J. C. & COHEN, G. R. 1986. Alterations in platelet concentration and aggregation in normal pregnancy and preeclampsia. *American journal of obstetrics and gynecology,* 155**,** 486-90.

PAPILE, L. A., BURSTEIN, J., BURSTEIN, R. & KOFFLER, H. 1978. Incidence and evolution of subependymal and intraventricular hemorrhage: a study of infants with birth weights less than 1,500 gm. *The Journal of pediatrics,* 92**,** 529-34.

PARODI, G., MARCUCCI, R., VALENTI, R., GORI, A. M., MIGLIORINI, A., GIUSTI, B., BUONAMICI, P., GENSINI, G. F., ABBATE, R. & ANTONIUCCI, D. 2011. High residual platelet reactivity after clopidogrel loading and long-term cardiovascular events among patients with acute coronary syndromes undergoing PCI. *JAMA : the journal of the American Medical Association,* 306**,** 1215-23.

PERACOLI, M. T., MENEGON, F. T., BORGES, V. T., DE ARAUJO COSTA, R. A., THOMAZINI-SANTOS, I. A. & PERACOLI, J. C. 2008. Platelet aggregation and TGF-beta(1) plasma levels in pregnant women with preeclampsia. *Journal of reproductive immunology,* 79**,** 79-84.

PREVITALI, E., BUCCIARELLI, P., PASSAMONTI, S. M. & MARTINELLI, I. 2011. Risk factors for venous and arterial thrombosis. *Blood transfusion = Trasfusione del sangue,* 9**,** 120-38.

QUIROGA, T., GOYCOOLEA, M., MUNOZ, B., MORALES, M., ARANDA, E., PANES, O., PEREIRA, J. & MEZZANO, D. 2004. Template bleeding time and PFA-100 have low sensitivity to screen patients with hereditary mucocutaneous hemorrhages: comparative study in 148 patients. *Journal of thrombosis and haemostasis : JTH,* 2**,** 892-8.

RAJASEKHAR, D., BARNARD, M. R., BEDNAREK, F. J. & MICHELSON, A. D. 1997. Platelet hyporeactivity in very low birth weight neonates. *Thrombosis and haemostasis,* 77**,** 1002-7.

REILLY, I. A. & FITZGERALD, G. A. 1986. Eicosenoid biosynthesis and platelet function with advancing age. *Thrombosis research,* 41**,** 545-54.

REININGER, A. J., HEIJNEN, H. F., SCHUMANN, H., SPECHT, H. M., SCHRAMM, W. & RUGGERI, Z. M. 2006. Mechanism of platelet adhesion to von Willebrand factor and microparticle formation under high shear stress. *Blood,* 107**,** 3537-45.

ROBB, A. O., DIN, J. N., MILLS, N. L., SMITH, I. B., BLOMBERG, A., ZIKRY, M. N., RAFTIS, J. B., NEWBY, D. E. & DENISON, F. C. 2010. The influence of the menstrual cycle, normal pregnancy and pre-eclampsia on platelet activation. *Thrombosis and haemostasis,* 103**,** 372-8.

ROBERTS, J., MONTGOMERY, R. AND WHITE, G. 2014. *Progress in the Diagnosis and Management of Type 1 von Willebrand Disease* [Online]. The Hematologist. [Accessed 09/12/14.

ROEST, M., REININGER, A., ZWAGINGA, J. J., KING, M. R. & HEEMSKERK, J. W. 2011. Flow chamber-based assays to measure thrombus formation in vitro: requirements for standardization. *Journal of thrombosis and haemostasis : JTH,* 9**,** 2322-4.

RUGGERI, Z. M. 1997. von Willebrand factor. *The Journal of clinical investigation,* 100**,** S41-6.

RUGGERI, Z. M. 2007. Von Willebrand factor: looking back and looking forward. *Thrombosis and haemostasis,* 98**,** 55-62.

RUGGERI, Z. M. & MENDOLICCHIO, G. L. 2007. Adhesion mechanisms in platelet function. *Circulation research,* 100**,** 1673-85.

RUGGERI, Z. M. & WARE, J. 1992. The structure and function of von Willebrand factor. *Thrombosis and haemostasis,* 67**,** 594-9.

RUGGERI, Z. M. & WARE, J. 1993. von Willebrand factor. *FASEB journal : official publication of the Federation of American Societies for Experimental Biology,* 7**,** 308-16.

SADLER, J. E. 1998. Biochemistry and genetics of von Willebrand factor. *Annual review of biochemistry,* 67**,** 395-424.

SADLER, J. E. 2003. Von Willebrand disease type 1: a diagnosis in search of a disease. *Blood,* 101**,** 2089-93.

SATO, Y., FUJIWARA, H. & KONISHI, I. 2010. Role of platelets in placentation. *Medical molecular morphology,* 43**,** 129-33.

SATO, Y., FUJIWARA, H., ZENG, B. X., HIGUCHI, T., YOSHIOKA, S. & FUJII, S. 2005. Platelet-derived soluble factors induce human extravillous trophoblast migration and differentiation: platelets are a possible regulator of trophoblast infiltration into maternal spiral arteries. *Blood,* 106**,** 428-35.

SAVAGE, B., SALDIVAR, E. & RUGGERI, Z. M. 1996. Initiation of platelet adhesion by arrest onto fibrinogen or translocation on von Willebrand factor. *Cell,* 84**,** 289-97.

SCHNEIDER, S. W., NUSCHELE, S., WIXFORTH, A., GORZELANNY, C., ALEXANDER-KATZ, A., NETZ, R. R. & SCHNEIDER, M. F. 2007. Shear-induced unfolding triggers adhesion of von Willebrand factor fibers. *Proceedings of the National Academy of Sciences of the United States of America,* 104**,** 7899-903.

SEIDEL, H., RAHMAN, M. M. & SCHARF, R. E. 2011. Monitoring of antiplatelet therapy. Current limitations, challenges, and perspectives. *Hamostaseologie,* 31**,** 41-51.

SESTITO, A., SCIAHBASI, A., LANDOLFI, R., MASERI, A., LANZA, G. A. & ANDREOTTI, F. 1999. A simple assay for platelet-mediated hemostasis in flowing whole blood (PFA-100): reproducibility and effects of sex and age. *Cardiologia,* 44**,** 661-5.

SEYFERT, U. T., HAUBELT, H., VOGT, A. & HELLSTERN, P. 2007. Variables influencing Multiplate(TM) whole blood impedance platelet aggregometry and

turbidimetric platelet aggregation in healthy individuals. *Platelets,* 18**,** 199-206.

SHATTIL, S. J., KIM, C. & GINSBERG, M. H. 2010. The final steps of integrin activation: the end game. *Nature reviews. Molecular cell biology,* 11**,** 288-300.

SHENKMAN, B., EINAV, Y., SALOMON, O., VARON, D. & SAVION, N. 2008. Testing agonist-induced platelet aggregation by the Impact-R [Cone and plate(let) analyzer (CPA)]. *Platelets,* 19**,** 440-6.

SHENNAN, A. T., DUNN, M. S., OHLSSON, A., LENNOX, K. & HOSKINS, E. M. 1988. Abnormal pulmonary outcomes in premature infants: prediction from oxygen requirement in the neonatal period. *Pediatrics,* 82**,** 527-32.

SHEU, J. R., HSIAO, G., SHEN, M. Y., LIN, W. Y. & TZENG, C. R. 2002. The hyperaggregability of platelets from normal pregnancy is mediated through thromboxane A2 and cyclic AMP pathways. *Clinical and laboratory haematology,* 24**,** 121-9.

SHUSTER, L. T., RHODES, D. J., GOSTOUT, B. S., GROSSARDT, B. R. & ROCCA, W. A. 2010. Premature menopause or early menopause: long-term health consequences. *Maturitas,* 65**,** 161-6.

SIBBING, D., BRAUN, S., MORATH, T., MEHILLI, J., VOGT, W., SCHOMIG, A., KASTRATI, A. & VON BECKERATH, N. 2009. Platelet reactivity after clopidogrel treatment assessed with point-of-care analysis and early drug-eluting stent thrombosis. *Journal of the American College of Cardiology,* 53**,** 849-56.

SIEDLECKI, C. A., LESTINI, B. J., KOTTKE-MARCHANT, K. K., EPPELL, S. J., WILSON, D. L. & MARCHANT, R. E. 1996. Shear-dependent changes in the three-dimensional structure of human von Willebrand factor. *Blood,* 88**,** 2939-50.

SINGH, G. 2006. Determination of Cutoff Score for a Diagnostic Test. *The Internet Journal of Laboratory Medicine,* 2.

SITARU, A. G., HOLZHAUER, S., SPEER, C. P., SINGER, D., OBERGFELL, A., WALTER, U. & GROSSMANN, R. 2005. Neonatal platelets from cord blood and peripheral blood. *Platelets,* 16**,** 203-10.

SMITH, J. M., CURRIE, S., CANNON, T., ARMBRUSTER, D. & PERRI, J. 2014. Are national policies and programs for prevention and management of

postpartum hemorrhage and preeclampsia adequate? A key informant survey in 37 countries. *Global health, science and practice,* 2**,** 275-84.

SOLA, M. C., DEL VECCHIO, A., EDWARDS, T. J., SUTTNER, D., HUTSON, A. D. & CHRISTENSEN, R. D. 2001. The relationship between hematocrit and bleeding time in very low birth weight infants during the first week of life. *Journal of perinatology : official journal of the California Perinatal Association,* 21**,** 368-71.

SOLA-VISNER, M. 2012. Platelets in the neonatal period: developmental differences in platelet production, function, and hemostasis and the potential impact of therapies. *Hematology / the Education Program of the American Society of Hematology. American Society of Hematology. Education Program,* 2012**,** 506-11.

SOLBERG, H. E. 1987. International Federation of Clinical Chemistry (IFCC), Scientific Committee, Clinical Section, Expert Panel on Theory of Reference Values, and International Committee for Standardization in Haematology (ICSH), Standing Committee on Reference Values. Approved Recommendation (1986) on the theory of reference values. Part 1. The concept of reference values. *Journal of clinical chemistry and clinical biochemistry. Zeitschrift fur klinische Chemie und klinische Biochemie,* 25**,** 337-42.

STAR, J., ROSENE, K., FERLAND, J., DILEONE, G., HOGAN, J. & KESTIN, A. 1997. Flow cytometric analysis of platelet activation throughout normal gestation. *Obstetrics and gynecology,* 90**,** 562-8.

STUBBS, T. M., LAZARCHICK, J., VAN DORSTEN, J. P., COX, J. & LOADHOLT, C. B. 1986. Evidence of accelerated platelet production and consumption in nonthrombocytopenic preeclampsia. *American journal of obstetrics and gynecology,* 155**,** 263-5.

TANTRY, U. S., BONELLO, L., ARADI, D., PRICE, M. J., JEONG, Y. H., ANGIOLILLO, D. J., STONE, G. W., CURZEN, N., GEISLER, T., TEN BERG, J., KIRTANE, A., SILLER-MATULA, J., MAHLA, E., BECKER, R. C., BHATT, D. L., WAKSMAN, R., RAO, S. V., ALEXOPOULOS, D., MARCUCCI, R., RENY, J. L., TRENK, D., SIBBING, D. & GURBEL, P. A. 2013. Consensus and update on the definition of on-treatment

platelet reactivity to adenosine diphosphate associated with ischemia and bleeding. *Journal of the American College of Cardiology,* 62**,** 2261-73.

TARANTINO, M. D., KUNICKI, T. J. & NUGENT, D. J. 1994. The estrogen receptor is present in human megakaryocytes. *Annals of the New York Academy of Sciences,* 714**,** 293-6.

THOMPSON, N. T., SCRUTTON, M. C. & WALLIS, R. B. 1986. Particle volume changes associated with light transmittance changes in the platelet aggregometer: dependence upon aggregating agent and effectiveness of stimulus. *Thrombosis research,* 41**,** 615-26.

TITANI, K., KUMAR, S., TAKIO, K., ERICSSON, L. H., WADE, R. D., ASHIDA, K., WALSH, K. A., CHOPEK, M. W., SADLER, J. E. & FUJIKAWA, K. 1986. Amino acid sequence of human von Willebrand factor. *Biochemistry,* 25**,** 3171-84.

UCAR, T., GURMAN, C., ARSAN, S. & KEMAHLI, S. 2005. Platelet aggregation in term and preterm newborns. *Pediatric hematology and oncology,* 22**,** 139-45.

ULRICHTS, H., UDVARDY, M., LENTING, P. J., PAREYN, I., VANDEPUTTE, N., VANHOORELBEKE, K. & DECKMYN, H. 2006. Shielding of the A1 domain by the D'D3 domains of von Willebrand factor modulates its interaction with platelet glycoprotein Ib-IX-V. *The Journal of biological chemistry,* 281**,** 4699-707.

VALERI, C. R., CASSIDY, G., PIVACEK, L. E., RAGNO, G., LIEBERTHAL, W., CROWLEY, J. P., KHURI, S. F. & LOSCALZO, J. 2001. Anemia-induced increase in the bleeding time: implications for treatment of nonsurgical blood loss. *Transfusion,* 41**,** 977-83.

VARON, D., DARDIK, R., SHENKMAN, B., KOTEV-EMETH, S., FARZAME, N., TAMARIN, I. & SAVION, N. 1997. A new method for quantitative analysis of whole blood platelet interaction with extracellular matrix under flow conditions. *Thrombosis research,* 85**,** 283-94.

WAGNER, C. L., MASCELLI, M. A., NEBLOCK, D. S., WEISMAN, H. F., COLLER, B. S. & JORDAN, R. E. 1996. Analysis of GPIIb/IIIa receptor number by quantification of 7E3 binding to human platelets. *Blood,* 88**,** 907-14.

WAGNER, D. D. 1993. The Weibel-Palade body: the storage granule for von Willebrand factor and P-selectin. *Thrombosis and haemostasis,* 70**,** 105-10.

WALSH, M. C. & KLIEGMAN, R. M. 1986. Necrotizing enterocolitis: treatment based on staging criteria. *Pediatric clinics of North America,* 33**,** 179-201.

WATSON, S. P. 2009. Platelet activation by extracellular matrix proteins in haemostasis and thrombosis. *Current pharmaceutical design,* 15**,** 1358-72.

WIEDMEIER, S. E., HENRY, E., SOLA-VISNER, M. C. & CHRISTENSEN, R. D. 2009. Platelet reference ranges for neonates, defined using data from over 47,000 patients in a multihospital healthcare system. *Journal of perinatology : official journal of the California Perinatal Association,* 29**,** 130-6.

WU, Y. P., VAN BREUGEL, H. H., LANKHOF, H., WISE, R. J., HANDIN, R. I., DE GROOT, P. G. & SIXMA, J. J. 1996. Platelet adhesion to multimeric and dimeric von Willebrand factor and to collagen type III preincubated with von Willebrand factor. *Arteriosclerosis, thrombosis, and vascular biology,* 16**,** 611-20.

YAGO, T., LOU, J., WU, T., YANG, J., MINER, J. J., COBURN, L., LOPEZ, J. A., CRUZ, M. A., DONG, J. F., MCINTIRE, L. V., MCEVER, R. P. & ZHU, C. 2008. Platelet glycoprotein Ibalpha forms catch bonds with human WT vWF but not with type 2B von Willebrand disease vWF. *The Journal of clinical investigation,* 118**,** 3195-207.

YAGO, T., WU, J., WEY, C. D., KLOPOCKI, A. G., ZHU, C. & MCEVER, R. P. 2004. Catch bonds govern adhesion through L-selectin at threshold shear. *The Journal of cell biology,* 166**,** 913-23.

Yakushkin, V.V., Zyuryaev, I.T., Khaspekova, S.G., Sirotkina, O.V., Ruda, M.YA. & Mazurov A.V. 2011. Glycoprotein IIb-IIIa content and platelet aggregation in healthy volunteers and patients with acute coronary syndrome. *Platelets, 22, 243–51.*

YIP, J., SHEN, Y., BERNDT, M. C. & ANDREWS, R. K. 2005. Primary platelet adhesion receptors. *IUBMB life,* 57**,** 103-8.

YUAN, H., DENG, N., ZHANG, S., CAO, Y., WANG, Q., LIU, X. & ZHANG, Q. 2012. The unfolded von Willebrand factor response in bloodstream: the self-association perspective. *Journal of hematology & oncology,* 5**,** 65.

YUAN, Y., KULKARNI, S., ULSEMER, P., CRANMER, S. L., YAP, C. L., NESBITT, W. S., HARPER, I., MISTRY, N., DOPHEIDE, S. M., HUGHAN, S. C., WILLIAMSON, D., DE LA SALLE, C., SALEM, H. H., LANZA, F. & JACKSON, S. P. 1999. The von Willebrand factor-glycoprotein Ib/V/IX interaction induces actin polymerization and cytoskeletal reorganization in rolling platelets and glycoprotein Ib/V/IX-transfected cells. *The Journal of biological chemistry,* 274**,** 36241-51.

ZAHAVI, J., JONES, N. A., LEYTON, J., DUBIEL, M. & KAKKAR, V. V. 1980. Enhanced in vivo platelet "release reaction" in old healthy individuals. *Thrombosis research,* 17**,** 329-36.

ZENG, S. M., YANKOWITZ, J., WIDNESS, J. A. & STRAUSS, R. G. 2001. Etiology of differences in hematocrit between males and females: sequence-based polymorphisms in erythropoietin and its receptor. *The journal of gender-specific medicine : JGSM : the official journal of the Partnership for Women's Health at Columbia,* 4**,** 35-40.

ZHANG, W., DENG, W., ZHOU, L., XU, Y., YANG, W., LIANG, X., WANG, Y., KULMAN, J. D., ZHANG, X. F. & LI, R. 2014. Identification of a juxtamembrane mechano-sensitive domain in the platelet mechanosensor glycoprotein Ib-IX complex. *Blood*.

ZHAO, H., SHAQFEH, E.S.G. AND NARSIMHAN 2012. Shear-induced particle migration and margination in a cellular suspension. *Physics of Fluids,* 24**,** 011902.

ZHOU, Y. F., ENG, E. T., ZHU, J., LU, C., WALZ, T. & SPRINGER, T. A. 2012. Sequence and structure relationships within von Willebrand factor. *Blood,* 120**,** 449-58.

Appendix A

Ethics approval for studies

Royal College of Surgeons in Ireland
The Research Ethics Committee
123 St. Stephens Green, Dublin 2, Ireland.
Tel: +353 1 4022373 Fax: +353 1 4022449 Email: recadmin@rcsi.ie

Dr. David Smith, Acting Chair
Ms. Stephanie O'Connor, Convenor

Royal College of Surgeons in Ireland
Coláiste Ríoga na Máinleá in Éirinn

RCSI

19th September, 2011

Dr Dermot Cox,
Royal College of Surgeons in Ireland,
Department of Molecular & Cellular Therapeutics,
3rd Floor,
123 St Stephens Green,
Dublin 2

Ethics Reference No:	REC676
Project Title:	Blood from human volunteers.
Researchers Name:	Dr Dermot Cox
Other Individuals Involved:	Ms. Olwen Foley, MCT. Researchers in RCSI requiring the use of blood from human volunteers.

Dear Dr Dermot Cox,
Thank you for your Research Ethics Committee (REC) application. We are pleased to advise that ethical approval has been granted by the committee for this study.

This letter provides approval for data collection for the time requested in your application and for an additional 6 months. This is to allow for any unexpected delays in proceeding with data collection. Therefore this research ethics approval will expire on 19th March, 2017.

Where data collection is necessary beyond this point, approval for an extension must be sought from the Research Ethics Committee.

This ethical approval is given on the understanding that:

- All personnel listed in the approved application have read, understand and are thoroughly familiar with all aspects of the study.
- Any significant change which occurs in connection with this study and/or which may alter its ethical consideration, must be reported immediately to the REC, and an ethical amendment submitted where appropriate.

We wish you all the best with your research.

Yours sincerely,

PP Ms. Stephanie O'Connor (Convenor)
Dr David Smith (Acting Chair)

LOCAL COMMITTEE DECLARATION AND SIGNATORY PAGE:

Name of Committee: National Maternity Hospital Research Ethics Committee.

Title of Study: platelet function in neonates

DECLARATION OF PRINCIPAL INVESTIGATOR:

1. I confirm that the information provided in this application for ethical review is correct to the best of my knowledge and assume full responsibility for it.
2. I agree to abide by the ethical principles governing the Declaration of Helsinki and European Guidelines of good Clinical Practice in the proper conduct of research.
3. I agree to submit annual reports on the progress of my research project and submit a copy of the study on its completion to the Research Ethics Committee. In addition, I will seek prior approval from Research Ethics Committee of any proposed changes/amendments to the protocol.
4. I agree to adhere to the study protocol as outlined in this submitted Research Ethics Application form if a favourable ethical opinion is given.
5. In the event of premature termination, suspension or deferral of this project, I agree to provide a report to the Research Ethics Committee outlining the circumstances for such termination, suspension or deferral.
6. All relevant information about serious adverse reactions and new events likely to affect the safety of the subjects will be reported the Research Ethics Committee in writing.
7. I understand that details relating to this research project are subject to the provisions of the Freedom of Information Act except where statutory exemptions apply.
8. I confirm that I have made the sponsor/Chief Investigator aware of this application and that the sponsor/Chief Investigator fully accepts all associated responsibilities.

Name of Principal Investigator: Eleanor Molloy

Signature of Principal Investigator:

Date: 31/10/2012

Ospidéal an Rotunda
Cearnóg Parnell, Baile Átha Cliath 1, É
The Rotunda Hospital
Parnell Square, Dublin 1, Ireland.
T: +353 1 817 1700 / F: +353 1 872 6523
www.rotunda.ie

2nd October, 2014

Dr Sieglinde Mullers,
Clinical Lecturer,
RCSI Unit,
Rotunda Hospital

Re: Role of hyper-reactive platelets in pre-eclampsia

Dear Dr Mullers,

Further to your enquiry, I am pleased to advise that the above named study was granted ethical approval by the Research Ethics Committee in April 2010.

Kind regards.

Yours sincerely,

Dr Peter McKenna,
Chairman,
Research Ethics Committee

Appendix B

Platelet tracking software

1 2 3

***Abstract*—Here, we report on the enhancements made to a method previously developed by this group to analyze complex dynamic platelet-protein surface behavior. Platelets are imaged on a defined von Willebrand factor (VWF) surface using a custom-designed microfluidic parallel plate flow chamber at arterial shear flow rates (Lincoln et al., Analytical Biochemistry 405 (2), 174-183). Using the centroids and area of each platelet at each time frame, a time history or track can be constructed for each platelet. Enhancements have been made to the tracking process through the design and verification of nine key trajectory parameters using idealized data sets where the values are known, specifically (1) total number of tracks, (2) the number of stably-adhered platelets, (3) the number of translocating platelets, (4) weighted median speed, (5) mean translocation distance, (6) percentage surface coverage, (7) percentage motion, (8) initial pause-time distribution and (9) adhesion rate, with absolute mean error determined for each variable. Hence, this novel analytical method provides rapid data pertinent to platelet translocation properties which can readily be applied for the analysis of different disease cohorts in the presence and absence of anti-platelet therapies (*e*.g. Aspirin, Clopidogrel).**

***Index Terms*—Platelet characterization, Image analysis, Weighted distance matrix, Microfluidic parallel-plate flow chamber, Algorithms, Computer Analysis.**

Enhancements to a platelet tracking method of shear-mediated platelet interactions with von Willebrand factor

Adam Ralph,Martin Somers,Jonathan Cowman,Bruno Voisin,Emma Hogan,
Hannah Dunne,Eimear Dunne,Barry Byrne,Antonio Ricco,Dermot Kenny,Simon Wong

I. Introduction

PLATELETS play key roles in maintaining normal hemostasis, and in the pathogenesis of ischemic syndromes occurring in the vicinity of ruptured atherosclerotic arteries. Thus, understanding the intrinsic relationship between platelet activation states and their kinetic properties upon association with matrix proteins such as von Willebrand factor (VWF) under defined flow conditions provides physiologically relevant information directly relating to the initial responses to vascular injury. It is well established that cardiovascular disease (CVD) is a major cause of mortality and morbidity, which places considerable financial burden on healthcare systems. Platelet adhesion and aggregation, essential responses to arterial vascular injury [1], depend on the initial capture and translocation of platelets on adhered VWF. Such interactions are shear stress-dependent, are influenced by blood flow conditions [2]–[5], are rapidly reversible and result in start-stop platelet movements [3]–[7]. Platelets undergo changes in their respective physiologies during thrombosis, suggesting that the monitoring of platelet morphologies (physical) and their functional state (biochemical) are clinically useful indicators of acute thrombotic events that, in turn, are useful predictors of thrombotic events.

Using the experimental methodology described previously [8] and the VWF-doped surfaces [9], we obtain a time-series set of images (or frames at a rate of 30 frames/s) of an $133 \times 133\mu m^2$ section of the surface. Platelets are incubated with a fluorescent dye, (3,3'-Dihexyloxacarbocyanine Iodide, DioC6) which localizes to the endoplasmic reticulum and mitochondria of platelets, so that they can be imaged. However, only those that interact with the surface are captured by the imaging software (Metamorph®Image Analysis Software). Experiments are conducted to capture the early stages of platelet adhesion before large-scale platelet aggregation occurs, in the order of 16.7s (equivalent to 500 frames). However, during this process platelets will translocate with the direction of the flow and recruit others. Thus, during this period platelets merge and separate over time making it difficult to apply other cell tracking algorithms [10]–[14]. The challenge then is not to locate the platelet on each frame, but to track the platelets, over time, from one frame to the next with the centroid position and area for each frame where a platelet is visible, referred to as the platelet's track. While a limited amount of information can be obtained from the static images, interrogation of platelet tracks produces a range of outputs that can be qualitatively and quantitatively measured, such as: translocation speed, translocation distance and percentage of time in motion.

With reference to the previously described method of tracking platelet behavior [8], a challenge for this system is that of platelet track fragmentation, where a single platelet track is recorded as a set of smaller tracks. The major source of platelet track fragmentation is the merging and separating of platelets over time (figure 1, platelet B). The enhancement of the tracking method described here, compared to that we described previously [8], is to identify individual platelets which are part of a platelet group and to track them as they merge and split from the group. This will allow construction of the full platelet track. This is in contrast to another method, described by [15], where watershed segmentation was used to separate joined platelets on the image. We did not implement watershed segmentation in the tracking algorithm as the average number of platelets per frame was high (in the order of a few hundred), some were substantially overlapped ($> 20\%$) and in a range of sizes, making it time consuming and difficult to implement.

Adam Ralph, Bruno Voisin, Emma Hogan, Simon Wong are with Irish Centre for High-end Computing, National University Ireland, Galway, Ireland.
Tel.: +353-1-5241608
Fax: +353-1-7645845

Martin Somers, Barry Byrne are with Biomedical Diagnostics Institute, Dublin City University, Dublin 9, Ireland.

Jonathan Cowman, Hanna Dunne, Eimear Dunne, Antonio Ricco, Dermot Kenny are with Biomedical Diagnostics Institute, Royal College of Surgeons in Ireland, Dublin 2, Ireland.

II. Material and Methods

A. Conversion Factor

A conversion factor was calculated so that all measurements on the aforementioned microscope system can be quantitatively related to the physical movements of platelets within the parallel platelet flow chamber. This was achieved through the use of a fluorescently-labelled (Cy3) fibrinogen microcontact-printed array comprised of $\sim 6\mu m$ dots separated in all planes by $\sim 15\mu m$. Due to the microcontact-printing process these distances can vary by 1-2% [16]. A single image was taken under conditions that mimic the settings for the assay. A series of eight dots (figure 2), measured 5 times, were used to determine the conversion factor from pixels to micrometers

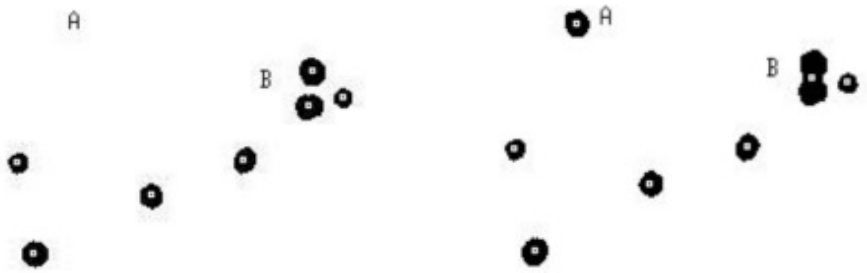

(a) Frame n (b) Frame n+1

Fig. 1. Two consecutive frames of masked images, the left being the current frame and the right the next. Most platelets can be assigned uniquely, except A is new and B merges. The flow is up the page $(+y)$ and the images have been inverted black to white.

(μm), with ImageJ processing [17] used to quantify pixel dimensions.

The distance over 8 spots from center to center was calculated to be $111\mu m$, *e.g.* $(7 \times 15\mu m) + 3\mu m + 3\mu m$, which correlated to an average distance of 431.91 pixels. Hence, a conversion factor of 0.2569 $(111\mu m/431.91$ pixels) was calculated, implying this (rounded to 0.26) could be used for converting pixel dimension into micrometers.

B. Tracking Process

Previous platelet tracking algorithms have used a probability function and cut-off based on the typical movement of a platelet on a clutter-free, smooth surface. That is to say, there is a strong preference for movement in a narrow angle in the direction of the flow [8], [15]. This can result in tracking errors due to merging and splitting of platelet groups and/or movement around obstructions. Previous results [15] demonstrate that tracking is adversely affected by probability functions that are strongly directional, in the direction of the flow, but not by ones that are more omnidirectional. The distance weighting method, described herein, is much less directional.

Initially, platelets are identified in each frame of an image sequence of 500 frames using the auto-threshold method [8]. This method reliably detects and records the (x, y) centroid position and approximate size of each platelet in an image frame against a continuously changing background using the Image Processing Toolkit of MatLab [18]. Next, a platelet track is constructed by identifying the same platelet from one frame to the next and recording the change in (x, y) over time. To this end, a weighted distance matrix is generated between a track's current position and all other platelets on the next frame. The weighting method gives preference to platelet movement in the direction of flow over cross-stream movement. Each track is extended by assigning a platelet in the next frame, if possible, by applying a set of rules to the weighted distance matrix. Complementary changes in platelet area allow the detection of two or more platelets merging into one object or conversely splitting. The result is a list of tracks with (x, y) positions and area (A) over time, linking each platelet in an image sequence.

The weighted distance is calculated between the ends of the currently active tracks (R_i) with the platelets on the subsequent frame (N_j) (eq. 1). Each object (R_i and N_j) has its centroid and area calculated with the flow in the $+y$ direction. Using the tracking rules outlined in table I tracks are amended using six scenarios. The current tracks can be extended by assigning a platelet on the next frame (N_j), new tracks started or currently active tracks are deactivated because they cannot be assigned a platelet on the next frame. This procedure is then repeated on the next frame, with the updated set of active tracks, and so on until the final frame is reached.

$$d(R_i, N_j) = (\sin^2(\theta/2) + 1/2) \times \sqrt{(\Delta x^2 + \Delta y^2)} \quad (1)$$

where

$$\Delta x = x_i - x_j,$$
$$\Delta y = y_i - y_j,$$
$$\theta = \arctan(\Delta x/\Delta y), -\pi \leq \theta \leq \pi$$

Six possible scenarios are considered when amending the tracks:

1) R_i is unambiguously assigned to a new platelet N_j,
2) R_i and R_k merge to form N_j on the next frame,
3) Merged tracks R_i and R_k split on the next frame to form N_j and N_l ,
4) R_i splits to form N_j and N_l hence forming a new track because R_i was considered a single platelet,
5) R_i cannot be assigned to a new platelet because it has disappeared,
6) N_j cannot be assigned to a previously recorded track because it is new.

When two platelets merge, the two tracks have the same (x, y, A) values but are managed as two separate tracks. In subsequent frames they are matched as one object but both tracks (i and k) are extended until they split, at which point the (x, y, A) for each track is different. Mergers and splits are not restricted to just two platelets, three or more could be involved and the algorithm keeps a record of how many platelets form a group, to ensure a group cannot split into more tracks than group members. It is also possible that initially a platelet is recorded as a singlet, only to split later

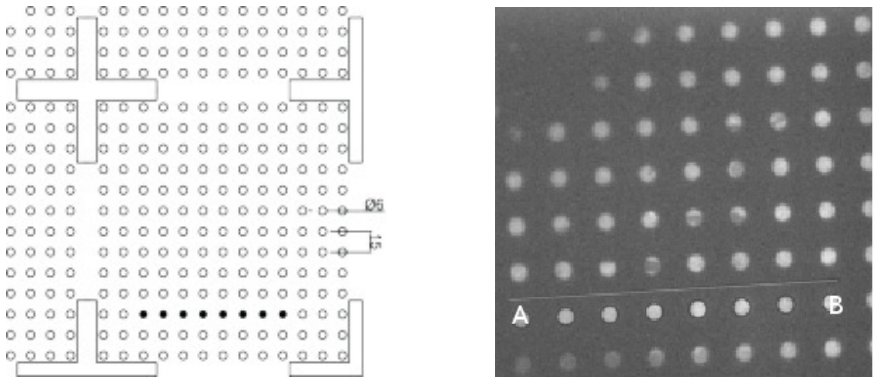

(a) Schematic (b) Image

Fig. 2. Microcontact-printed fibrinogen array, comprised of $6\mu m$ dots labelled with Cy3, which were center to center $15\mu m$ apart. Eight individual dots were imaged and subsequently selected for determining a conversion factor for estimating μm distances, based on pixel content. Left is a schematic and right the imaged array, the eight dots used are between A and B.

(scenario 4). In this instance, the platelet is in fact a multiple and it is tracked retrospectively as a multiple. Appearance and disappearance of platelets is not restricted to the top and bottom of the image, respectively, but can occur anywhere. Platelets can also disappear if they move out of the imaging area, in the direction of the flow. Furthermore, Glycoprotein Ib alpha (GPIbα) (as this is the part of the subunit of the platelet that interacts with A1 domain of VWF) tethering can break, due to the pressure exerted, under arterial shear, leading to platelets disappearing anywhere on the imaged surface. Finally, platelets can apparently disappear if they become too faint. Tracks are allowed to reappear in the space of 5 frames, which can happen if the high-intensity platelets move out of frame, lowering the masking level so that dim platelets reappear in the masked image. This occurs very infrequently and no special conditions are applied in this case.

The distance matrix along with the area changes are used to distinguish between the various different tracking possibilities. Table I matches each scenario with the necessary conditions. No cut-offs were applied to the weighted distance function but instead hard limits (similar to y_c in [8]) were applied to stop recorded tracks being extended over distances, which were considered physically impossible. Specially, if the distances observed were $|\Delta x| > 5.2\mu m$ or $\Delta y > 5.2\mu m$ upstream or $\Delta y > 26.0\mu m$ downstream, the assignment was rejected. These values were set empirically from manual inspection of the algorithm's performance. They are larger than those you might obtain from fluid flow dynamics, to ensure that platelets are tracked correctly when merging and separating.

Finally after all of the tracks are constructed from the image set, some are rejected. Rejections are based on two criteria: if the tracks are 10 frames or less and if the platelet area is less than $\sim 3\mu m^2$. The first criterion is to remove unavoidable fragmented tracks. The second is to remove tracked objects that are not platelets. The limit is smaller than the area of a small platelet ($\sim 4\mu m^2$).

TABLE I
RULES UNDER WHICH NEW PLATELETS ARE ASSIGNED TO PREVIOUSLY RECORDED TRACKS, FOR THE SIX SCENARIOS DESCRIBED ABOVE.

Scenario	Tracking Results
1	R_i and N_j are closest to each other.
2	R_i and R_k are closest to N_j, with a suitable increase in area in N_j.
3	N_j and N_l are closest to R_i (or R_k) which are multiples, with a suitable reduction in areas for both N_j and N_l.
4	same as 3 but R_j is a singlet.
5	all the suitable new platelets have been assigned.
6	all the suitable recorded tracks have been assigned.

C. Validation

To validate the tracking algorithm, ideal image sets were created. A set of tracks was created with known properties, which were then used to generate the images. The image set can be run through the tracking process populating the variables. As the ideal tracks have known properties, we can compare values obtained through the process against the expected values. Many different ideal image sets were created, outlined below, with different track properties to cover the range of properties we find experimentally.

Using the centroid values for each platelet on each image (from the ideal tracks) roughly same sized circular platelets were placed at each point. Due to pixelation of the image, platelets cannot be all the same size or indeed completely circular. Each object had the maximum intensity with a background of zero, *i.e.* no noise. Figure 3 shows an example of an ideal image. On each start frame (frame 1), 25 platelets were randomly placed, with the only restriction being the absence of overlapping platelets. Each image set had a known number of ideal tracks (object count), which is equal to the number of platelets on the final frame (frame 500). On subsequent frames, platelets were added at regular intervals so that on the final frame, the expected number of tracks was achieved. Again, platelets were placed randomly in areas where they

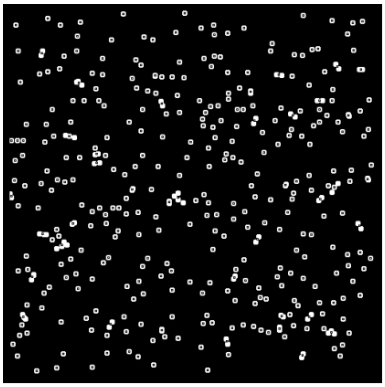

Fig. 3. Example of a single image from an image set used to validate the tracking process.

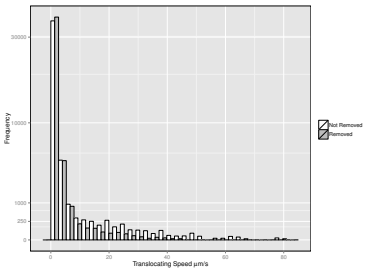

Fig. 4. Histogram of platelet translocating speeds (calculated as described in the section II-E4). Speeds with artificial movement removed (grey bars) and not removed (white bars) from the same image set. The grey bars have been displaced to enable comparison. The y-axis is square rooted.

would not overlap other platelets. As no platelets overlapped when they first appeared, a perfect tracking system would record all tracks. Any deviation from the expected number would be due to mistracking. A fraction of platelets were assigned as translocating. Each translocating platelet had the same track, *e.g.* they moved for 100 pixels at 1.0 pixel/frame and then stopped. Static platelets did not move at all, hence having a translocating distance of zero. Care was taken so that no platelet was removed from the image. The translocating platelets moved only in the direction of the flow with no restrictions on the number of mergers and separations after its initial frame.

For each dataset, five variables were fixed: the final object count (50, 100, 150, 200, 250, 300, 350, 400), the fraction of static platelets (10%, 20%, 30%), the translocating speed (0.5, 1.0, 1.5 pixels/frame), the translocating distance (50, 100, 150 pixels) and the initial pause time (10, 20 and 30 frames). Three different runs were generated with the same values for each of the 5 variables. The accuracy of each of the variables above was determined by comparing the expected value, which is known *a priori* against that obtained from the tracking process. Errors from runs with same expected value are averaged together to give the results shown in Section III.

Several runs were generated with no merging or separation events. These error-free runs gave the expected values for each variable (results not shown), allowing for detection and elimination of inherent errors in the algorithm.

D. Artificial Movement

When considering platelet mergers and separations, there is a large source of systematic error in the motion of the platelet which must be addressed. When platelets merge and separate there is an apparent movement that is larger than their actual movement. This is due to the centroid moving to a different location within the platelet or less frequently outside its area. An example of artificial movement is presented in figure 1, where two platelets (B) merge to form a single object on the next frame. In the track for the upper platelet it appears to move upstream and for the lower platelet it jumps downstream. This artificial movement, if not accounted for, will affect the values of platelet speed and distance traveled. Figure 4 shows the histogram of speeds from a single run with and without artificial movement removed. When artificial movement is not removed there is a longer tail of high velocities, which is exactly what we would expect.

A second case of artificial movement is platelet wobble. From frame-to-frame, platelets may appear to change shape because the masking threshold changes or they change shape when moving. This causes some uncertainty in each platelet's actual centroid position. This sort of artificial movement is difficult to remove and will affect the instantaneous velocity (currently we are not using shape information as part of the tracking process). In the next section we describe the use of moving averages to ameliorate the effect of platelet wobble.

E. Measured Variables

Below are the definitions for each of the variables, 9 in total, which are being assessed.

1) Total Number of Tracks: The total number of tracks is the number of platelet tracks, which the algorithm has deemed to be unique, after rejecting tracks where the platelets are too small.

2) Number of Stably-Adhered:

3) and Translocating Platelets: Translocating and stably-adhered (or static) platelets are categorized from the set of tracks, after all rejections are removed. A platelet is considered as translocating or static, not both. The classification of static and translocating platelets is an important one because many of the other variables are calculated from the translocating platelets. For this reason the classification was based on the movements of the singlet platelets only, ignoring all motions when part of a platelet group. A platelet is classed as translocating if it has moved more than 1.5x its average radius over the length of the track (when a singlet).

4) Weighted Median Speed: As can be seen from figure 4 a typical speed distribution will be severely skewed, limiting the usefulness of mean-based metrics. Additionally, erroneous speeds exist due to platelet wobble and mistracking. As previously mentioned, platelet wobble is the artificial change in the

platelet centroid and will typically overestimate the number of smaller speeds. To reduce the effect of platelet wobble, instantaneous velocities were averaged in a 5-frame window. That is to say, both speed and direction were used. The result is reduced to a speed, which is then used in the calculation of the weighted median. The artificial movements introduced by merging and separating platelets, which can be identified, are removed. Mistracking events cannot be predetermined and will typically lead to an overestimation of higher speeds. Using a weighted median will reduce the effect of these erroneous speeds and provide more meaningful speed measurements.

5) Mean Translocating Distance: The translocating distance (TD) for one track is calculated from eq. 2. The per frame x and y displacements (dx and dy) are summed separately (including sign) and then squared and added. Artificial movements due to merging and separation events are removed. Thus, the distance is not the same as that calculated from the start and end points of the track. The mean is calculated from all the translocating platelets for an image set.

$$TD = \sqrt{(\sum_{frames} dx)^2 + (\sum_{frames} dy)^2} \quad (2)$$

6) Surface Coverage: Surface coverage is the percentage of the sum of platelet areas on a particular frame over 512×512 pixels^2. Two variations were used: the surface coverage on the last frame and the difference in surface coverage between the first and last frames.

7) Percentage Motion: Percentage motion for a single translocating platelet is the ratio of the time in motion to the time it is attached to the surface. Thus, if the platelet continually translocates, then the percentage motion would be 100%. Typically a platelet may translocate, stop, and then translocate again. In this case, the percentage motion is less than 100%. When considering a set of tracks, it is the sum of the frames where a platelet is in motion (over all translocating platelets) divided by the sum of the track lifetimes (in frames over all translocating platelets).

Motion per frame is calculated the same way as the speed, *i.e.* it is the distance moved over a 5-frame window, removing artificial movements from merging and separating. If this value is bigger than the cutoff, then the platelet is defined as having moved that frame. A cutoff value is essential, otherwise percentage motion will always be near 100%. The cutoff used is twice the mean motion per frame of the stably-adhered platelets. The motion of the stably-adhered is assumed to be noise only.

8) Initial Pausetime Distribution: The initial pause time is the number of frames that a translocating platelet is stationary before it starts to move. The pausetimes for every valid track from the run is used in the distribution.

9) Adhesion Rate: Adhesion rate is the rate at which new tracks appear, which we assume to be roughly linear. For ease of calculation the rate is in fact obtained from the number of platelets per frame, which would be exact only if no platelets moved out of frame. If the rate is clearly non-linear then the rate is calculated from the linear part. Calculating the rate from the number of platelets per frame has the advantage in that image-processing irregularities are easily detected.

III. Results

A. Ideal Data Sets

The main influence on the errors for all of the variables was the object count. This is correlated with the number of merging and separating events and hence, the number of mistracking events *i.e.* the higher object count, the more mistracking events. For this reason we present the mean absolute error over the 8 object count levels in table II, for 7 of the nine variables. Figures are used to illustrate the variation in error for some of the variables. Figures 5-7 have the variable measurements on y and object count on x. There are 3 static fraction values which are color coded. Runs were produced and plotted in triplicate for a fixed value of object count, translocating distance and speed, initial pausetime and static fraction. The statistics have been produced by the statistical package R [19] and plots by the R ggplot2 package [20].

1) Total Number of Tracks: The error in the total number of tracks is correlated with the object count and tends to be overestimated. This is evident at higher object counts where more platelets merge and separate, which can cause mistracking. Mistracking can lead to track fragmentation or to joining different tracks. The former is more frequent as there is an overestimation of the number of tracks, which agrees with what we see when inspecting image sets manually.

2) Number of Stably-Adhered:

3) and Translocating Platelets: Figure 5 shows the error in the number of stably-adhered. The magnitude of the error will depend on the object count and the fraction of statics. It is clear that the error can vary over the three runs using the same parameters but in most cases there is an over-estimate. The errors are caused by mistracking, which increases with object count (which tends to increase the total number of tracks). However, if a platelet has been a singlet for only a few frames (< 10) then it will tend to be classed as a stably-adhered. Given that most of the other variables are calculated from the translocating platelets, it makes sense to class these platelets as static; the downside being that the number of stably-adhered could be overestimated. The error in the number of translocating platelets is directly correlated with that of the stably-adhered.

4) Weighted Median Speed: The observed error for the weighted median speed was very low and uncorrelated with the object count. This shows that the weighted median speed is indeed not influenced by the outliers. This is a substantial improvement over the error for the mean speed, which is in the order of 5-10%.

5) Mean Translocating Distance: The results were combined from runs where platelets translocated from 50 to 150 pixels with the translocating speed kept constant at 1 pixel/frame. As can be seen in figure 6, the mean distance is mostly underestimated and the greater error is observed for higher object counts and static fractions. In higher object count runs there is an overestimation of the number of tracks, implying track fragmentation. Fragmented tracks are shorter than expected, thus reducing the mean. Mistracking events that lead to a translocating platelet track being matched with a static platelet produces shorter than expected track. Increasing

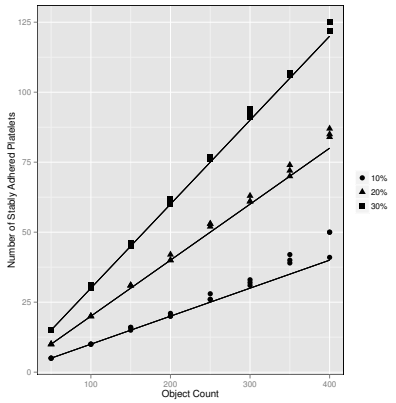

Fig. 5. Number of stably-adhered platelets verses object count. Translocating distance (50 pixels) and speed (1 pixel/frame) are constant. The straight lines are the expected values for each fraction of static platelets.

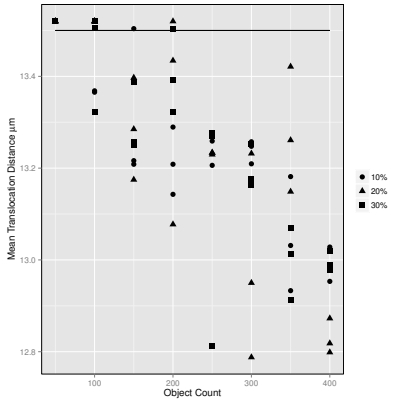

Fig. 6. Mean translocating distance versus object count for a fixed translocating speed (1.0 pixel/frame) and distance (50 pixels). The black line is the expected value.

the number of statics increases the likelihood of these type of mistracking events, again leading to a reduction in the mean.

6) Surface Coverage: Table II shows that surface coverage has a error of $\sim 10\%$ which is always underestimated. The expected value is just the fraction of the sum of the platelet areas. One source of error will be that masked platelet areas will be smaller than the actual value. In addition, merged platelets will have a slightly smaller area than if they were separated. For both these reasons the surface coverage will be underestimated.

7) Percentage Motion: The error in percentage motion increases with object count and it is mostly under-estimated (see figure 7). There will be several factors acting on percentage motion: platelets could appear to move when merged increasing percentage motion but misclassification of stably-adhered platelets would lower it. As the number of stably-

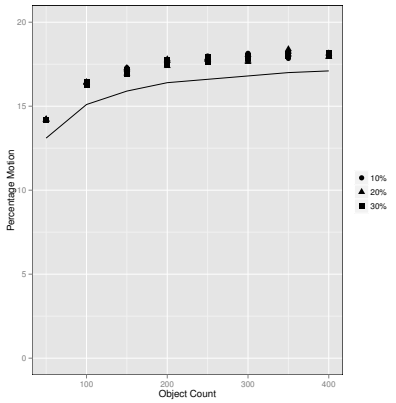

Fig. 7. Percentage of time in motion versus object count. The black line represents the expected values. Translocating speed (1.0 pixels/frame) and distance (50 pixels) are kept constant.

TABLE III
PERCENTAGE OF CORRECTLY MEASURED INITIAL PAUSETIMES VERSUS DIFFERENT EXPECTED PAUSETIMES.

Expected Pausetime (frames)	10	20	30
Percentage Correct (%)	92	88	85

adhered platelets tends to be under-estimated, this is the main source of error.

8) Initial Pausetime Distribution: Three initial pausetimes were used: 10, 20 and 30 frames with a fixed translocating distance of 50 pixels. Speed, static fraction and object count were varied and all the results combined for a fixed pausetime. The errors are due to mistracking and both shorter and longer initial pausetimes were measured (see table III).

9) Adhesion Rate: The error increases with object count and is always an underestimate, with the maximum absolute error of $\sim 17\%$. This is because the recorded values are the number of platelets on each frame and not the number of tracks. The number of platelets on a frame will always be less than or equal to the number of tracks at that point in time.

B. Anti-P2Y1 Test

To further validate the accuracy of the distance-weighted algorithm, we investigated the effect of MRS2179, a selective antagonist of the ADP receptor P2Y1 on platelet trajectories. The P2Y1 receptor is involved in platelet shape change and initiation of platelet aggregation. Furthermore, it has been shown that compounds that inhibit the P2Y1 platelet receptor effect the shape of the platelet when bound to VWF attached to a surface and hence the translocation speed [21]. We performed a test on blood from 8 healthy volunteers who were free from any medication known to affect platelet function within previous 10 days, with ethical approval from the Royal College of Surgeons in Ireland. Blood samples were treated with/without $20\mu M$ MRS2179 (P2Y1 inhibitor), see Section IV for the experimental details. Figure 8 shows

TABLE II
MEAN ABSOLUTE ERROR OF A MEASURED VARIABLE VERSUS OBJECT COUNT.

Variable	**Mean Absolute Error (%)** (Object Count)							
	50	100	150	200	250	300	350	400
Number of Tracks	0.4	0.7	0.5	0.5	0.8	0.9	1.1	1.6
Number of Statics	2.1	3.8	8.1	7.6	8.1	13.4	18.3	15.5
Mean Translocating Distance	1.7	3.9	5.9	7.7	8.5	9.7	10.9	12.1
Weighted Median Speed	0.1	0.1	0.1	0.1	0.1	0.1	0.1	0.1
Surface Coverage	5.5	12.0	12.2	12.5	12.2	13.0	13.2	14.1
Percentage Motion	6.5	10.3	13.7	10.9	13.7	15.0	17.6	19.7

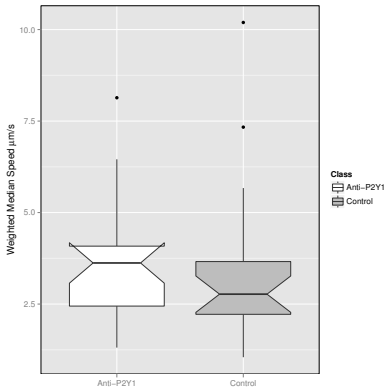

Fig. 8. Boxplot of weighted median translocating speed, combining results for all donors. The notches are the 95% confidence interval on the median and the dots are considered outliers using the standard 1.5 times the interquartile range.

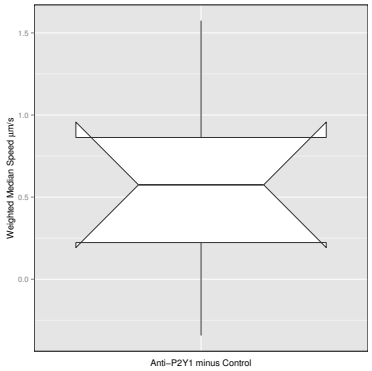

Fig. 9. Boxplot of the differential translocating speed between treated and untreated blood samples from the same donor. Notches are the 95% confidence interval on the median.

the translocating speed, combining results from treated and untreated samples, respectively. The notches on the boxplots give the 95% confidence interval about the median. At this significance level there is no difference between the speeds for the anti-P2Y1 and the control, p-value=0.12. However it is clear there are some outliers in the data (presented by open circles). Figure 9 shows the difference in translocating speed between the mean of the samples for 7 donors. One donor was removed because two of the outliers were from this donor, also the other outlier from the anti-P2Y1 group was removed. As you can see from figure 9 there is a significant difference in the differential translocating speed, p-value=0.039. Both figures were plotted using ggplot2 [**?**] and the p-values were calculated from a one-sided Wilcox test [22]. A one-sided test was used because we were looking for an increase in speed.

C. Platelet Count and Number of Tracks

Blood was obtained from healthy donors with platelet counts ranging from 150,000 to 350,000 per μL of blood. Five donors with 150,000 per μL, five with 250,000 per μL and two with 350,000 per μL. Each donor had at least two runs, with a total of 35 assay runs. Increasing platelet count resulted in a significant increase in the number of platelets interacting with VWF. Using a simple linear regression model the p-value for the slope is ~ 0.00002 (see figure III-C). Results were obtained using the lm function from R [19].

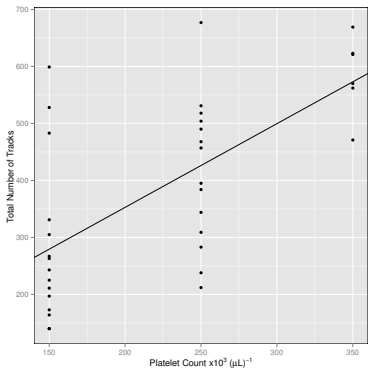

Fig. 10. Plot of all runs for each donor of total number of tracks verses platelet count in the three classes. The black line is the linear regression fit.

IV. Experimental Setup

A. Assembly and Preparation of Parallel Plate Flow Chambers

To perform flow-based analysis to investigate the effect of MRS2179 (Vide Infra), parallel plate flow chambers were comprised of 3 layers, the top layer being a polymethylmethacrylate (PMMA) top plate with an inlet and outlet attached via epoxy glue. The second layer consists of pressure-sensitive adhesive (PSA) containing the microfluidic channel of interest. Finally, a glass coverslip containing the immobilized analyte (VWF, $100\mu g$ coated overnight at 4°C) was used as a base. Prior to analysis, the channel was washed 3 times with phosphate buffered saline (PBS), blocked with 1% (w/v) BSA for 1 hour at room temperature, followed by final rinsing with PBS buffer prior to blood perfusion.

B. Preparation of Whole Blood Prior to Perfusion

Blood was obtained from 8 healthy volunteers who were free from any medication known to affect platelet function within previous 10 days (e.g. Aspirin). Prior to phlebotomy, written informed consent was obtained from all healthy volunteers. Blood was drawn through a 19-gauge butterfly needle into polypropylene syringe (Becton Dickinson, Oxford, UK) containing a 3.2% solution of the anti-coagulant, trisodium citrate dihydrate. $200\mu l$ of blood was aliquoted to a 2ml eppendorf tube. Blood samples were treated with/without $20\mu M$ MRS2179 (P2Y1 inhibitor) and labelled with $1\mu M$ DiOC6 (Invitrogen, USA) fluorescence dye, which localizes to the endoplasmic reticulum and mitochondria of platelets for 10 minutes at 37°C.

C. Perfusion of Whole Blood and Image Acquisition in a Parallel Plate Flow Chamber using MRS2179

Parallel plate flow chambers were mounted on an inverted microscope (Zeiss Axiovert-200 epi-fluoresence). Blood treated with/without P2Y1 inhibitor was drawn through a bio-compatible platinum-cured silicone tubing (Nalgene, 1/16 in internal diameter, Thermo Fisher Scientific, Denmark). Blood was then perfused through the flow chamber using a nemESYS syringe pump (Nem-8001-02-C, Cetoni, Germany), at a controlled flow rate of $75\mu l$/min, giving a fluid shear rate of $1500s^{-1}$ corresponding to physiologically relevant arterial shear rates. Images were captured using a vacuum-cooled (-80°C) digital EM-CCD camera (iXON EM+, Andor Technology, Belfast, Ireland) connected to MetaMorph® (version 7.7, Molecular Devices Ltd., UK) illuminated with an Osram 103-W mercury light source and a fluorescein isothiocyanat (FITC) filter set (ExS490/20x, EmS528/38m, Chroma Technology Corp, Vermont, USA). Images were acquired at 30 frames per second (fps) for 500 frames.

V. Conclusions

Given the number of image sets generated to-date and the complexity of the images themselves, routine manual inspection of images is not viable. An automatic image analysis process is then required, but such a system can never be 100% accurate for non-trivial image sets; when platelets move at random times, appear and disappear anywhere on the imaged surface and the transitory nature of platelet-platelet interactions. Hence there is a need to validate such a system, even if the test image sets are, of necessity, simplified.

It is clear that the major influence on the errors for each of the variables is the number of platelets per frame. The more platelets per frame, the more chance of mergers and separations between platelets occurring and hence mistracking events. However, some variables are affected more than others. For instance the weighted median speed is weakly influenced but stronger for the number of statics. In deciding to track platelet groups but maintain individual tracks, artificial movements are introduced which need to be removed to reduce the bias in the measured variables. There is a penalty, in that any real platelet movements which come with a merging or separation event are also discarded. It might be possible to estimate the real movement in these cases but this has not currently been implemented.

In image sets with real platelets, tracking will inevitably become more difficult. The mean absolute errors presented above therefore represent a lower limit on the actual error one would expect from a real experiment. Although in making all the platelets the same shape and size means that in some cases tracking becomes harder. As can be shown from the anti-P2Y1 results it is still possible to elucidate differential platelet properties between different drugs, disease states and healthy individuals given enough data.

In summary, we have designed and verified the accuracy of a novel platelet tracking algorithm based on a weighted distance matrix using custom-developed idealized data sets, determining the percentage systematic error for key individual parameters of platelet translocation of biological relevance. The ability to interrogate and elucidate platelet translocation dynamic characteristics and utilize them in such a combinatorial manner facilitates the interrogation of healthy and disease cohorts, thus providing unique insights into platelet trajectory profiles in the presence and absence of anti-platelet therapies.

Acknowledgement

This material is based upon work supported by the Science Foundation Ireland under Grant No.10/CE/B1821.

References

[1] Z. M. Ruggeri, "Platelets in atherothrombosis," *Nat Med*, vol. 8, no. 11, pp. 1227–1234, 11 2002.

[2] Y. Ikeda, M. Handa, K. Kawano, T. Kamata, M. Murata, Y. Araki, H. Anbo, Y. Kawai, K. Watanabe, and I. Itagaki, "The role of von willebrand factor and fibrinogen in platelet aggregation under varying shear stress." *The Journal of Clinical Investigation*, vol. 87, no. 4, pp. 1234–1240, 4 1991.

[3] B. Savage, E. SaldÌvar, and Z. M. Ruggeri, "Initiation of platelet adhesion by arrest onto fibrinogen or translocation on von willebrand factor," *Cell*, vol. 84, no. 2, pp. 289–297, 01 1996.

[4] B. Savage, F. Almus-Jacobs, and Z. M. Ruggeri, "Specific synergy of multiple substrate–receptor interactions in platelet thrombus formation under flow," *Cell*, vol. 94, no. 5, pp. 657 – 666, 1998.

[5] S. Kulkarni, S. M. Dopheide, C. L. Yap, C. Ravanat, M. Freund, P. Mangin, K. A. Heel, A. Street, I. S. Harper, F. Lanza, and S. P. Jackson, "A revised model of platelet aggregation." *J Clin Invest*, vol. 105, no. 6, pp. 783–791, Mar 2000.

[6] R. K. Andrews, J. López, and M. C. Berndt, "Molecular mechanisms of platelet adhesion and activation," *The International Journal of Biochemistry and Cell Biology*, vol. 29, no. 1, pp. 91 – 105, 1997.

[7] R. K. Andrews, Y. Shen, E. E. Gardiner, J.-f. Dong, J. A. López, and M. C. Berndt, "The glycoprotein ib-ix-v complex in platelet adhesion and signaling," *Thrombosis and Haemostasis*, vol. 82, no. 8, pp. 357–364, 1999.

[8] B. Lincoln, A. J. Ricco, N. J. Kent, L. Basabe-Desmonts, L. P. Lee, B. D. MacCraith, D. Kenny, and G. Meade, "Integrated system investigating shear-mediated platelet interactions with von willebrand factor using microliters of whole blood," *Analytical Biochemistry*, vol. 405, no. 2, pp. 174 – 183, 2010.

[9] N. Kent, L. Basabe-Desmonts, G. Meade, B. MacCraith, B. Corcoran, D. Kenny, and A. Ricco, "Microfluidic device to study arterial shear-mediated platelet-surface interactions in whole blood: reduced sample volumes and well-characterised protein surfaces," *Biomedical Microdevices*, vol. 12, no. 6, pp. 987–1000, 2010.

[10] P. Ruhnau, C. Guetter, T. Putze, and C. Schnörr, "A variational approach for particle tracking velocimetry," *Measurement Science and Technology*, vol. 16, no. 7, p. 1449, 2005.

[11] M. J. Saxton and K. Jacobson, "Single-particle tracking:applications to membrane dynamics," *Annual Review of Biophysics and Biomolecular Structure*, vol. 26, no. 1, pp. 373–399, 1997, pMID: 9241424.

[12] R. N. Ghosh and W. W. Webb, "Automated detection and tracking of individual and clustered cell surface low density lipoprotein receptor molecules," *Biophysical journal*, vol. 66, no. 5, pp. 1301–1318, 05 1994.

[13] J. Gelles, B. J. Schnapp, and M. P. Sheetz, "Tracking kinesin-driven movements with nanometre-scale precision," *Nature*, vol. 331, no. 6155, pp. 450–453, 02 1988.

[14] S. S. Work and D. M. Warshaw, "Computer-assisted tracking of actin filament motility," *Analytical Biochemistry*, vol. 202, no. 2, pp. 275 – 285, 1992.

[15] M. Machin, A. Santomaso, M. Mazzucato, M. R. Cozzi, M. Battiston, L. De Marco, and P. Canu, "Single particle tracking across sequences of microscopical images: Application to platelet adhesion under flow," *Annals of Biomedical Engineering*, vol. 34, no. 5, pp. 833–846, 2006.

[16] A. Perl, D. N. Reinhoudt, and J. Huskens, "Microcontact printing: Limitations and achievements," *Advanced Materials*, vol. 21, no. 22, pp. 2257–2268, 2009.

[17] D. M. D. Abràmoff, D. P. J. Magalhães, and D. S. J. Ram, "Image processing with imagej," *Biophotonics International*, vol. 11, no. 7, pp. 36–42, July 2004.

[18] MATLAB, *version 7.12.0 (R2011a)*. Natick, Massachusetts: The MathWorks Inc., 2011.

[19] R Core Team, *R: A Language and Environment for Statistical Computing*, R Foundation for Statistical Computing, Vienna, Austria, 2012, ISBN 3-900051-07-0.

[20] H. Wickham, *Ggplot: Elegant graphics for data analysis*. Springer, 2009.

[21] M. Mazzucato, M. R. Cozzi, P. Pradella, Z. M. Ruggeri, and L. De Marco, "Distinct roles of adp receptors in von willebrand factor-mediated platelet signaling and activation under high flow." *Blood*, vol. 104, no. 10, pp. 3221–3227, Nov 2004.

[22] D. F. Bauer, "Constructing confidence sets using rank statistics," *Journal of the American Statistical Association*, vol. 67, no. 339, pp. 687–690, 1972.